EVALUATION OF MASS TRANSFER IN A CATALYTIC DISTILLATION COLUMN USING HYDROGENATION OF 1-HEXENE AS A TEST REACTION

by

Mamabolo Geoff Mphahlele

A Half-Thesis presented to the University of Cape Town in partial fulfilment of the requirement for the degree of Master of Science in Chemical Engineering

Cape Town, Western Cape, South Africa, 2003

I hereby declare that I am the sole author of this thesis. I authorize the University of Cape Town to lend this thesis to other institutions or individuals for the purpose of scholarly research. I further authorize the University of Cape Town to reproduce this thesis by photocopying or by other means, in total or in part, at the request of institutions or individuals for the purpose of scholarly research

Abstract

Catalytic distillation (CD) is formally defined as a process in which a heterogeneously catalysed chemical reaction and distillation of the reagents and products occur simultaneously within a distillation column (Podrebarac *et al.*, 1997). The heterogeneous packing serves both as distillation packing and a catalyst. Catalytic distillation is different from reactive distillation (RD), in which a homogeneous catalyst is used. With a catalyst in the column, the distillation operation becomes a two-phase counter current flow, fixed bed reactor. CD is classified as counter current because the liquid and vapour flow in opposite directions inside the column. Other reactors have flow configurations of the vapour and liquid phases in co-current downward flow – a trickle bed reactor (TBR) - or co-current upward flow, as in a slurry reactor.

Despite the CD technology being commercialised, limited studies on the effect of selective hydrogenation reaction on mass transfer in a CD column have been carried out. In contrast, the effect of hydrogenation reaction on mass transfer in a trickle bed reactor has been well investigated (Kelkar *et al.*, 1992; Chou, 1997).

Mass transfer to or from single spheres, packed beds of spheres and fluidized beds of spheres has and continue to receive attention because of the importance of, amongst other chemical engineering operations, catalytic reactors and catalytic distillation columns. Podrebarac (1992) found that mass transfer in the CD process had a major effect on the observed catalyst activity for the oligomerization of 1-butene. Proper design of CD columns through the non-equilibrium model (NEQ) requires knowledge of gas-liquid and liquid-solid mass transfer correlations and interfacial areas (Huang *et al.*, 1998*a*; Baur *et al.*, 2000, 2001*a*; *b*). However, so far very few correlations exist for predicting these mass transfer correlations and the interfacial areas. Huang and co-workers (1998*a*) have shown that mass transfer has a significant effect on the overall CD performance.

Abstract

The aim of this project is to evaluate experimentally the overall vapour/liquid mass transfer coefficient, and to develop a simple model for evaluating the effect of chemical reaction on the overall vapour/liquid mass transfer coefficient.

Following the extensive literature review, the following hypotheses were made:

- The overall vapour/liquid mass transfer coefficient increases with increasing vapour or liquid flow rate.
- The catalytic chemical reaction will affect the vapour-liquid mass transfer rate. Since the hydrogenation reaction is fast, the gas phase mass transfer will be the controlling step. Hence, a larger vapour-liquid mass transfer will be observed in the presence of hydrogenation.

The overall vapour/liquid mass transfer coefficients in the absence of hydrogenation reaction were experimentally determined in a bench-scale batch catalytic distillation operating at total reflux. The reboiler and condenser concentrations at varying liquid/vapour rates were measured at steady state, and the overall vapour/liquid mass transfer coefficients were determined using the Height of Transfer Units method. The liquid/vapour flow rates were varied by changing the reboiler duty.

To evaluate the effect of chemical reaction, hydrogen gas was introduced into the column to facilitate the hydrogenation of 1-hexene to n-hexane, and the reboiler and condenser concentrations were measured at varying liquid-vapour rates. The overall vapour-liquid mass transfer coefficients in the presence of reaction were then inferred from a simple film theory model.

The model developed in this study was based on numerous assumptions and is therefore considered simplistic. The model has been shown to conform to all expected behaviour, and therefore the inferred overall vapour-liquid mass transfer coefficients make sense.

Abstract

The experimental work in this study indicated that in the absence of hydrogenation reaction the overall vapour-liquid mass transfer increases with increasing gas molar flow rate. This result is consistent with the work of other investigators (Bravo *et al.*, 1985; Zheng and Xu, 1992; Dudukovic, 1996; Subawalla *et al.*, 1997; Huang *et al.*, 1998a; Van Baten and Krishna, 2002). Statistical analysis of the experimental results showed that the mass transfer coefficients are reproducible up to 95% level of confidence.

The model developed in this study was validated by comparing the experimentally measured reboiler compositions of 1-hexene to those predicted by the model. The relative error between the experimental and measured values was considered acceptable. It was also shown by inference from the simple film model that the vapour-liquid mass transfer rate is enhanced by the chemical reaction.

Acknowledgements

Carrying out research in Catalytic Distillation is certainly not a 'walk in the park'. The presence of chemical reaction in addition to the separation by distillation makes the whole process complicated. Putting together a thorough thesis takes a lot of effort and many people have contributed to this process.

First of all, I would like to thank my supervisor, Dr. Klaus P. Moller, for providing me with the guidance and encouragement during the project. I also would like to thank Dr. Miklos Stark of Sasol Research and Development for providing the 1-hexene and the Nickel/Alumina catalyst used in the experiments. Prof. Eric Van Steen provided some useful assistance to the project through discussions when my supervisor was away.

I thank Joan Muller and my colleagues in Chemical Engineering department for the stimulating friendship that helped me to get through the testing times during the project. I must also thank all the folks that were, at some stage or the other, my squash partner/s. This really helped in reducing the stress induced by the project.

Lastly, I would also like to express my appreciation to my brother Stanley and my parents for their support and encouragement. Hopefully it won't be too soon that they will stop asking: so, when are you finishing the thesis?

Table of Contents

List of Tables

List of Figures

Nomenclature

A = frequency factor [s^{-1}]

a = interfacial area per unit height of packing [m^2/m]

a_p = total surface area of packing [m^2/m^3]

a_w =wetted surface area of packing [m^2/m^3]

a_t = specific surface of packing [m^2/m^3]

a_1, a_2 = constants in Equation (1.17)

C = concentration [mol/m^3]

c_S = saturated concentration [mol/m^3]

c_1, c_2, c_3 = constants in Equation (1.13)

d_p = equivalent diameter of the packing $(4\varepsilon/a_t)$ [m]

D = diffusivity [m^2/s]

d_C = diameter of the column [m]

d_{eq} = equivalent diameter of channel [m]

d_h = hydraulic diameter [m]

d_1, d_2, d_3, d_4 = constants in Equation (1.24)

E = activation energy [J/mol]

G = gas or vapour superficial velocity [m/s]

g = gravitational acceleration constant [m^2/s]

H = height of packing [m]

H = Henry's constant

h_d = dynamic liquid holdup

h_L = specific liquid hold-up

j_D = j-factor in liquid – solid phases $\{\frac{k_S a}{d\nu_L}\left(\frac{\mu_L}{\rho_L D_{SL}}\right)^{2/3}\}$

j_G = j-factor in vapour – liquid phases $\{\frac{Sh_G}{\mathrm{Re}_G Sc_G^{1/3}}\}$

k_g = mass transfer coefficient for the gas-phase based on a partial pressure driving force [$mol/(m^2.s.kPa)$]

K_{OG} = overall mass transfer coefficient based on the vapour phase with the partial pressure driving force [$kmol/m^2.s.kPa$]

Nomenclature

K_{OL} = overall mass transfer coefficient based on the liquid phase with the concentration driving force [m/s]

k_C =mass transfer coefficient for the liquid-phase based on concentration driving force [m/s]

k_Sa = overall mass transfer coefficient between liquid-solid phases [m^2/s]

K_X = overall mass transfer coefficient based on the liquid phase with a mole-fraction driving force [$mol/m^2.s$]

K_Y = overall mass transfer coefficient based on the vapour phase with a mole-fraction driving force [$mol/m^2.s$]

k_ya = mass transfer coefficient for the vapour phase based on a mole-fraction driving force [mol/m.s]

k_xa = mass transfer coefficient for the liquid phase based on a mole-fraction driving force [mol/m.s]

L = liquid flow rate [mol/s]

m = equilibrium constant between vapour and liquid compositions

N = molar concentration

N_i = mass transfer flux of component i [$mol/m^2.s$]

P = pressure [kPa]

Q = volumetric flow rate [m^3/s]

R = universal gas constant [J/mol. K}

r = reaction rate on the solid surface [$mol/m^3.s$]

Re = Reynolds number $(d v \rho / \mu)$

Re'_G = modified Reynolds number for the gas phase $(4G\rho_G / a_t \mu_G)$

Re'_L = modified Reynolds number for the liquid phase $(4L\rho_L / a_t \mu_L)$

S = fractional rate of surface renewal

Sc = Schmidt number $(\mu / \rho D)$

Sh_G = Sherwood number $(K_Y a / CD)$

Sh'_G = modified Sherwood number for the gas phase $(K_Y a d_p / a_t C D_G)$

Sh'_L = modified Sherwood number for the liquid phase $(K_X a d_p / a_t D_L)$

t = contact time [s]

t_C = contact time [s]

T = absolute temperature of the gas [K]

Nomenclature

u = superficial velocity based on empty column [m/s]

$U_{g,eff}$ = effective gas or vapour velocity through channel [m/s]

$U_{L,eff}$ = effective liquid velocity through channel [m/s]

v = fluid superficial velocity [m/s]

w_1, w_2, w_3, w_4 = constants in Equation (1.32)

X = mole fraction in liquid phase

Y = mole fraction in vapour phase

Z = depth into the film thickness

Abbreviations

CD = catalytic distillation

CO_2 = carbon dioxide

RD = reactive distillation

H_2O = water

HOAc = acetic acid

ID = internal diameter

EQ = equilibrium

GC = gas chromatography

LLMT = low limit

MeOH = methanol

MeOAc = methyl acetate

$Na_2CO_3 - NaHCO_3$ = sodium bicarbonate

NEQ = non-equilibrium model

TBR = trickle bed reactor

ULMT = upper limit

VLE = vapour and liquid equilibrium

Greek letters

ε = void fraction in the bed

μ = fluid viscosity [Pa.s]

ρ = fluid density [kg/m^3]

α = relative volatility

δ = film thickness [m]

δ = dynamic diffusivity [kmol/(m. s)]

υ_Z = equivalent linear dimension $(\eta^2/\rho^2 g)$ [m]

η = dynamic viscosity [Pa. s]

Γ = mass flow rate of liquid per unit wetted perimeter [kg/s. m]

Superscripts/subscripts

A = species A

B = species B

AB = species A in solution of B

b = bottom

b = bulk

d = dry

e = experiment

i = component I

i = interface

H = height

H_2 = hydrogen

max = maximum

l = liquid

G = gas or vapour

r = reboiler

s = solid

LS = liquid-solid phase

OG = overall gas/vapour-phase

OL = overall liquid-phase

t = top

vap = vapour

Y = gas phase

* = equilibrium or saturation

1 = inlet conditions

2 = exit conditions

1. INTRODUCTION AND LITERATURE REVIEW

1.1. Catalytic distillation and its applications

Catalytic distillation (CD) is formally defined as a process in which a heterogeneously catalysed chemical reaction and distillation of the reagents and products occur simultaneously within a distillation column (Podrebarac *et al.*, 1997). The heterogeneous packing serves both as distillation packing and a catalyst. Catalytic distillation is different from reactive distillation (RD), in which a homogeneous catalyst is used. With a catalyst in the column, the distillation operation becomes a two-phase counter current flow, fixed bed reactor. CD is classified as counter current because the liquid and vapour flow in opposite directions inside the column. Other reactors have flow configurations of the vapour and liquid phases in co-current downward flow – a trickle bed reactor (TBR) - or co-current upward flow, as in a slurry reactor.

The traditional flow sheet of a chemical process consists of a reactor followed by a separation unit to remove the undesired reactants from the desired product and recycle these back to the reactor, as shown in Fig 1.1:

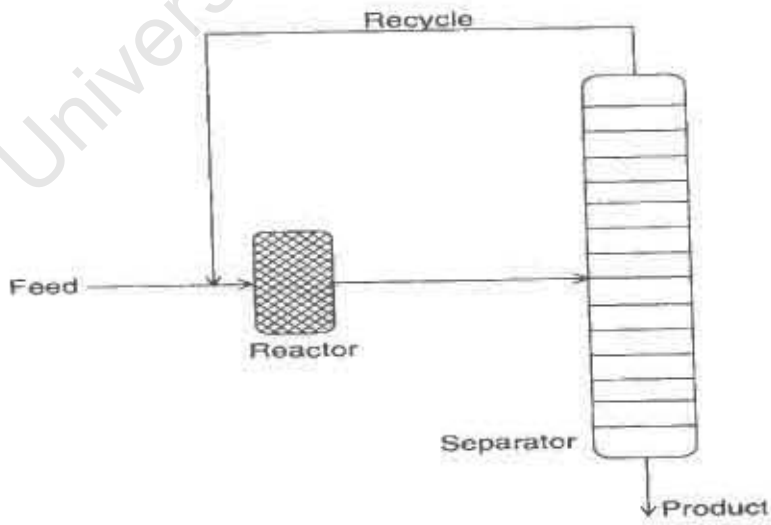

Fig 1.1: Conventional flowsheet of a process consisting of a reactor followed by a separation unit (Krishna, 2002).

The success story of reactive distillation technology has been the production of methyl acetate through a homogeneous reaction. The manufacture of high-purity methyl acetate by the sulphuric acid-catalysed esterification reaction of acetic acid with methanol:

$$HOAc + MeOH \leftrightarrow MeOAc + H_2O, \quad (1.1)$$

is made difficult by the following factors (Krishna, 2002):

- Reaction equilibrium limitations;
- Difficulty of separating HOAc and H_2O;
- Presence of MeOAc – H_2O and MeOAC – MeOH azeotropes.

The conventional process uses one or more liquid phase reactions with large excess of one reactant in order to achieve high conversions of the other, as shown in fig 1.2:

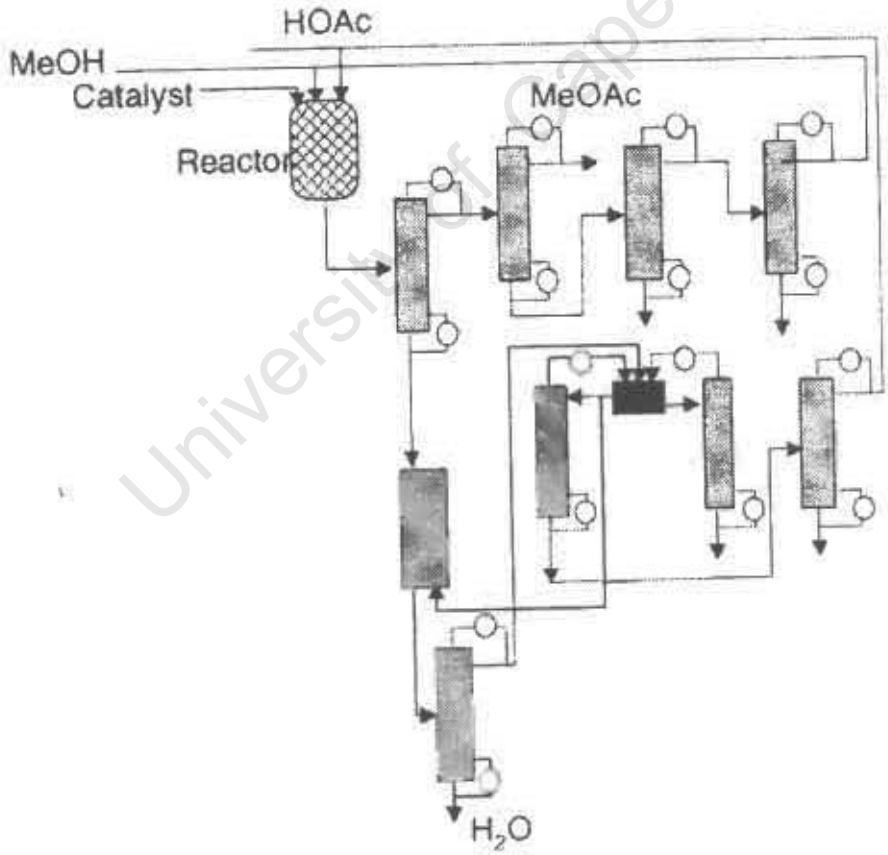

Fig 1.2: Conventional processing scheme for producing high-purity methyl acetate (Krishna, 2002).

A typical flow sheet for the production of high-purity MeOAc involves a reaction section followed by eight distillation columns, one liquid-liquid extractor and a decanter. This process requires a large capital investment, high-energy costs and a large inventory of solvents (Krishna, 2002).

In the CD process for the production of MeOAc, invented by Eastman chemical company, the entire process is carried out in a single column, as shown in fig 1.3:

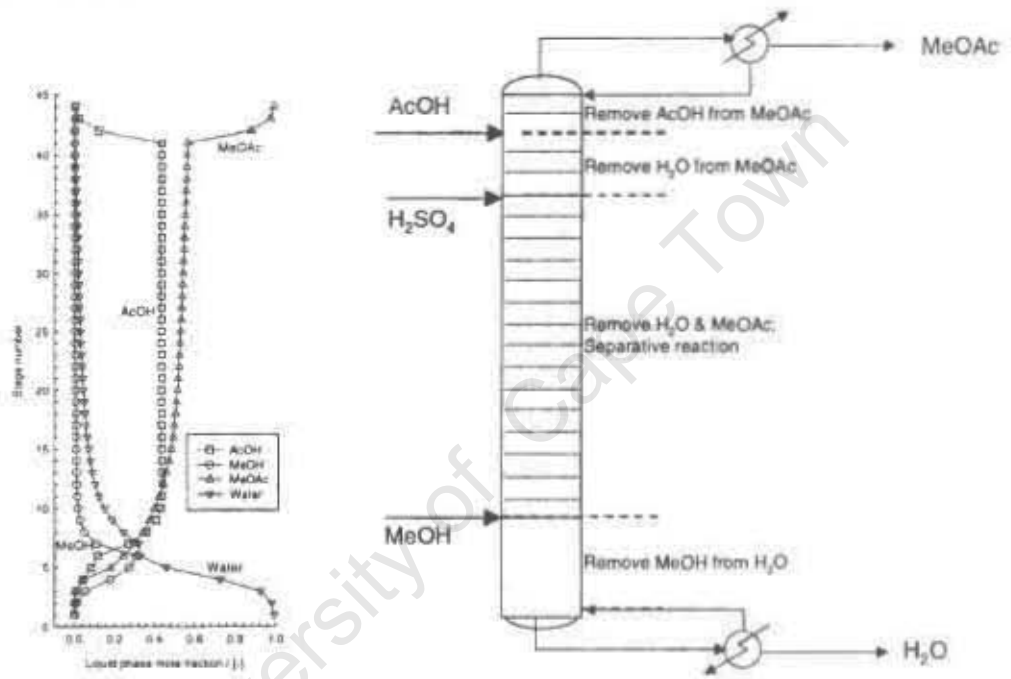

Fig 1.3: The Eastman reactive distillation process for methyl acetate manufacture (Krishna, 2002). The reaction takes place predominantly in the middle section, below H_2SO_4 feed.

In this single column high-purity methyl acetate is made with no additional purification steps and with no unconverted reactant streams to be recovered. By flashing off the methyl acetate from the reaction mixture, conversion is increased without using excess of one of the reactants. The CD column has stoichiometrically balanced feed. The Sulphuric acid leaves the column in the aqueous phase. The CD column represents an entire chemical plant and costs one-fifth of the capital investment of the conventional process and consumes only one-fifth of the energy (Krishna, 2000).

CD technology, as opposed to conventional distillation, has found limited success in industry due to the special attention that it needs in order for it to be successful. On any reactive tray or packing, the requirements for chemical reaction, i.e. high liquid hold-up for maximising conversion, are not always in consonance with the requirement for good separation, i.e. high interfacial area. For conventional distillation, the spray regime is the preferred operation regime of separation whereas for reactive trays the liquid-hold up needs to be increased until a bubbly flow or froth regime is obtained.

Catalyst particles used in common catalytic reactors such as TBR are typically small spherical or cylindrical particles, resulting in a bed porosity of 0.3 to 0.4 (Podrebarac *et al.*, 1997). However, catalytic distillation packings typically have a void fraction of about 0.7, with a few achieving a void fraction of 0.97 (Podrebarac *et al.*, 1997; Fair and Bravo, 1990). Generally, the low void fraction of the catalyst bed makes countercurrent operation difficult to carry out, and hence flow rates must be controlled to avoid flooding the catalyst bed. However, TBRs do not flood under a wide variety of liquid and gas flow rates (Podrebarac *et al.*, 1997). Hence easier operation and wide operation "window" makes TBR far more common in the chemical industry.

Catalytic distillation is used in a variety of industrial processes. These processes include (Podrebarac *et al.*, 1997):

- Etherification. This is a process in which MTBE is produced from an acid-catalyzed reaction between methanol and isobutylene.
- Hydration of olefins. The hydration of isobutylene to t-butyl alcohol is often carried out in CD columns to avoid the severe conditions experienced in conventional fixed bed reactors.
- Dehydration of alcohols. CD columns have been used to perform the bimolecular dehydration of isopropyl alcohol to form diisopropyl ether.

It is therefore clear that CD columns play an important role in chemical industry. Hence, there is a scientific and industrial interest in their performance.

1.1.1 Advantages and disadvantages of CD

Catalytic distillation has many advantages over conventional fixed-bed reactors (Podrebarac *et al.*, 1997), and the key benefits are the following:

- CD uses the exothermic heat of reaction efficiently. In conventional reactors, the reaction heat is removed by cooling coils or heat exchangers. In CD, the catalyst is surrounded by boiling liquid, and the reaction heat generates more vapour. Therefore, the distillation process is enhanced. In addition, this 'natural' heat integration provides significant energy savings because reboiler duties can be reduced in CDs.
- A common problem in reactors running highly exothermic reactions such as hydrogenation reaction is formation of "hot spots" in the catalyst bed. However, in a CD column this problem is avoided, because the catalyst is surrounded by boiling liquid. The temperature of the liquid phase in the CD column cannot exceed its boiling point. Therefore, as long as the liquid flow rate keeps the catalyst wet enough, the catalyst temperature will remain near the boiling point of the liquid phase.
- In catalytic distillation, two operations – catalytic reaction and separation – are carried out in one unit operation. In conventional reaction engineering, these two operations would be separate. Therefore, CD offers significant capital savings over a conventional reactor-distillation column scheme.
- Most CD processes, for example production of MTBE, can be operated such that certain reaction products are selectively removed from the reaction zone by distillation. Le Chatelier's principle implies that the removal of product from a system at equilibrium will cause more product to form. Therefore, the conversion of an equilibrium-limited reaction beyond its thermodynamic limit is possible in a CD column.
- Distillation columns normally operate at higher liquid and vapour flow rates than conventional reactors. Hence, faster removal of products from the reaction zone of the column is possible. This can reduce the probability of

consecutive reactions taking place and thus increase the product selectivity.

Unfortunately, as in other conventional reactors, CD cannot be applied to all reactions. The following conditions must be satisfied for CD to work properly (Podrebarac *et al.*, 1997):

- Distillation has to be a practical method of separating the reagents and products.
- The reaction has to take place in the liquid phase since the catalyst pellets have to remain completely wetted.
- The reaction has to take place at a temperature equivalent to the boiling point of the liquid in the column. The boiling point depends on the column overhead pressure. Therefore, the boiling temperature can be varied by changing the column pressure. However, two phases – vapour and liquid – are needed for distillation, and therefore there is a limit to the temperature that can be used. Hence, the reaction temperature has to be below the critical temperature of at least one of the components present in the column.
- A heterogeneous catalyst with a rather long life span must be used. It is expensive and labour intensive to change the catalyst from the unique packing – such as "tea bags", wire mesh etc, in a CD column. Typically the catalyst must last 1 or 2 years in service to be commercially viable (Podrebarac *et al.*, 1997).

1.1.2 Hydrogenation using CD system

Selective hydrogenation of the olefinic cut is of prime importance to refiners globally. Selective hydrogenation increases the amount of normal butenes available for alkylation, and thereby improves the octane of alkylate from alkylation units. In addition, diolefins can deactivate catalysts in downstream operations or take part in undesired side reactions. At present, the following selective hydrogenation schemes are carried out in commercial CD columns (Rock *et al.*, 1997):

- selective hydrogenation of olefins (CDHydro process).

- C_4 butadiene selective hydrogenation.
- C_5 pentadiene selective hydrogenation.
- C_8 hexadiene selective hydrogenation.
- hydrogenation of benzene.
- hydrogenation of aromatics.

CDHydro was commercialized in early 1994 at two locations for the selective hydrogenation of butadiene. Shell started up the first unit in a C_4 splitter at Norco, La., in February 1994. In July 1994, Idemitsu Kosan began the operation of the second unit in an MTBE debutanizer at Chiba, Japan. Both installations perform selective hydrogenation of butadiene to butene in distillation columns. Two more units were installed in late 1994.

The CDHydro process combines distillation with hydrogenation. Propriety devices containing catalyst are installed in the distillation column's top section (1) as shown in Fig 1.4:

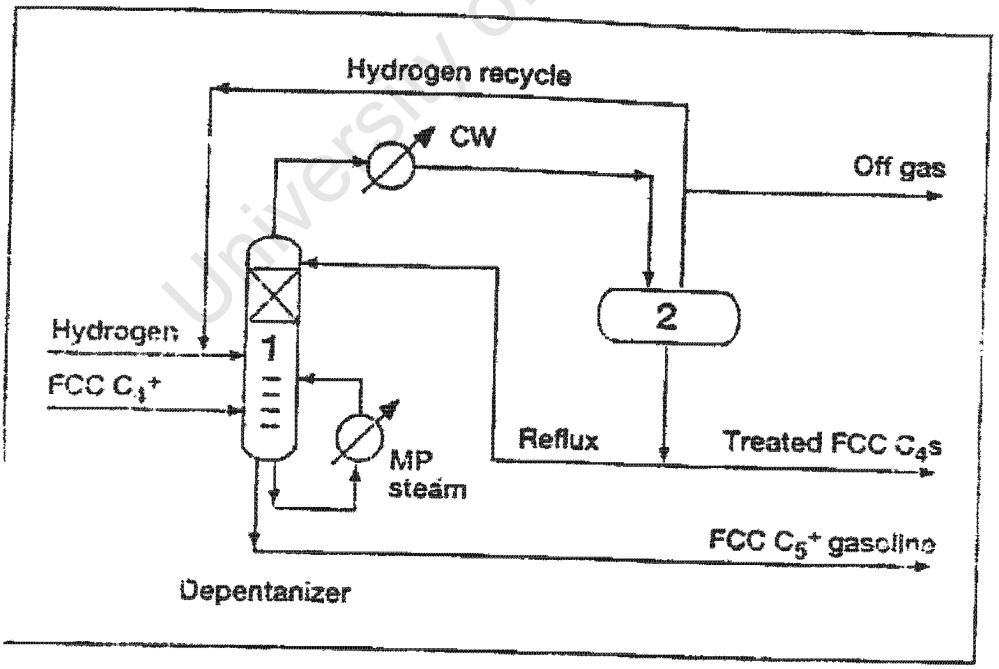

Fig 1.4: CDHydro process for selective hydrogenation of diolefins (Hydrocarbon Processing, 1994).

Hydrogen is introduced beneath the catalyst zone. Distillation carries light components into the catalyst zone where the reaction with hydrogen occurs. Distillation also sends heavy materials to the bottom. This prevents foulants and heavy catalyst poisons in the feed from contacting the catalyst. In addition, clean hydrogenated reflux continuously washes the catalyst zone. These factors combine to give a long catalyst life. In addition, mercaptans can react with diolefins to make heavy, thermally stable sulfides. The sulfides are fractionated to the bottoms product. This eliminates the need for a separate mercaptan removal step.

Despite the CD technology being commercialised, limited studies on the effect of selective hydrogenation reaction on mass transfer in a CD column have been carried out. In contrast, the effect of hydrogenation reaction on mass transfer in a trickle bed reactor has been well investigated (Kelkar *et al.*, 1992; Chou, 1997).

1.2 Mass transfer

The design and operational issues for CD systems are more complex than those involved in either conventional reactors or conventional distillation columns. The introduction of an in situ separation function within the reaction zone leads to complex interactions between vapour-liquid equilibrium, vapour-liquid mass transfer, intra-catalyst diffusion and chemical kinetics. These interactions have been shown to lead to the phenomena of multiple steady states and complex dynamics, which have been verified in experimental laboratory and pilot plant units (Baur *et al.*, 2000*a*, *b*).

Mass transfer to or from single spheres, packed beds of spheres and fluidized beds of spheres has and continue to receive attention because of the importance of, amongst other chemical engineering operations, catalytic reactors and catalytic distillation columns. Podrebarac (1992) found that mass transfer in the CD process had a major effect on the observed catalyst activity for the oligomerization of 1-butene.

Proper design of CD columns through the non-equilibrium model (NEQ) requires knowledge of gas-liquid and liquid-solid mass transfer correlations since a three-phase operation takes place. This is evident from the work by various authors in literature (Huang *et al.*, 1998a; Baur *et al.*, 2000*a*, *b*, 2001*a*; *b*). Huang *et al.* (1998*a*, 2000) and Zheng *et al.* (2001) have shown that the rate based method applied to the simulation of the aldol condensation of acetone to diacetone alcohol agreed with the experimental data well. The temperature profiles along the length of the column and the outlet concentrations predicted by the NEQ model agreed with the experimentally measured values. Huang and co-workers have also shown that mass transfer has a significant effect on the overall CD performance.

1.2.1 Gas-liquid mass transfer theories.

Fluid-fluid mass transfer phenomena with and without chemical reaction has been well explained by the following theories:

- Film theory;
- Two-film theory;
- Penetration theory;
- Surface renewal theory, and
- Film-penetration theory

Detailed discussion of these models is provided by Sherwood (1975); Welty *et al.* (1984); Henley and Seader (1998) and Bird *et al.* (2002).

1.2.1.1 Film theory

Film theory, first proposed by Nerst in 1925, for turbulent mass transfer to or from a fluid-phase boundary assumes that the entire resistance to mass transfer is in a thin, stagnant region of that phase at the interface, called a film as shown in Fig 1.5.

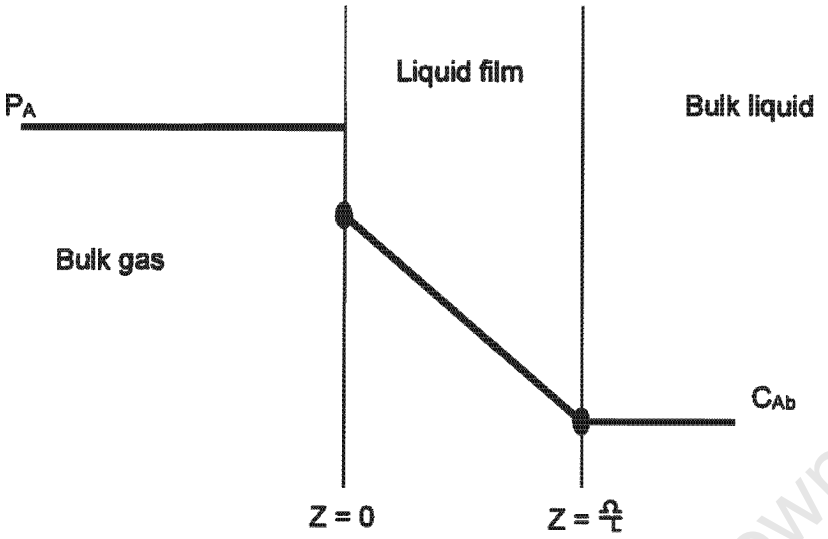

Fig 1.5: Film theory for mass transfer from a fluid-fluid interface into a liquid (Henley and Seader, 1998).

In the thin, stagnant liquid film thickness of δ, molecular diffusion only occurs with a driving force of $C_{Ai} - C_{Ab}$. Assuming no accumulation of the species A in the film, neglecting bulk flow and assuming dilute solutions, the mass transfer flux of A is given by (Henley and Seader, 1998):

$$N_A = k_C(C_{Ai} - C_{Ab}) = \frac{cD_{AB}}{\delta}(x_{Ai} - x_{Ab}) \quad (1.2)$$

Hence, film theory predicts that the mass transfer coefficient, k_C, is directly proportional to the molecular diffusivity. This dependency contradicts experimental data which indicate a dependency of D_{AB}^n, where n ranges from 0.5 to 0.75 (Henley and Seader, 1998).

1.2.1.2 Two-film theory

Whitman suggested an extension of the film theory to two fluid films in series. Each film presents a resistance to mass transfer, but concentrations in the two fluids at the interface are in equilibrium. Hence, there is no additional interfacial resistance to mass transfer. According to Henley and Seader

(1998), the two film theory has found extensive application in modelling steady-state gas-liquid separation processes when the fluid phases are in laminar or turbulent flow.

This postulation predicts linear concentration gradients as shown in Fig 1.6:

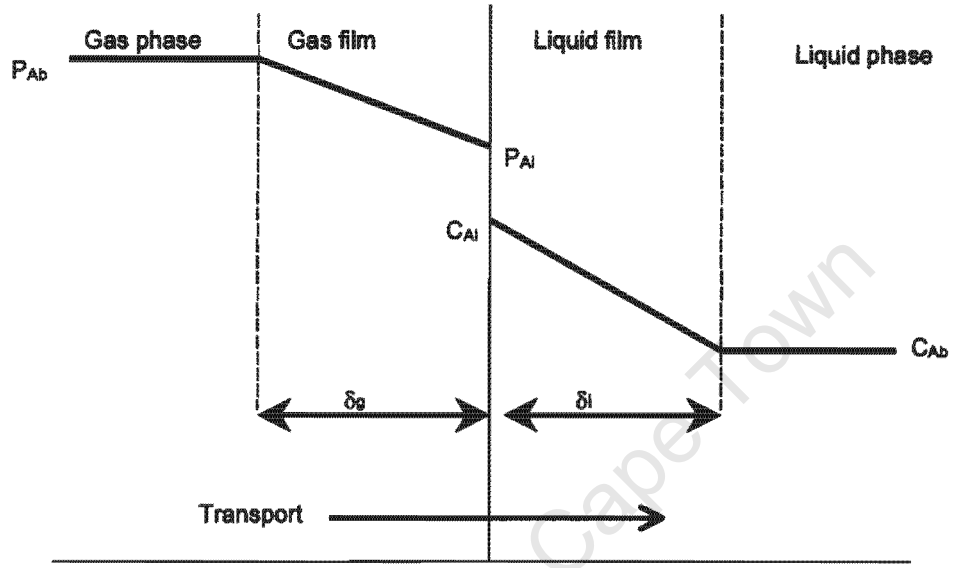

Fig 1.6: Concentration gradients as described by two-film theory (Henley and Seader, 1998).

Because the interfacial concentrations are not known, it is necessary to define the overall driving force for mass transfer based on gas and liquid bulk concentrations. The overall driving force in the gas phase is defined as

$$\left(P_{Ab} - P_A^*\right) \tag{1.3}$$

where,

$$P_A^* = \frac{C_{Ab}}{H_A} \tag{1.4}$$

The mass transfer flux is then given by:

$$N_A = K_{OG}\left(P_{Ab} - P_A^*\right) = \frac{\left(P_{Ab} - P_A^*\right)}{\left(1/k_g\right) + \left(1/H_A k_C\right)} \tag{1.5}$$

where the overall mass transfer coefficient is given by:

$$\frac{1}{K_{OG}} = \frac{1}{k_g} + \frac{1}{H_A k_c} \tag{1.6}$$

By similar analysis, the overall mass transfer coefficient based on the liquid phase is given by:

$$\frac{1}{K_{OL}} = \frac{H_A}{k_g} + \frac{1}{k_c} \tag{1.7}$$

1.2.1.3 Penetration theory

The penetration theory, suggested by Higbie (1935), provides a more realistic physical model of mass transfer from a fluid-fluid interface into a bulk liquid. Fig 1.7 describes the penetration theory:

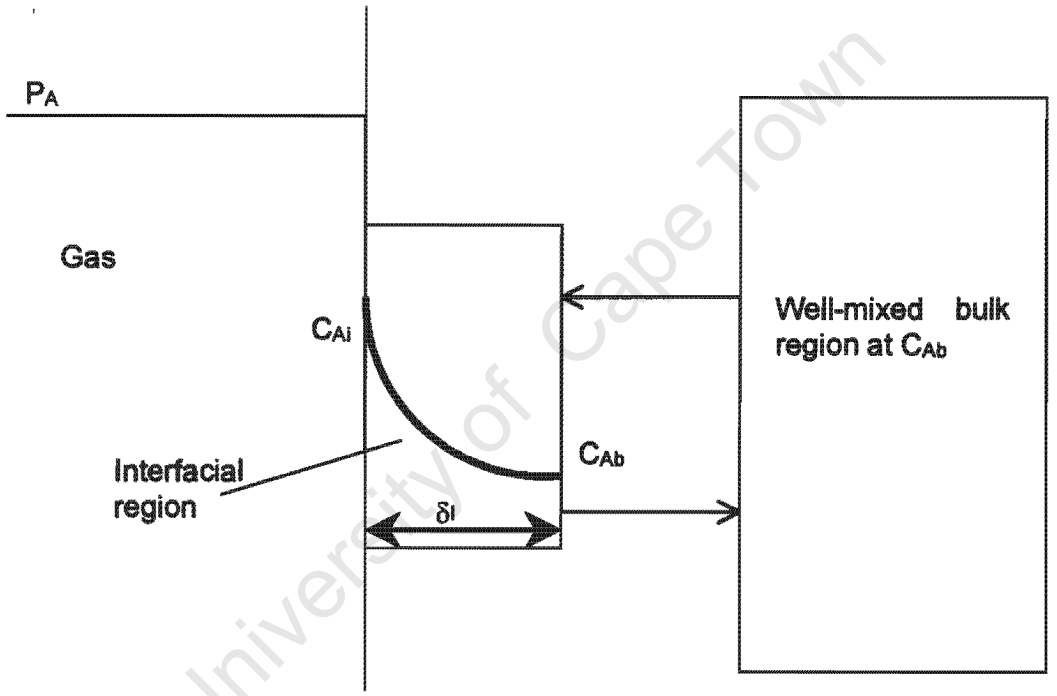

Fig 1.7: Penetration and surface renewal theories for describing mass transfer from a fluid-fluid interface into a liquid (Henley and Seader, 1998).

The stagnant-film concept, of the two-film theory, is replaced by the so-called Boussineq eddies that undergo the following process (Henley and Seader, 1998):

- move from the bulk fluid to the fluid-fluid interface (single component transferred);

- stay at the interface for a short, fixed period of time during which they remain static so that unsteady-state molecular one-dimensional diffusion takes place in a direction normal to the interface, and
- leave the interface to mix with the bulk stream.

When an eddy moves to the interface, it replaces another static eddy. Thus, the eddies are intermittently static and moving. In the penetration theory, unsteady state diffusion takes place at the interface during the time the eddy is static. The average mass transfer flux of species A in the absence of bulk flow is given by (Henley and Seader, 1998):

$$N_A = k_C(C_{Ai} - C_{Ab}) = 2\sqrt{\frac{D_{AB}}{\pi t_C}}(C_{Ai} - C_{Ab}) \tag{1.8}$$

Therefore, penetration theory supposes that k_c is proportional to the square root of the molecular diffusivity, which happens to be the lower limit of experimental data (Henley and Seader, 1998).

Penetration theory is most useful when mass transfer involves flow over random packings (Henley and Seader, 1998). For a packed tower, where the liquid flows as a film over particles of random packing, mixing can be assumed to occur each time the liquid passes from one piece of packing to another.

1.2.1.4 Surface renewal theory

One of the shortcomings of penetration theory is the assumption of a constant contact time for all eddies that temporarily reside at the fluid-fluid interface (Fig 1.7). Danckwerts (1951) improved penetration theory by assuming the contact time of all eddies is given by a gaussian residence time distribution. Danckwerts supposes that probability of an eddy at the surface being replaced by a fresh eddy is independent of the age of the surface eddy.

The average mass transfer flux of species A is then given by:

$$N_A = k_C(C_{Ai} - C_{Ab}) = \sqrt{D_{AB}s}(C_{Ai} - C_{Ab}) \tag{1.9}$$

where

$$s = 1/\sqrt{t}\,, \tag{1.10}$$

the fractional rate of surface renewal. So, surface renewal theory, like penetration theory, also supposes that the mass transfer coefficient is proportional to the square root of the diffusivity. However, estimation of s is just as difficult as t_c in penetration theory.

1.2.1.5 Film-Penetration theory

Toor and Marchello (1958) modified the film, penetration and surface renewal theories to develop a film-penetration theory (Fig 1.8). This theory predicts a dependency of the mass transfer coefficient, k_c, on the diffusivity, that varies from $\sqrt{D_{AB}}$ to D_{AB}. Film-penetration theory assumes that the entire resistance to mass transfer resides in a film of fixed thickness δ. Eddies move to and from the bulk fluid and this film. Age distribution for time spent in the film is of the Higbie or Danckwerts type.

The average mass transfer flux of A is given by:

$$N_A = (C_{Ai} - C_{Ab})\left(\frac{D_{AB}}{\delta}\right)\left[1 + 2\sum_{n=1}^{\infty}\frac{1}{\left(1 + n^2\pi^2\frac{D_{AB}}{s\delta^2}\right)}\right] \tag{1.11}$$

Hence, film-penetration theory predicts that:

$$k_c = \left(\frac{D_{AB}}{\delta}\right)\left[1 + 2\sum_{n=1}^{\infty}\frac{1}{\left(1 + n^2\pi^2\frac{D_{AB}}{s\delta^2}\right)}\right] \tag{1.12}$$

For a high rate of surface renewal, $\frac{s\delta^2}{D_{AB}}$, film-penetration theory reduces to the surface renewal theory. For low rates of renewal, the theory reduces to film theory. At conditions in between, k_c is proportional to D_{AB}^n, where n is in the range of 0.5 to 1.0 (Henley and Seader, 1998). However, estimation of s and δ is rather difficult, but the dependence on molecular diffusivity brackets experimental data (Henley and Seader, 1998).

1.2.2 Liquid-solid mass transfer theories

Fluid-solid mass transfer phenomena is best described using the boundary layer theory. A thorough explanation of this theory is given by Levich (1962), Skelland (1974), Schlichting (1979), Welty *et al.* (1984) and Bird *et al.* (2002).

Boundary layer theory applies to dilute solutions in laminar flow. The flow near the solid is divided into two distinct regions, the flow near the solid wall which is within the boundary layer where the pressure gradient is non-existent and inviscid flow away from the wall driven by pressure gradient.

The generalized equations of change of concentration within the boundary layer are then formulated. Boundary conditions at the edge of the boundary layer and at the fluid-solid interface are then formulated, and the resulting two-dimensional partial differential equation is solved. This is best solved using computational fluid dynamics routines.

1.3 Mass transfer correlations for CD columns

Correlations in literature for vapour-liquid mass transfer in distillation trays (Savkovic-Stevanovic, 1992; Billet and Shultes, 1993; Chen and Chuang, 1994, 1995), and liquid-solid mass transfer in trickle bed reactors (Onda *et al.*, 1968; Satterfield *et al.*, 1978; Krishna and Standart, 1979; Zhukova *et al.*, 1990; Sims *et al.*, 1993) are not applicable to CDs because of the unique catalyst packing geometry and that in CD operations the liquid is boiling in addition to the reaction present.

Zheng and Xu (1992*a*), and Huang *et al.* (1998*b*) reported both gas and liquid phase mass transfer coefficients in the reaction section of a CD column, however these correlations are packing dependent. Their mass transfer studies were carried out at atmospheric pressure, and so far no studies have been performed on mass transfer in a CD column at elevated pressures. Yet industrial operations carried out in a CD column, such as hydrogenation of benzene, are operated at elevated pressures.

1.3.1 Gas-liquid mass transfer

There are two experimental methods for determining gas-liquid mass transfer coefficients:

- Distillation method, usually under total reflux, in which a closely boiling mixture is boiled off, and the exiting compositions are determined from which the gas-phase mass transfer coefficient is determined, and
- Absorption method, in which a gas (for example air) is absorbed by a system with a large equilibrium constant, such as carbon dioxide in water, when measuring overall liquid-film mass transfer coefficient. A gas (for example air) absorbed by a system, such as ammonia in water, with small equilibrium constant may be employed to measure overall gas-film mass transfer coefficient.

1.3.1.1 Experimental evaluation.

Huang *et al.* (1998*b*) measured the overall vapour-liquid mass transfer in a batch CD column under total reflux at 101.3 kPa using ethanol/1-propanol, 2-propanol/1-propanol and n-hexane/1-hexene.

The mass transfer data was compared to the flow conditions using the Chilton-Colburn correlation:

$$j_G = \frac{Sh_G}{\mathrm{Re}_G\, Sc_G^{1/3}} = c_1 \mathrm{Re}_G^{c_2} \tag{1.13}$$

where,

$$Sh_G = K_Y a / C D_G \tag{1.14}$$

$$\mathrm{Re} = d_P v_G \rho_G / \mu_G \tag{1.15}$$

$$Sc_G = \mu_G / \rho_G D_G \tag{1.16}$$

Huang and co-workers (1998*b*) defined d_P as the diameter of the packing, C is the gas-phase concentration, K_Y is the overall gas-phase mass transfer and a is the interfacial area for mass transfer per unit height of packing.

The Chilton-Colburn correlation is normally used for local mass transfer coefficients. However, in a distillation process, the concentration of the lower

boiling component in the vapour at the vapour-liquid interface is greater than that in the vapour stream. As a result, there is a net diffusion of the lower boiling component away from the liquid surface. Chilton and Colburn (1935) assumed that the continual evaporation of liquid and condensation of vapour at the interface proceed at a higher rate such that the surface layer of vapour is always in equilibrium with the liquid, and therefore resistance to mass transfer lies in the gas phase. Hence, it is reasonable to assume that from two-resistance theory the gas phase resistance is essentially equal to the overall resistance. However, Welty *et al.* (1984) warn that the assumption of negligible interfacial resistance has not been adequately verified. It is also stated that many investigators have shown that a resistance does exist if dust particles or other foreign particles are carried by the liquid phase.

The estimated correlation parameters are provided in Table 1.1:

Table 1.1: Overall mass transfer coefficient parameters (Huang *et al.*, 1998*b*)

Parameter	Ethanol/1-propanol	1-hexene/n-hexane
C_1–reactive section	0.484	0.54
C_2 – reactive section	-0.212	-0.215
C_1–non-reactive section	0.555	1.288
C_2–non-reactive section	-0.013	-0.117

$$Sh_G = C_1 \mathrm{Re}_G^{C_2+1} Sc_G^{1/3}$$

Subawalla *et al.* (1997) have studied gas-liquid mass transfer in a 5.3 cm CD column operated under total reflux using two systems, cyclohexane/n-heptane and acetone/methyl ethyl acetone, at 138 and 241 kPa. The column was packed with a combination of Sulzer-BX and catalytic bale packing filled with Amberlyst-15 catalyst. Bravo *et al.* (1985) have studied mass transfer in gauze-type Sulzer–BX packings in a 25 and 50 cm CD columns at 101.3 kPa under total reflux. The systems used included the ortho/para-xylenes, methanol/ethanol, ethylene/propylene glycol and ethylbenzene/styrene. In both cases the gas phase mass transfer coefficients were calculated using the wetted-wall formulation of Johnstone and Pigford (1942):

$$Sh_G = a_1 \mathrm{Re}_G^{a_2} Sc_G^{1/3} \qquad (1.17)$$

where,

$$Sh_G = k_G d_{eq} / D_G \tag{1.18}$$

$$\mathrm{Re}_G = \left(d_{eq}\rho_G / \mu_G\right)\left(U_{g,eff} + U_{L,eff}\right), \tag{1.19}$$

and d_{eq} is the equivalent diameter of channel and U_{eff} is the effective velocity which takes into account liquid/gas holdup. The following definitions were adopted:

$$U_{g,eff} = \frac{u_V}{(\varepsilon - h_L)} \tag{1.20}$$

$$U_{L,eff} = u_L / h_L \tag{1.21}$$

where h_L is the total liquid holdup for the packing and ε is the void fraction of the column. The estimated correlation parameters are listed in Table 1.2:

Table 1.2: Gas-phase mass transfer correlation parameters in Equation (1.17)

Author	a_1	a_2
Subawalla *et al.*(1997)	0.054	0.8
Bravo *et al.*(1985)	0.0338	0.8

$Sh_G = a_1 \mathrm{Re}_G^{a_2} Sc_G^{1/3}$

Bravo and co-workers claim that the mass transfer model in Equation (1.17) fitted the experimental data set with an average deviation of 14.6%, and 90 % of the points fell within ±25%.

In both cases, the liquid film mass transfer coefficient was calculated using penetration theory (Higbie, 1935):

$$k_L = 2\left(\frac{D_L}{\pi t_C}\right)^{1/2} \tag{1.22}$$

with contact time defined as

$$t_C = d_h / \left(U_{g,eff} + U_{L,eff}\right) \tag{1.23}$$

where d_h is the hydraulic or channel diameter. In both cases, it was assumed that the interfacial area is equal to the total surface area of the packing. Bravo

and co-workers (1985) also found that the liquid-side mass transfer resistance was very small.

Zheng and Xu (1992*a*) carried out vapour-liquid mass transfer in a flow-through fixed bed reactor packed like a CD column at 101.3 kPa and 25 °C, measuring both the gas film mass transfer and the liquid film mass transfer coefficients using the absorption procedure as opposed to the distillation method employed by Huang and co-workers (1998*c*) and Subawalla and co-workers (1997). The gas phase consisted of air with a little ammonia being absorbed by 1N H_2SO_4 when the gas film mass transfer coefficient was measured, while pure CO_2 was absorbed by Na_2CO_3-$NaHCO_3$ buffer solution when the liquid film mass transfer coefficient was measured. Kolodziej *et al* (2001) measured mass transfer coefficients for the gas and liquid phases in a 250 mm ID CD column packed with MULTIPAK® structured packings. They performed absorption experiments using the carbon dioxide-air-water system, when measuring liquid-phase mass transfer coefficient, and ammonia-air-water system when measuring gas-phase mass transfer coefficient.

The gas-film mass transfer data was then correlated to the flow conditions using the following correlation:

$$Sh_G = d_1 \mathrm{Re}_G^{d_2} \mathrm{Re}_L^{d_3} Sc_G^{d_4} \tag{1.24}$$

where Zheng and Xu (1992*a*) defined the dimensionless groups as:

$$Sh_G = k_G a d_p RT / a_t D_G \tag{1.25}$$

$$\mathrm{Re} = 4v\rho / a_t \mu \tag{1.26}$$

whereas Kolodziej and co-workers (2001) used the definitions:

$$Sh_G = K_G d_e / \delta_G \tag{1.27}$$

$$Sh_L = K_L \upsilon_Z / \delta_L \tag{1.28}$$

$$Sc = \mu / \delta M \tag{1.29}$$

$$\mathrm{Re} = G d_e / \varepsilon \mu \tag{1.30}$$

Kolodziej and co-workers (2001) defined G as the mass superficial velocity, δ is the dynamic diffusivity, M is the molecular mass, and υ_Z is the equivalent linear dimension.

$$\upsilon_Z = \left(\eta^2/\rho^2 g\right)^{1/3} \tag{1.31}$$

where η is the dynamic viscosity and g is the acceleration of gravity. The parameters in the correlation are listed in Table 1.3.

Table 1.3: Gas-film mass transfer coefficient parameters in Equation (1.24)

Author	d_1	d_2	d_3	d_4
Zheng and Xu (1992*a*)	1.072×10^{-3}	0.92	0.24	0.5
Kolodziej *et al* (2001)	0.126	0.536	0.241	0.33

$$Sh_G = d_1 \,\mathrm{Re}_G^{d_2}\, \mathrm{Re}_L^{d_3}\, Sc_G^{d_4}$$

Equation (1.24) indicates that the gas-phase mass transfer coefficient increases with increasing liquid and gas velocities.

The liquid-film mass transfer data were correlated to the following correlation:

$$Sh_L = w_1 \,\mathrm{Re}_L^{w_2}\, \mathrm{Re}_G^{w_3}\, Sc_L^{w_4} \tag{1.32}$$

The parameters in the correlation are listed in Table 1.4:

Table 1.4: Liquid-film mass transfer coefficient parameters in Equation (1.32)

Author	w_1	w_2	w_3	w_4
Zheng and Xu (1992*a*)	0.149	0.3	0	0.5
Kolodziej *et al* (2001)	2.1×10^{-3}	0.636	0.190	0.5

$$Sh_G = w_1 \,\mathrm{Re}_G^{w_2}\, \mathrm{Re}_L^{w_3}\, Sc_L^{w_4}$$

The results in Table 1.4 clearly indicate that the liquid-film mass transfer coefficient increases with increasing liquid velocity. The results of Kolodziej and co-workers suggest that the liquid-film coefficient also increases with increasing gas velocity, however those of Zheng and Xu (1992*a*) suggest that it is independent of the gas velocity.

1.3.1.2 Comparison of correlations.

In a wetted-wall column, the gas-phase mass transfer coefficient is directly proportional to $\mathrm{Re}_G^{0.83}$ (Welty *et al.*, 1984), where

$$\mathrm{Re}_G = d_C v\rho/\mu \tag{1.33}$$

and d_C is the diameter of the column. This agrees with Equation (1.13) and (1.17), but this correlation disagrees with the data obtained. So, clearly the wetted-wall correlation agrees with the gas-phase coefficient measured using the distillation procedure as opposed to the absorption method. The discrepancy between wetted-wall and CD correlations is partly due to the increased mass transfer rates inherent in CD operations.

The liquid-phase mass transfer coefficient is proportional to $\mathrm{Re}_L^{0.4}$ (Welty *et al.*, 1984), where

$$\mathrm{Re}_L = 4\Gamma/\mu \tag{1.34}$$

and Γ is the mass flow rate of liquid per unit wetted perimeter. This correlation disagrees with data obtained as represented by Equation (1.32). The liquid-phase coefficient cannot be obtained from the distillation procedure as a negligible liquid-film resistance is assumed in this procedure, and therefore comparison is unwarranted.

1.3.2 Liquid-solid mass transfer

According to Satterfield (1975), liquid-solid mass transfer resistance is significant when the following relation is satisfied:

$$\left(10d_p/c_s\right) r\left(1-\varepsilon\right) > k_S \tag{1.35}$$

where d_p is the particle diameter, r is the rate of reaction, ε is the bed void fraction, k_S is the liquid-solid mass transfer and c_s is the concentration of the transferring species at saturation.

Therefore, the liquid film around the catalyst particles becomes the controlling resistance for either of the following situations:

- Highly active catalysts or fast reactions, and/or

- Large catalyst particles.

Hydrogenation reaction is a relatively fast reaction and comparatively large catalyst pellets (typically 3mm by 3mm) are used in CD operations, and therefore it is important to investigate liquid-solid mass transfer.

1.3.2.1 Experimental evaluation.

There are three predominant methods for the measurement of mass transfer coefficients between liquid and solid. These are (Zheng and Xu, 1992*a*):

- determination of the solubility in liquid phase for granules of a sparingly soluble solid,
- determination of electrochemical reaction rate, and
- determination of the reaction rate for a mass transfer controlled reaction.

The dissolution method is most widely used as it can also be used to measure the liquid-solid wetting efficiency for the packing. However, there are practical problems associated with this method. The solid can evaporate from the liquid phase into the gas phase either within the reactor or when sampling/analysing. Hence, the liquid solution being analysed may contain lower solid concentration than it should be. This was confirmed by Al-Dahhan *et al.* (2000) in the dissolution of naphthalene in water.

Huang and co-workers (1998*b*) studied the liquid–solid mass transfer in a CD column using a benzoic acid/water/air system at 25 °C and 100 kPa, while Zheng and Xu (1992*a*) used a naphthalene/water/air system at similar conditions. Huang and co-workers (1998*b*) took the non-ideal flow pattern into account by performing tracer experiments. The dispersion numbers obtained ranged from 0.008 at low gas/liquid flow rates to 0.031 at high gas/liquid flow rates. This clearly indicates that at low flow rates plug flow approximation, assumed in the mass balance for calculation of mass transfer coefficients, is acceptable. At high flow rates, however, there is deviation from plug flow. The mass transfer coefficient was then correlated with the flow conditions using the following equation:

$$j_D = \frac{k_S a}{d_P v_L}\left(\frac{\mu_L}{\rho_L D_{LS}}\right)^{2/3} = b_1 \mathrm{Re}_L^{b_2}\,\mathrm{Re}_G^{b_3}, \qquad (1.36)$$

where D_{LS} is the diffusivity of benzoic acid in water. Huang and co-workers (1998*b*) defined Re as $\frac{d_P v \rho}{\mu}$ where d_P is the diameter of the packing and v is the fluid superficial velocity while Zheng and Xu (1992*a*) defined Re as $\frac{4v\rho}{a_t \mu}$ where a_t is the specific surface of packing. The estimated parameters for liquid – solid mass transfer are listed in Table 1.5:

Table 1.5: Overall mass transfer correlation parameters

Parameter	Huang *et al.* (1998*b*)	Zheng and Xu (1992*a*)
b_1	48.163	0.586
b_2	-0.608	-0.28
b_3	-0.103	-0.27

$$\frac{k_S a}{d_P v_L}\left(\frac{\mu_L}{\rho_L D_{LS}}\right)^{2/3} = b_1 \mathrm{Re}_L^{b_2}\,\mathrm{Re}_G^{b_3}$$

The results in Table 1.5 clearly indicate that at fixed liquid velocity, the liquid-solid mass transfer coefficient decreases with increasing gas superficial velocity. Conversely, at fixed gas velocity, the mass transfer coefficient increases with increasing liquid velocity.

1.3.2.2 Comparison of correlations.

Most experimental liquid-solid mass transfer correlations found in literature (McCune and Wilhelm, 1949; Linton and Sherwood, 1950; Williamson *et al.*, 1963) are for single-phase flow over packed beds, and are therefore inapplicable to CD operations. Those that were obtained for two-phase flow (Morsi *et al.*, 1984; Rode *et al.*, 1994; Sedahmed *et al.*, 1996; Highfill and Al-Dahhan, 2001) were, however, mostly applicable in TBR operations where the liquid/gas flow is not countercurrent

The results in Table 1.5 clearly indicate that Zheng and Xu (1992*a*) predict higher mass transfer coefficient for a given flow rate than Huang and co-workers. The discrepancy is partly attributed to the following reasons:

- Wall effect. Huang used only one catalyst bag while Zheng and Xu used many tiny bags, and therefore a large proportion of liquid by-pass occurs in Huang's case. The use of many catalyst bags also promotes the total mass transfer area per unit height of packing.
- Zheng and Xu used small solid particles than Huang, and therefore had a significant amount of flow passing through the bags of catalyst.

Nevertheless, the two empirical correlations indicate a sensitive relationship between mass transfer coefficient, $k_S a$ and liquid phase Reynolds number. Huang's correlation shows that $k_S a$ is proportional to $(\mathrm{Re}_L)^{0.392}$, but Zheng and Xu shows that $k_S a$ is proportional to $(\mathrm{Re}_L)^{0.72}$. Both correlations indicate similar relationship between $k_S a$ and vapour flow rate.

It must be pointed out that Zheng and Xu did not carry out dispersion studies to check their assumption of plug flow behaviour. In addition, no effort was made to carry out gas analysis to determine the amount of naphthalene absorbed by the air stream. It is important to bear in mind that a comparatively small amount of the solid is absorbed into the liquid phase as it is absorbed into the gas phase. Therefore, it is possible that the mass transfer coefficient was not accurately measured.

1.4 Effect of pressure and temperature on mass transfer coefficients

1.4.1 Gas-phase mass transfer

From film theory (cf. Equation (1.2)):

$$k_G = \frac{D_{AB}P}{\delta_G RT} \tag{1.37}$$

Since $D_{AB}P$ is relatively independent of the pressure, then k_g is independent of the total pressure of the system.

The gas phase diffusivity is inversely proportional to the total pressure, and the gas viscosity is not dependent on pressure (Reid and Prausnitz, 1977). The ideal gas law indicates that the gas phase density and concentration are both directly proportional to pressure. Therefore Equation (1.13) indicates that the gas-phase mass transfer coefficient is not dependent on the total pressure, which agrees with the film theory.

As Equation (1.13), (1.17) and (1.24) suggest, the gas-phase mass transfer coefficient depends on the Reynolds and Schmidt number. The gas-phase viscosity varies with temperature as follows:

$$\mu_G \propto T^{1/2} \tag{1.38}$$

From ideal gas law model:

$$\rho \propto T \tag{1.39}$$

The gas-phase diffusivity is expressed as follows (Welty *et al.*, 1984):

$$D_G \propto T^{3/2} \tag{1.40}$$

Therefore from Equation (1.13):

$$k_G \propto T^{(3C_2-4)/6} \tag{1.41}$$

which indicates a strong dependency to gas-phase temperature.

1.4.2 Liquid-phase mass transfer

According to the Wilke-Chang correlation (Welty *et al.*, 1984), the liquid-phase diffusivity is independent of the total pressure. Therefore, from equation (1.22), k_L is independent of pressure.

According to the Wilke-Chang correlation (Welty *et al.*, 1984) the liquid-phase diffusivity is directly proportional to the temperature. Therefore, from Equation (1.22):

$$k_L \propto T^{1/2} \tag{1.42}$$

which shows a dependency on liquid-phase temperature.

1.4.3 Liquid-solid mass transfer

According to Reid and Prausnitz (1977), the liquid viscosity is independent of pressure. Therefore Equation (1.36) suggests that:

$$k_S \propto P_G^{a_3} \tag{1.43}$$

Hence, the liquid-solid mass transfer is dependent on the gas-phase pressure.

The liquid-phase viscosity is expressed in terms of the Andrade correlation (Reid and Prausnitz, 1977):

$$\mu_L \propto e^{1/T} \tag{1.44}$$

The liquid density is not a strong function of temperature (Reid and Prausnitz, 1977), and therefore Equation (1.36) indicates that k_S is a strong function of temperature.

1.5 The hydrogenation reaction

1.5.1 Mechanism

There are three steps involved in the hydrogenation of an alkene in the liquid phase on a heterogeneous catalyst:

1) the transport of gaseous hydrogen into the liquid phase and the diffusion of hydrogen and the alkene through the solution to the catalytic surface,
2) the chemisorption of these reactants, their reaction at the catalyst surface, and their associative desorption as product, and
3) the diffusion of the product away from the catalyst.

The detailed mechanism, the Horiuti-Polanyi mechanism, for the hydrogenation of olefins in general has been well investigated (Bond, 1962; Augustine, 1965; Kieboom *et al.*, 1977).

1.5.2 Kinetics

Boutonnet *et al.* (1980) studied hydrogenation of 1-hexene over platinum catalyst supported on alumina at 30 and 50 °C and 0.9 atm hydrogen

pressure. The amount of n-hexane formed in the reaction showed a direct linear relationship with time elapsed, indicating that the reaction is of zero-order with respect to 1-hexene and first order with respect to hydrogen. The intrinsic reaction rate was therefore assumed to be directly proportional to the hydrogen pressure.

The reported activation energy for the reaction was 21.5 kJ/mol. Further experimental work by Boutonnet and co-workers showed that the reaction was not diffusion controlled, and hence this was the true activation energy. The reaction rate constant extracted from the data reported is:

$$k(T) = Ae^{-E/RT} \tag{1.45}$$

where A = 1807.04 1/s and E = 21.5 kJ/mol.

Carturan and Scrivanti (1979) also studied hydrogenation of 1-hexene over saline hydride-reduced palladium catalyst at 25 °C and 1 atm hydrogen pressure. Their results also indicated first order dependence of the reaction rate on hydrogen pressure. However, the experimental data presented was not adequate to work out reaction rate parameters. No credible studies of hydrogenation of 1-hexene over Nickel/Alumina catalyst were found in literature.

1.6 Effect of chemical reaction on mass transfer

1.6.1 Gas-liquid mass transfer

The effect of heterogeneous reaction on gas phase mass transfer for two phase, countercurrent flow, as is the case in a CD column, has received little consideration. Mass transfer process at the vapour-liquid interface is best described by the generalised Maxwell-Stefan approach (Sundmacher and Hoffman, 1996). Barbosa and Dorhety (1988) studied the effect of equilibrium chemical reactions on vapour-liquid equilibrium and homogeneous (reactive) distillation processes using reactive-phase diagrams and residue maps. They found that chemical reactions can either create or break distillation boundaries depending on the equilibrium constant. In this study, the effect of

heterogeneous chemical reaction on gas-liquid mass transfer process would be investigated.

1.6.2 Liquid-solid mass transfer

The effect of heterogeneous reaction on liquid-solid mass transfer in a two-phase countercurrent mode, as is the case for CD operations, has received little attention thus far. Higler *et al.* (2000) developed a nonequilibrium model for heterogeneous CD process for simulating the production of MTBE and TAME in which simultaneous mass transfer and equilibrium chemical reaction inside the catalyst particle were taken into account. Liquid-solid mass transfer inside the porous catalyst particles were described using the dusty fluid model. Simulation of a MTBE CD process showed that the overall conversion, i.e. global rate of reaction, was affected by the mass transfer resistance inside the porous catalyst. The introduction of extra mass transfer resistance led to the observed drop in the maximum conversion. This is supported by the observations of Higler *et al.* (1999).

Simulation of a TAME CD process showed that the overall conversion is not affected significantly by the mass transfer resistance inside the porous catalyst. Hence, the MTBE process is relatively sensitive to mass transfer resistances whereas the TAME process is not. A possible reason for this contradiction is that the TAME reaction rate is much lower than that for the MTBE process. The forward reaction rate constant for TAME is about an order of magnitude lower than that for the MTBE process. Therefore, the production rate of TAME will be much less sensitive to changes in the mass transfer resistance.

Higler *et al.* (2000) also developed the so-called 'dusty fluid model' for modelling diffusion and equilibrium reaction inside the catalyst particles, obtained by modifying the 'dusty gas model' developed by Krishna and Wesselingh (1997). The mass transfer from the liquid bulk to the catalyst phase (solid phase) is described by the correlation of Van Krevelen and Krekels (1948):

$$\frac{k_{i,j}^{LS}}{D_{i,j}^{L} a_P} = 1.8 \left(\frac{\rho \cdot u}{\mu \cdot a_P} \right)_L^{1/2} \left(\frac{\mu}{\rho D_{i,j}} \right)_L^{1/3} \tag{1.46}$$

where,

$$0.013 < \left(\frac{\rho \cdot u}{\mu \cdot a_P} \right)_L < 12.6 \tag{1.47}$$

It is common knowledge that in distillation operations the superficial liquid velocity, u_L, is much higher than in conventional reactors. With increased velocities, and with all else equal, Equation (1.46) predicts that the liquid-solid mass transfer is enhanced.

1.7 Project aims and hypotheses

The aim of this project is to evaluate experimentally the overall vapour/liquid mass transfer coefficient, and to develop a simple model for evaluating the effect of chemical reaction on the overall vapour/liquid mass transfer coefficient.

Following the extensive literature review, the following hypotheses are made:

- The overall vapour/liquid mass transfer coefficient increases with increasing vapour or liquid flow rate.
- The catalytic chemical reaction will affect the vapour-liquid mass transfer rate. Since the hydrogenation reaction is fast, the gas phase mass transfer will be the controlling step. Hence, a larger vapour-liquid mass transfer will be observed in the presence of hydrogenation.

2. EXPERIMENTAL PROCEDURE

2.1 Apparatus.

A simple distillation device shown in Fig 2.1 was set up to determine the overall gas-phase mass transfer coefficients. The column was made of stainless steel type 316. The column diameter was 5 cm and the packed height was 50 cm. The reboiler holds about 0.5 litre of liquid feed while the condenser has a capacity of 1 litre. There was a 60 cm long tube with 2 cm internal diameter leading to the condenser. This tube was heated to temperatures around 100 °C to maintain vapour into the condenser and to eliminate condensation prior to the condenser. A Voltac variable transformer (Yokohama electric works Ltd) was used to provide variation in reboiler settings. The reboiler duty was controlled by manually adjusting the voltage applied to the reboiler heater. The column was operated at the heat duties shown in Table 2.1.

Table 2.1: Heat duties for operation of a CD column.

Reboiler power [W]	Boil-up rate [mmol/s]	Cooling rate [l/hr]	Inlet temperature [°C]	Exit temperature [°C]	Condenser duty [W]
50.62	1.77	230	-5	15	5386.3
43.65	1.53	185	0	25	5386.7
37.19	1.30	150	0	24	4194.3
31.25	1.09	100	2	30	3254.1
25.83	0.90	80	5	32	2506.6
20.92	0.73	50	5	35	1739.3

Although the boil-up rates listed in Table 2.1 seem to be small, they are typical flow rates used in laboratory CD column apparatus as used by, amongst others, Aiouache and Goto (2003) and Huang *et al* (1998*b*).

Since the operation was at total reflux, then the reflux rate (or the liquid flow rate) in the absence of chemical reaction was equal to the vapour boil up rate.

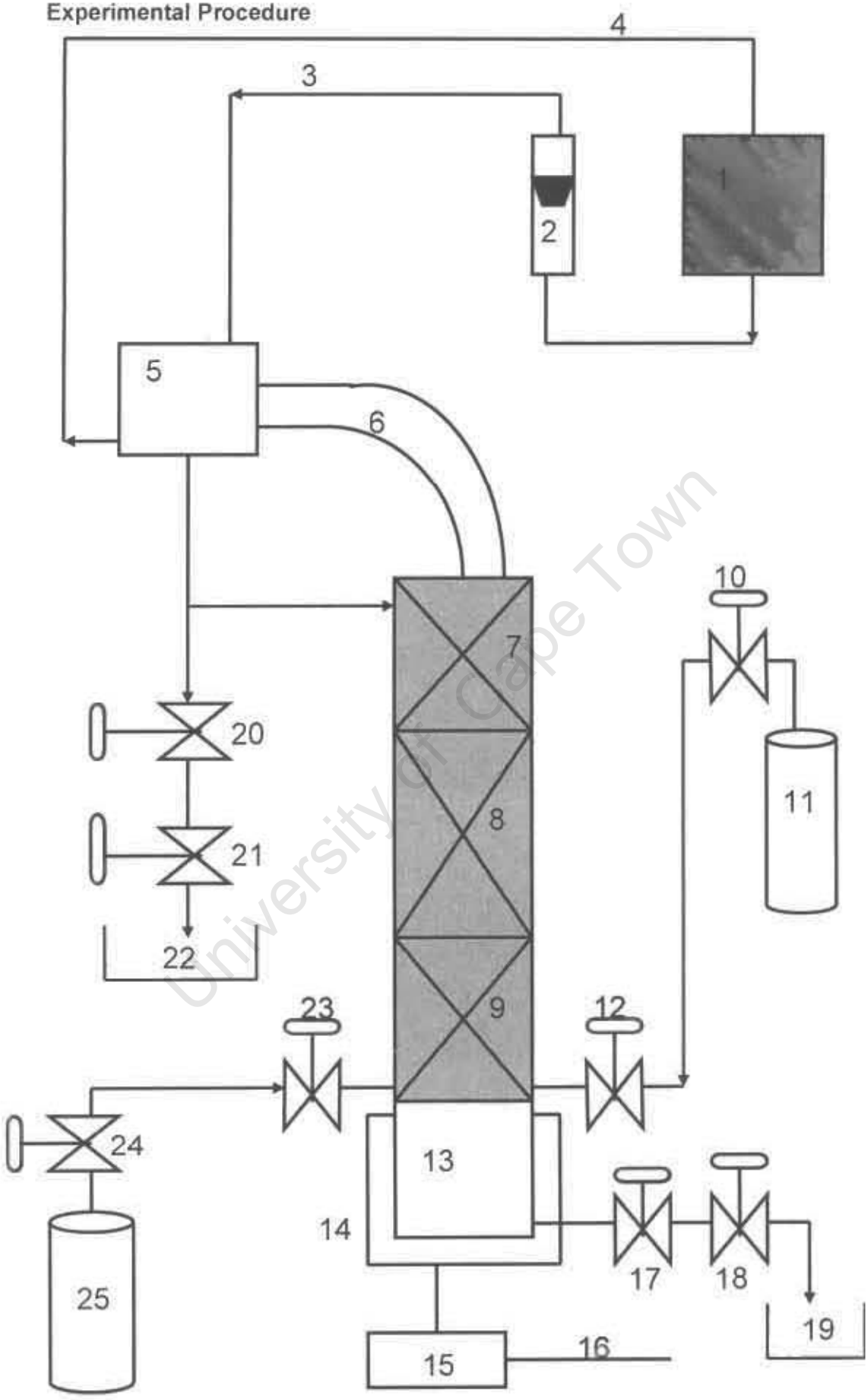

Fig 2.1: Experimental flowchart for a bench-scale CD column.
1. Ethylene Glycol bath; 2: Flow rotameter; 3. Cooling water in; 4. Cooling water out; 5. Condenser; 6. Condenser arm; 7. Sulzer BX packing; 8. Catalytic packing; 9. Sulzer BX packing; 10. Control flow valve; 11. H_2 gas cylinder; 12. Flow valve; 13. Reboiler; 14. Reboiler heating jacket; 15. Transformer; 16. Power input/source; 17. Needle valve; 18. Flow valve; 19. Reboiler sample collector; 20. Needle valve; 21. Flow valve; 22. Condenser sample collector; 23. Flow valve; 24. Control flow valve; 25. N_2 cylinder.

Operation at total reflux in the absence of chemical reaction also facilitated a steady-state operation and eliminated uncertainties in knowing the reflux ratio exactly.

For the gas-phase mass transfer in the presence of hydrogenation reaction, the reflux rate was not equal to the vapour boil up rate due to the presence of stagnant H_2 gas. The estimated reflux rates are shown in Table 2.2. The reflux rates were based on the diffusion rate of n-hexane through the stagnant hydrogen gas in the condenser. The resulting reflux rates were too low compared to the boil-up rate which might have resulted in incomplete wetting of the catalyst. This would have resulted in side reactions, such as gas-phase reactions and cracking.

Table 2.2: Estimated reflux rates in the column during hydrogenation

Reboiler duty [W]	Condenser duty [W]	Boil-up rate [mmol/s]	Reflux rate [mmol/s] $\times 10^3$
50.62	5386.3	1.77	3.01
43.65	5386.7	1.53	2.16
37.19	4194.3	1.30	1.70
31.25	3254.1	1.09	1.54
25.83	2506.6	0.90	1.39
20.92	1739.3	0.73	1.15

Sasol Alpha Olefins, Sasolburg, R.S.A supplied liquid 1-hexene with 99% purity, while n-hexane with 99% purity was supplied by Aldrich, Cape Town, R.S.A. A Gefran 500 temperature controller was used to maintain and control

the temperatures at the packed and condenser arm sections. A WIKA pressure gauge with ratings 0 – 30 bar(g) was located at the condenser inlet and a similar gauge was located at the distillation section, just above the reboiler.

2.2 Catalyst

2.2.1 Catalyst physical properties

The catalyst used for these experiments was KL6560-TL2.5 (Kata-Leuna, CRI, Houston, Texas, U.S.A). The catalyst was composed of approximately 18 wt % nickel on an alumina support. The catalyst properties, as supplied by the manufacturer, are provided in Table 2.3:

Table 2.3: Catalyst properties

Nickel content	Approximately 18	Weight %
Alumina content	Approximately 82	Weight %
Bulk density	650 – 750	kg/m^3
Average length	4	Mm
BET-surface area	120 – 140	m^2/g
Pore volume	0.48 – 0.56	cm^3/g
Side crush strength	≥ 12	N/mm
Approximate diameter	2.5	Mm

The catalyst was held inside a stainless steel wire mesh 'sausage' bags (100 mesh). Each bag was approximately 2 cm in diameter and 20 cm long. 10 g of catalyst was loaded into each of the two catalyst bags, and the bags were then sewn closed at the top. The other three catalyst bags were filled with inert glass beads. The five bags were wrapped with demister wire to bring the diameter up to 5 cm, and thus ensuring that no dead volume is left within the reactive zone. The wrapped structure was then inserted into the middle section of the distillation column. The demister wire provided a high internal gas voidage in the reactive section of the column. This high gas voidage ensured a low pressure-drop in the reactive zone of the column.

2.2.2 Catalyst wetting efficiency

So far no studies on the external catalyst wetting efficiency in a CD system have been carried out. For the purposes of the experimental work, it was assumed that the specific surface packing, a_P, was equal to the wetted area of the catalyst packing, a_W.

2.2.3 Catalyst activation procedure

Considering that the CD operates in a batch mode, the activation procedure provided by the manufacturer meant for flow reactor systems was altered slightly. The activation procedure followed is as follows:

Firstly, the system was purged with nitrogen. Hydrogen at the system pressure of 1 – 5 bar(g) was introduced into the column. The catalyst bed temperature was increased to 120 °C, at 1 °C/min, and this temperature was maintained for about 1 hour. The temperature was then increased to 230 °C at a rate of 100°C/hr, maintaining this temperature for a further hour. At this stage the reduction water will have ceased to occur and would have evaporated into the gaseous phase. Then hydrogen together with the evaporated reduction water was purged from the system by simply opening the valve at the condenser outlet. Precaution was taken to ensure that no air was sucked back into the column by purging with nitrogen. The oxygen in the air can affect the catalyst at higher temperatures due to oxidation. The system was then cooled down to the run temperature. The catalyst was then activated and ready for use. Whenever not in use, 5 bar (g) positive nitrogen pressure over the catalyst was maintained.

2.2.4 Liquid and gas holdup in the catalyst packing

The liquid holdup plays an important role in CD hydrodynamics and mass transfer. Liquid holdup also affects the catalyst wetting efficiency, which, in turn, affects the reaction selectivity depending on whether the reaction takes place solely on the wetted catalyst area or on dry and wetted catalyst areas alike. The liquid holdup is made up of the static and dynamic holdup. The total liquid holdup is essentially the reaction volume, and therefore it is important to keep the liquid holdup as high as possible without flooding the column.

The dynamic liquid holdup correlation below the flooding point developed by Xu *et al* (1997) is given by:

$$h_d = a u_G^b u_L^c \qquad (2.4)$$

where $a = 0.0336$, $b = 0.0109$ and $c = 0.429$. This shows a strong dependence of the dynamic liquid holdup on the liquid superficial velocity than on the gas velocity. It is therefore important to keep the liquid superficial velocity as high as possible. At low liquid velocities, the liquid holdup can become so small that the packing can be incompletely wetted.

2.3 Non-catalytic packings

2.3.1 Geometric properties.

The non-reactive zones located above and below the reactive zone were filled with Sulzer-BX packing (Bravo *et al.*, 1985). The length of each packing was 16 cm. The packing above the catalyst zone was intended to distribute the liquid over the catalyst bag, and thereby mimic the operation of a large pilot-scale CD column.

The geometric information concerning the Sulzer BX packing is listed in Table 2.4:

Table 2.4: Geometric data for Sulzer BX packing

Void fraction, ε	0.9
Packing surface area, a_p [m^2/m^3]	492
Crimp height, h [mm]	6.4
Channel base, B [mm]	12.7
Channel side, S [mm]	8.9
Hydraulic radius, r_h [mm]	1.8
Equivalent diameter, d_{eq} [mm]	7.2
Channel flow angle from horizontal, degrees	60

The Sulzer metal BX packing consisted of parallel corrugated sheets. The sheets were installed vertically with the corrugations inclined relative to the axis of the column. For adjacent sheets the angle of inclination was reversed. The packing was self-wetting due to the capillary action of the gauze material.

2.3.2 Liquid and gas holdup.

According to Henley and Seader (1998), to ensure complete wetting of packing, the superficial liquid velocities in a metal type of packing (such as the Koch-Sulzer BX packing used in this study) should exceed 9×10^{-4} m/s. However, in this study this high liquid velocities could not be established due to the limited reboiler duty and the low condenser duty. So, it is clear that the packing was incompletely wetted.

2.4 Operating procedure and conditions.

At the start of each batch CD experiment, a 50:50 mixture of 1-hexene/n-hexane making up 0.5 litres was charged into the reboiler. The entire column, except the condenser, was insulated with ceramic wool to prevent heat loss. The temperature at the distillation section was set to 80 °C while that of the condenser arm was set to 100 °C to ensure that no liquid is formed at the condenser inlet. Cooling water containing 25% ethylene glycol was pumped through the condenser from an Endocal refrigerated bath. A needle valve was used to set the cooling water flow rate between 50 and 220 l/hr. The cooling water flow was estimated using a rotameter. The cooling water temperature, with inlet and exit temperatures shown in Table 2.1, was set to ensure that the condensate would always be supercooled.

Reboiler heating at a set power commenced, and the temperature and pressure reading and product sample was taken from the reboiler and condenser outlets every 1 hour. The sample size taken for analysis at each time interval was approximately 2 ml, and this did not have an impact on the total liquid volume within the column. At the end of each run, the liquid volume in the reboiler was typically in excess of 480 ml.

The sampling time used to determine steady state reached depended on the boil-up rate and was generally determined by the time at which consecutive samples from reboiler and condenser showed no variation with time. Typically the sampling time was approximately 8 hours. The composition of the samples was determined using gas chromatography (GC).

2.4.1 Isomerization of the feed.

Preliminary experiments showed that the olefin feed isomerized on the Ni/Al_2O_3 catalyst. This was probably due to the acidic Al_2O_3 sites present as the support to the catalyst. This was observed by distilling the feed, in the absence of hydrogen using a fully activated catalyst, at total reflux. The undesired 1-hexene isomers start to form after approximately 2 hours of time on stream. Other than 1-hexene isomerization which was the dominant side reaction, cracking, oligomerisation and deactivation reaction products were observed in trace amounts.

Under these conditions of operations, a strategy to reduce the time on stream or residence time of the liquid allowed to wet the catalyst down to 1.5 hours was implemented, and hydrogen was then introduced into the column for the reaction to begin. A heavy component, toluene (boiling point 110 °C) with the known concentration relative to the feed was introduced into the column and the reboiler concentrations were reported relative to this compound. Unfortunately, the composition of the light components at the condenser outlet cannot be accurately measured if liquid sampling is used. With on-line gas sampling and analysis not possible, the reaction rate will therefore be reported in terms of reboiler concentrations. It was assumed that the diffusion rate of the isomers are the same as that of the main product n-hexane and therefore the system remains ternary – consisting of n-hexane, hydrogen and the unreacted 1-hexene. Therefore, the reaction rate measured will not be the true rate, but will be the lumped rate of hydrogenation and isomerization rate combined.

2.4.2 Diffusion of n-hexane in hydrogen

The hydrogen introduced into the column for reaction occupied all the reactor volume and is non-condensable at operating conditions. The main product formed n-hexane diffused through the stagnant hydrogen gas in the 0.5 m condenser arm before condensing back to the main column. Therefore, the question arose as to whether this diffusion rate was fast enough as compared to the liquid molar rate in the main section of the column. Calculations to work out the diffusion rate of n-hexane through the stagnant H_2 were performed based on the following assumptions:

- The 1-hexene isomers formed are lumped together with n-hexane – they are expected to have the same diffusion coefficient and concentration as n-hexane;
- Ideal binary gas mixture between H_2 and n-hexane was assumed;
- The Hirschfelder, Bird and Spotz correlation was used to work out the diffusion coefficient.

The diffusion rate was calculated using the well-known diffusion flux across the condenser:

$$N_A = \frac{cD_{AB}}{(z_2 - z_1)} \ln \frac{(1 - y_{A2})}{(1 - y_{A1})} \tag{2.5}$$

where subscript 1 and 2 denote inlet and exit conditions to the condenser, A represent n-hexane and B is hydrogen gas, c is the gas phase concentration as expressed by ideal gas law, z is the length of the condenser tube and y is the estimated gas phase composition. As shown in Table 2.2, the molar diffusion rate (i.e. reflux rate) through the condenser arm was much slower than the liquid molar flow in the main section of the column. Therefore, this had the following consequences:

- The catalyst wetting was effectively reduced. This caused gas-phase hydrogenation reaction to take place.
- Formation of cracked products as the catalyst was too hot.

There were two options to this problem. Firstly, some of the hydrogen could be vented off. However, the vented hydrogen will also result in the undesired removal of the light components formed from the system. Alternatively, the unreacted hydrogen could be pumped back to the reactive zone. But this

required a complicated set-up as the condensed liquid has to be prevented from being pumped together with hydrogen. This would necessitate a completely new design of the condenser arm. Neither option was used, and the calculated rate of n-hexane diffusion was used as the reflux rate.

2.4.3 Hydrodynamics regimes

Three hydrodynamic regimes are possible for a two-phase gas-liquid flow through a catalyst packing. These are a film regime, a bubble regime and an emulsification regime. The film regime, which is the desired operating regime, occurs below the flooding point. The undesirable operating regimes, bubble and emulsification, occur beyond the flooding point. Therefore, it is clear that the combination of liquid and gas superficial velocities used in this study resulted in operation of the bed in a film regime.

2.4.4 Flooding conditions

What is reassuring is that Xu *et al.* (1997) found that the flooding point is at high gas velocities, with the minimum conditions causing flooding at u_G = 1 m/s and u_L = 1.39 × 10^{-3} m/s. So, it is clear that at all the experimental conditions used in this study, the column did not flood.

2.5 Estimation and control of reflux ratio.

It was important to maintain constant pressure for different vapour and liquid flow rates so that proper studies on mass transfer can be carried out. The maximum power, P_{max}, supplied by the reboiler heater is 500 W, corresponding to 220 V of voltage, V_{max}. Using the basic electrical equations, Equation 2.5 was used to estimate the power input, P_1, at a certain voltage setting, V_1, to the reboiler:

$$P_1 = P_{max}\left(\frac{V_1}{V_{max}}\right)^2 \qquad (2.6)$$

Therefore, Equation 2.6 was used to estimate the reflux ratio given P_1:

$$R = \frac{P_1}{\left[\sum_{i=1}^{N} \Delta H_{vap,i} x_{feed,i}\right]} \quad (2.7)$$

It was assumed that P_1 remains constant during the operation and the resistance was constant with changing temperature.

2.6 Estimation of mass transfer coefficient with chemical reaction.

2.6.1 Gas phase mass transfer

The operation procedure was similar to the case in the absence of hydrogenation reaction with the exception of the following:

The 1-hexene/n-hexane mixture was allowed to reach total reflux, which required about 1.5 hours on stream. The desired column pressure of 1 bar(g) indicated that steady total reflux had been reached. Then hydrogen gas was introduced into the column at the location just below the non-reactive zone, just above the reboiler, bringing the column pressure to a set pressure of 2 bar(g). Hydrogen was the limiting reactant and the olefins provided the excess reactant. The top and bottom concentrations were collected until all the hydrogen gas was consumed.

2.7 Collection and analysis of liquid samples.

It was observed that the liquid collected at the condenser outlet had some gas bubbles in it. Due to the low vapour pressure of 1-hexene and its isomers, these gas bubbles would quickly escape the sample bottle while collecting the sample. Hence, the composition analysed at the condenser outlet might have been slightly underestimated.

The liquid at the reboiler outlet had no visible gas bubbles in it. So the global reaction rate was based on the reboiler outlet composition alone. But the vapour-liquid mass transfer coefficient was estimated from both outlet compositions.

0.5 μl of liquid solution was injected into the column using a SGE syringe. For each sample, the liquid was analysed twice to minimise composition error.

3. THEORETICAL DEVELOPMENTS AND MODELLING

3.1 Theory and Assumptions.

3.1.1. Gas-phase mass transfer coefficient.

3.1.1.1 Non-reacting system

The gas-phase mass transfer is defined in terms of the required height per transfer unit (*H.T.U*) (Chilton and Colburn, 1935):

$$H.T.U = \frac{H}{n} = \frac{G}{K_G a \prod M_m} \tag{3.1}$$

where n is the number of transfer units (Chilton and Colburn, 1935):

$$n = \frac{2.3}{(\alpha - 1)} \log \frac{y_2(1 - y_1)}{y_1(1 - y_2)} + 2.3 \log \frac{(1 - y_1)}{(1 - y_2)} \tag{3.2}$$

where subscripts 1 and 2 indicate reboiler and condenser conditions respectively. The equilibrium relation between y^* and x is expressed in terms of the relative volatility (α) of the components:

$$y^* = \frac{\alpha x}{1 + (\alpha - 1) x} \tag{3.3}$$

It was assumed that α was constant over the distillation range and the mass transfer coefficients and flow rates, G and L, were taken to be constant throughout the column. The assumption of constant α is justified for mixtures with close boiling points and those that do not deviate from Raoult's law (Chilton and Colburn, 1935). This resulted in a constant gas phase mass transfer coefficient across the entire length of the column.

In a batch CD operation, there is a rapid continual evaporation of liquid and condensation of vapour at the vapour-liquid interface, and hence the surface layer of the vapour is always in equilibrium with the liquid (Chilton and Colburn, 1935). Therefore, the gas phase mass transfer resistance usually dominates the overall mass transfer resistance. Huang *et al.* (1998) also confirmed this by modelling the aldol condensation of acetone in a CD column. The Chilton-Colburn j-factor analogy was used to relate the

measured overall mass transfer coefficient to the flow conditions in the column using Equation (1.15). It is important to note that since the column is operated at total reflux, the liquid molar flow rate equals the vapour molar flow rate, and therefore the Reynolds numbers for liquid and vapour phases are dependent on each other. In this study, the Reynolds number for a packed column was defined as (Chilton and Colburn, 1935):

$$\mathrm{Re} = \frac{d_e G}{\mu} = \frac{4G}{a\mu} \tag{3.4}$$

The Schmidt number was defined by Equation (1.18). The definition of the Sherwood number depend on the units of the mass transfer coefficient:

$$Sh = \frac{K_G a}{CD} \tag{3.5}$$

for a case in which the units of $K_G a$ are mol/(m packed height).(s), or alternatively:

$$Sh = \frac{K_G a R T d_e}{D a_t} \tag{3.6}$$

where $K_G a$ has the units mol/(s) (m^3 packed volume) (kPa)

3.1.1.2 Reacting system

Two approaches were adopted to model the reacting system. In the first approach, a detailed analysis taking into account the ternary vapour-liquid equilibrium and mass transfer rates was carried out and in the second method it was assumed that H_2 does not affect the 1-hexene vapour-liquid equilibrium (VLE) even though the pressure variation is affected. Therefore H_2 was treated as a pseudo-inert gas for the VLE in the non-reactive zones. Furthermore, it is assumed that the hydrogenation reaction takes place only on the catalyst surface and not in the gas or the liquid phase. The activity of the catalyst is assumed to remain constant with time.

(a) Model for evaluating the effect of hydrogenation reaction on mass transfer phenomena in a CD column

The solid-liquid-vapour phase interaction in a catalytic distillation process is best represented using film theory which provides a convenient method of evaluating effect of hydrogenation reaction on overall gas-phase mass transfer and liquid-solid mass transfer, as represented in Fig 3.1.

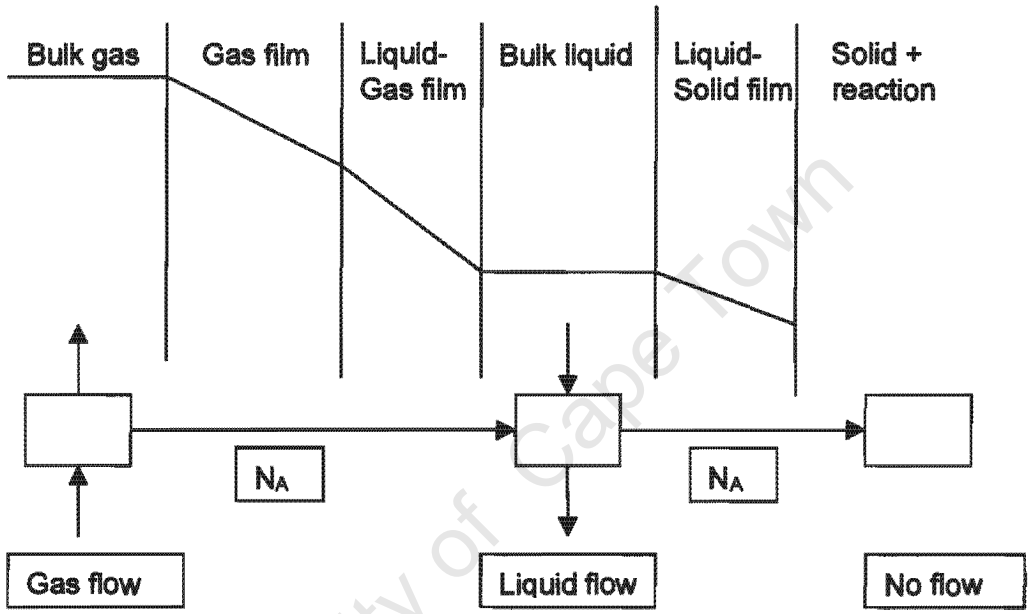

Fig 3.1: Film model representation of the CD process to evaluate the influence of hydrogenation reaction on gas-phase and liquid-solid mass transfer phenomena.

Hydrogen is essentially stagnant within the batch CD column and therefore can be taken out of the column mole balance. Hence the system can be treated as pseudo binary while still allowing the kinetics to be evaluated. The following assumptions are made to simplify the model:

- H_2 is evenly distributed throughout the column, i.e. it has the same concentration throughout and is independent of the position in the packing. The gradients caused by the reaction and the "flow" of H_2 are small due to the fast diffusion of H_2 because it is a small molecule.
- The mixture of n-hexane/1-hexene gas 'flows' up the column and the condensate flow down with V = L. This excludes hydrogen since it is

noncondensable at the operating conditions and does not pass through the condenser. The vapour "flowing" up thus diffuses through the stagnant H_2. This means that there should be a concentration gradient for the hydrocarbons and thus, because of constant pressure, also in H_2. This effect has been ignored. This is justified by noting that the hydrocarbons are in vapour-liquid equilibrium up the column and thus concentration gradients in the packing will be smoothed out by evaporation from the liquid phase. The liquid flow rate is limited by the rate at which the vapour can condense, which in turn is limited by the rate at which the vapour can diffuse through the column. As the hydrogen reacts and gets depleted, the diffusion behaviour of the vapour will more closely approximate the conditions of normal 1-hexene/n-hexane distillation with flowing vapour and liquid.

- The hydrogen concentration in the liquid phase is ignored in both mass balances and VLE calculations. This is validated by the low operating pressure (2 bar).

Using a first order reaction for H_2 the concentration of H_2 can be eliminated in both the solid and liquid phase, and this represents the reaction rate. The rate constant will include the effects of gas-liquid and liquid-solid mass transfer. A transient model which requires knowledge of the gas and liquid holdup, volume(s) of the column, condenser and reboiler is needed.

The gas phase hexene mole balance is given by:

$$-Vy_i'A\big|_z + Vy_i'A\big|_{z+\Delta z} - N_i A\Delta z = A\Delta z\varepsilon_g \frac{d}{dt}\left(y_i \frac{P}{RT}\right) \tag{3.7}$$

where A is the column cross-sectional area, V is the gas phase molar flow rate, N_i is the gas molar flux and ε_g is the gas void fraction per column volume. The distance z is measured from the reboiler through to the condenser. Equation (3.7) is simplified as follows:

$$\varepsilon_g \frac{d}{dt}\left(y_i \frac{P}{RT}\right) = V\frac{dy_i'}{dz} - K_y a\left(y_i - y_i^*\right) \tag{3.8}$$

where,

$$y_i' = \frac{y_i}{(1-y_H)} \tag{3.9}$$

and,

$$N_i = K_y a\left(y_i - y_i^*\right) \tag{3.10}$$

y_H is the hydrogen mole fraction, and so Equations (3.7) through to (3.10) are on a hydrogen-free basis.

The liquid phase hexene mole balance is given by:

$$Lx_i A\big|_z - Lx_i A\big|_{z+\Delta z} + N_i A\Delta z + R_i A\Delta z = A\Delta z \varepsilon_L \rho_L \frac{d}{dt}(x_i) \tag{3.11}$$

where L is the liquid mole flow rate, N_i is the liquid molar flux, ε_L is the liquid void fraction per column volume and ρ_L is the liquid density. Assuming no build up of material in the liquid-gas interface, the liquid and gas phase molar fluxes are equal, and Equation (3.11) is simplified to:

$$\varepsilon_L \rho_L \frac{d}{dt}(x_i) = -L\frac{dx_i}{dz} + K_y a\left(y_i - y_i^*\right) + R_i \tag{3.12}$$

where R_i is the rate of entering the liquid phase as a result of reaction in the solid phase. R_i thus represents a pseudohomogeneous liquid phase reaction rate taking into account the mass transfer rate of H_2 from the gas to the solid surface.

(b) Evaluation of the mass transfer controlled reaction rate

Simplifications made in this analysis are made possible by the reaction rate being first order in H_2 and zero order in hexene, and thus provides an evaluation of R_i. The overall reaction rate of hydrogen in a differential section is expressed as follows:

$$\varepsilon_g A\Delta z \frac{d}{dt}\left(y_H \frac{P}{RT}\right) = R_i A\Delta z \tag{3.13}$$

Dividing both sides by the differential volume, $A\Delta z$, yields the following:

$$\frac{\varepsilon_g}{RT}\frac{d}{dt}(P_H) = R_i \tag{3.14}$$

where

$$y_H = \frac{P_H}{(P_H + P_{C6} + P_{C6=})} \tag{3.15}$$

In Equation (3.15), P_{C6} and $P_{C6=}$ is the partial pressure of n-hexane and 1-hexene respectively while P_H is the hydrogen partial pressure. The overall pressure is expressed as:

$$P = P_H + P_{C6} + P_{C6=} \tag{3.16}$$

Assuming that the operating temperature is constant means the relative volatility α is also constant. Therefore, the sum of the pressure contribution by the hydrocarbons $(P_{C6} + P_{C6=})$, is constant with time, and hence:

$$\frac{dP}{dt} = \frac{dP_H}{dt} \tag{3.17}$$

In the solid phase, assuming quasi-steady state, the overall reaction rate is given by:

$$k_x a(x_i - x_{si})A\Delta z - R_i A\Delta z\left(\frac{V_s}{V}\right) = 0 \tag{3.18}$$

where $k_x a$ is the liquid-solid mass transfer coefficient, x_{si} is the mole fraction of species i absorbed to the solid phase, V_S is the volume of catalyst and V is the total column volume. The hydrogenation of 1-hexene by hydrogen reaction is expressed by:

$$H_2 + C_6H_{12} \rightarrow C_6H_{14} \tag{3.19}$$

Let A represent H_2, B be C_6H_{12} and C be C_6H_{14}. Assume that A is limiting, the reaction is first order in H_2 and there are no diffusion limitations in the catalyst, i.e. $C_A = C_{A,s}$. Then,

$$R_i = k_r C_{H_2} = k_r C_A = k_r C_t x_{S_A} \tag{3.20}$$

where k_r is the reaction rate constant and C_t represents the total concentration in the catalyst pores assumed to be the same as in the liquid phase:

$$C_t = \frac{1}{\sum_{i=1}^{N} \frac{x_i M_i}{\rho_i}} \tag{3.21}$$

where M_i and ρ_i are molecular mass and liquid density of each species respectively. Elimination of x_{S_A} using the solid balance yields:

$$x_{S_A} = \frac{k_x a \cdot x_A}{\left[k_x a + k_r C_t \left(\frac{V_S}{V}\right)\right]} \tag{3.22}$$

Therefore the liquid-solid mass transfer rate is given by:

$$N_L = k_L a\left(x_i - x_{S_i}\right) = \frac{k_x a \cdot k_r C_t \left(V_S/V\right) x_A}{k_x a + k_r C_t \left(V_S/V\right)} \tag{3.23}$$

which is valid for species A only. The other species are given by:

$$N_{L_B} = R_B \left(V_S/V\right) \tag{3.24}$$

$$N_{L_C} = R_C \left(V_S/V\right) \tag{3.25}$$

So the gas-liquid mass transfer rate of species B and C are independent of whether the transfer coefficients, $k_x a$, are equal or not and depends only on the rate of mass transfer of species A, a result of reaction stoichiometry at steady state. Evaluation of the liquid-solid mass transfer rate yields a coefficient K_x that depends on both reaction and film properties, thus:

$$N_{L_A} = K_{x_A} x_A \tag{3.26}$$

where,

$$K_{x_A} = \frac{k_x a \cdot k_r C_t \left(V_S/V\right)}{\left[k_x a + k_r C_t \left(V_S/V\right)\right]} \tag{3.27}$$

Assuming no accumulation of species in the interfaces and in the liquid phase, the steady state gas-liquid interface mole balance for H_2 gives:

$$K_{x_H} a\left(y_A - y_A^*\right) A\Delta z = K_{x_H} a\left(y_A - H x_A\right) A\Delta z = k' x_A A\Delta z \tag{3.28}$$

where Henry's law is used to describe vapour-liquid equilibrium for hydrogen. Equation (3.28) becomes upon simplification:

$$x_A = \frac{K_{x_A} a \cdot y_A}{k' + K_{x_A} a \cdot H} \tag{3.29}$$

Therefore the reaction rate is given by:

$$-R_A = \frac{k_x a \cdot k_r C_t \left(V_S/V\right)}{k_x a + k_r C_t \left(V_S/V\right)} x_A = k' x_A \tag{3.30}$$

Substituting Equation (3.29) into (3.30) yields the overall reaction rate per column volume as:

$$-R_A = \frac{y_A}{\frac{1}{K_{x_H} a} + \frac{H}{k_r C_i (V_S/V)} + \frac{H}{k_x a}} = K_A y_A \tag{3.31}$$

The rate constant K_A also includes the solid fraction and thus is specific to this system. Equation (3.31) represents the pseudo steady state reaction rate of H_2 in the CD column under batch operation as a function of all the mass transfer resistances in series.

In order to solve the system described by Equations (3.8) and (3.12), appropriate boundary conditions are required. Boundary conditions are obtained from the condenser and reboiler. In the condenser, negligible volume holdup is assumed owing to the pseudo steady state. The boundary condition in the condenser is then given by:

$$x_i\big|_{z=0} = \left.\frac{y_i}{1-y_A}\right|_{z=0} \tag{3.32}$$

In the reboiler equilibrium between vapour and liquid is assumed:

$$V_R \rho_L \frac{dx_{R_i}}{dt} = L x_i A\big|_{z=L} - V y_i' A\big|_{z=L} \tag{3.33}$$

where $y_i' = f(\alpha, x_{R_i})$ (3.34)

Vapour-liquid equilibrium is described using Raoult's law:

$$y_B = \alpha \frac{x_B(1-y_A)}{1+(\alpha-1)x_B} \tag{3.35}$$

where α is the relative volatility expressed using the combination of Raoult's and Dalton's laws:

$$\alpha = \frac{P_B^{vap}}{P_C^{vap}} \tag{3.36}$$

The liquid mole fraction of species B is given by:

$$x_B = \frac{y_B}{y_B + \alpha(1-y_A-y_H)} \tag{3.37}$$

The mole fraction of species A is given by the mole summation:

$$y_A = 1 - y_B - y_C \tag{3.38}$$

In Equation (3.35) up to (3.37) it is assumed that there is no hydrogen in the liquid phase due to its low solubility at the operating pressure and temperature. In strict terms, the system should be considered ternary due to the presence of hydrogen but to simplify the analysis it is assumed that hydrogen has a negligible effect on the vapour-liquid equilibrium behaviour.

(c) Pseudo steady state bottom-up solution

The vapour-liquid mass transfer coefficient in the CD column was determined using steady state compositions. Although the column does not reach steady state when chemical reaction is present, pseudo steady state was assumed so as to simplify the analysis. This is an important simplification which helps in comparison of the results in cases where the reaction is present and in which it is absent. As will be shown in the results section, the change in reboiler composition after a long time did not show a significant decrease as compared to the initial charge. Therefore the assumption of pseudo steady state is justified.

At steady state, Equations (3.8) and (3.12) become:

$$\frac{dy_i}{dz} = -\frac{k_y a(1-y_H)(y_i - y_i^*)}{V} \tag{3.39}$$

$$\frac{dx_i}{dz} = -\frac{k_y a(y_i - y_i^*)}{L} - \frac{R_i}{L} \tag{3.40}$$

where,

$$R_i = -K_H y_H \tag{3.41}$$

In Equation (3.37) it is assumed that the hydrogen mole fraction is independent of the column height, and hence the gas phase is well-mixed. The mole summation equations in the vapour phase make the balance of the Equations:

$$\sum_{i=1}^{3} y_i = 1 \tag{3.42}$$

The overall reaction rate for this model depends only on the partial pressure of hydrogen and thus the rate of change of moles of H_2 can be obtained:

$$\frac{dN_i}{dt} = R_i A z_{cat} \tag{3.43}$$

where R_i depends only on the partial pressure of hydrogen, P_{H_2}, and mass of catalyst (z_{cat} = length of catalyst bed) and mass transfer rate of the system, i.e. a standard first order rate constant.

An analytical solution is obtained by eliminating the liquid mole balance using a balance from bottom to any position in the column (including reaction):

$$Vy'_{o_i} + Lx_i + \int_0^z R_i dz = Vy'_i + Lx_{o_i} \tag{3.44}$$

With appropriate simplification, Equation (3.44) becomes:

$$x_i = \frac{V}{L}\left(y'_i - y'_{o_i}\right) + x_{o_i} - \frac{R_i z}{L} \tag{3.45}$$

The reaction rate is constant across the column and as the flow is downwards, the loss of 1-hexene must be added to the liquid flow as z increases. When no distillation takes place, the gas phase concentration remains constant ($\frac{V}{L}\left(y'_i - y'_{o_i}\right) = 0$) up the column and the liquid phase reacts when the liquid flows over the catalyst. The concentration of reactants in the liquid phase should reach a maximum at the top of the column ($x_i > x_{o_i}$). Thus differentiating with respect to x_i:

$$\frac{dx_i}{dz} = -\frac{R_i}{L} \tag{3.46}$$

For a reactant R_i is negative, thus x_i increases as z increases up the column as required.

Solving Equation (3.39) gives:

$$y_i(z) = \int_0^z -\frac{k_y a(1 - y_H)(y_i - y_i^*)}{V} dz \tag{3.47}$$

where y_i^* is described by Equation (3.35). The solution of Equation (3.46) and (3.47) requires the two parameters $k_y a$ and K_H. The initial conditions $y_H(t=0)$, $y_{o_i}(t=0)$ and $x_{o_i}(t=0)$ are all functions of time and this data can be used to determine the two parameters by fitting the model to measured compositions at the top of the column.

It was observed that the boundary condition at the top is not satisfied when reaction is included in the model. This is due to the fact that the system can never reach steady state when the reaction is present. Therefore the system behaves as a batch reactor with distillation taking place. In the model negligible holdup in the reboiler has been assumed by setting $y_i^* = x_i$ and similarly for the condenser, $x_i\big|_{z=0} = \left.\dfrac{y_i}{1-y_H}\right|_{z=0}$. This by definition means that no reaction can take place, and this is what is observed when the reaction term is removed. When reaction is added, it is impossible to have these boundary conditions at both ends for a batch system, as it cannot reach steady state. The solution to this is to have at least one boundary condition which does not specify equality between gas and liquid compositions. Now in a batch distillation at total reflux, most of the liquid will be in the reboiler and it seems reasonable to assume that there is negligible holdup in the column and condenser and that the rate of reaction is given by the rate of change of the reboiler composition. This provides the link to the reaction rate of 1-hexene and hydrogen.

(d) Pseudo steady state top-down solution

These assumptions lead to the following 'top down' approach. Assume a composition at the top with the negligible holdup assumption which leads to the boundary condition stated in Equation (3.32). Integrate down the column assuming negligible holdup. The deviation observed at the bottom given by Equation (3.32) gives the rate of reaction, with $L = V$. Or better still, the reboiler composition is given by equilibrium and is also measured as a

function of time. Thus given $k_y a$ and K_H and x_{R_i} it will be necessary to iterate the assumed value of the condenser composition such that the model corresponds to the value of x_{R_i}. Alternatively, and this was done here, if x_{D_i} and x_{R_i} are measured as a function of time, these can be obtained by least squares fitting to measured x_{R_i} using the given measured values of x_{D_i}. This then provides an estimate of the reaction rate and mass transfer rate at different pressures and varying vapour and liquid molar flow rates.

An interesting fact to note is that if 1-hexene is removed at the bottom of the system and H_2 is supplied at a steady rate equal to the reaction rate, then the CD system will reach steady state and make the analysis easy.

The steady state Equations for the 'top down' model with changing reboiler dynamics are similar to the 'bottom up' Equations except that now $z = -z$. Therefore Equations (3.39) and (3.40) become:

$$\frac{dy_i}{dz} = \frac{k_y a(1-y_H)(y_i - y_i^*)}{V} \tag{3.48}$$

$$\frac{dx_i}{dz} = \frac{k_y a(y_i - y_i^*)}{L} + \frac{R_i}{L} \tag{3.49}$$

Equations (3.35), (3.37), (3.38), and (3.42) make the balance of the Equations describing the system. An analytical solution is obtained by eliminating the x mole balance using a balance from top to any position in the column. Hence Equation (3.49) become:

$$y_i(z) = \int_0^z \frac{k_y a(1-y_H)(y_i - y_i^*)}{V} dz \tag{3.50}$$

Equation (3.50) is simplified to:

$$x_i = \frac{V}{L}(y_i' - y_{o_i}') + x_{o_i} + \frac{R_i z}{L} \tag{3.51}$$

Note that differentiating with respect to z causes x_i to decrease down the column as required when there is no distillation.

Making the column length dimensionless by setting:

$$z^* = \frac{z}{z_L} \tag{3.52}$$

Causes the length of the CD system (z_L) to be imbedded in the mass transfer and reaction rate coefficients in the following way:

$$\frac{dy_i}{dz^*} = A\left(y_i - y_i^*\right)\left(1 - y_H\right) \tag{3.53}$$

and,

$$\frac{dx_i}{dz^*} = A\left(y_i - y_i^*\right) + B \cdot y_H \tag{3.54}$$

where,

$$A = \frac{k_y a \cdot z_L}{L} = \frac{k_y a \cdot z_L}{V} \tag{3.55}$$

$$B = \frac{K_H \cdot z_L}{L} = \frac{R_i}{y_H} \tag{3.56}$$

A and B represent the 2 dimensionless parameters which describe this system. The condition for A arises, because of total reflux, because the number of moles of 1-hexene do not change and because H_2 does not "flow" through the system. B is not a function of z^* and is equivalent to the Damköhler number used frequently in reaction engineering. The analytical solution described by Equation (3.53) then becomes:

$$y_i(z) = \int_0^1 A\left(y_i - y_i^*\right)\left(1 - y_H\right) dz^* \tag{3.57}$$

and that of Equation (3.54) becomes:

$$x_i = \frac{V}{L}\left(y_i' - y_{o_i}'\right) + x_{o_i} + B \cdot y_H z^* \tag{3.58}$$

(e) Model evaluation and verification

It is important to verify the model described by the Equations stated above. If the model is theoretically sound it can then be validated with experimental work. The model was verified by solving a ternary system such that the liquid solution in the reboiler consisted of equimolar 1-hexene and n-hexane system as a feed. The boundary value system was solved using FORTRAN routines. The following parameters were used in the verification of the model:

The model is robust enough such that different values of the parameters listed in Table 3.1 were used successfully resulting in similar trends with respect to column composition. The values shown in Table 3.1 are simply representative of the range of values used in the evaluation of the model.

Table 3.1: Typical simulation parameters implemented in the model.

Simulation Parameter	Value
K_H	0.0001
$k_y a$	30
y_H	0.5
V/L	1
A	30
B	0.1

Fig 3.2 shows composition profiles for distillation without hydrogenation reaction.

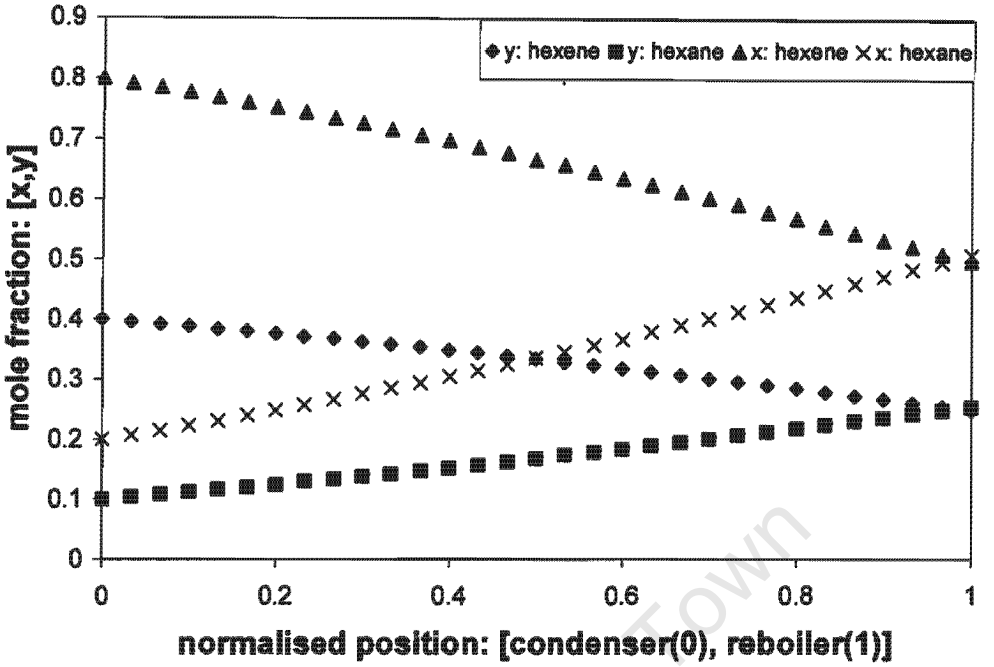

Fig 3.2: Composition profiles along the length of the column due to distillation in the absence of hydrogenation of 1-hexene reaction.

Fig 3.2 shows that the distillation process proceeds as expected, with 1-hexene (x_1) highest at the top (or condenser). Mass transfer coefficient is chosen to produce a reboiler mole fraction of 0.5.

Fig 3.3 shows the case where hydrogenation reaction without distillation takes place. A case for distillation in the absence of hydrogenation reaction is shown for comparison.

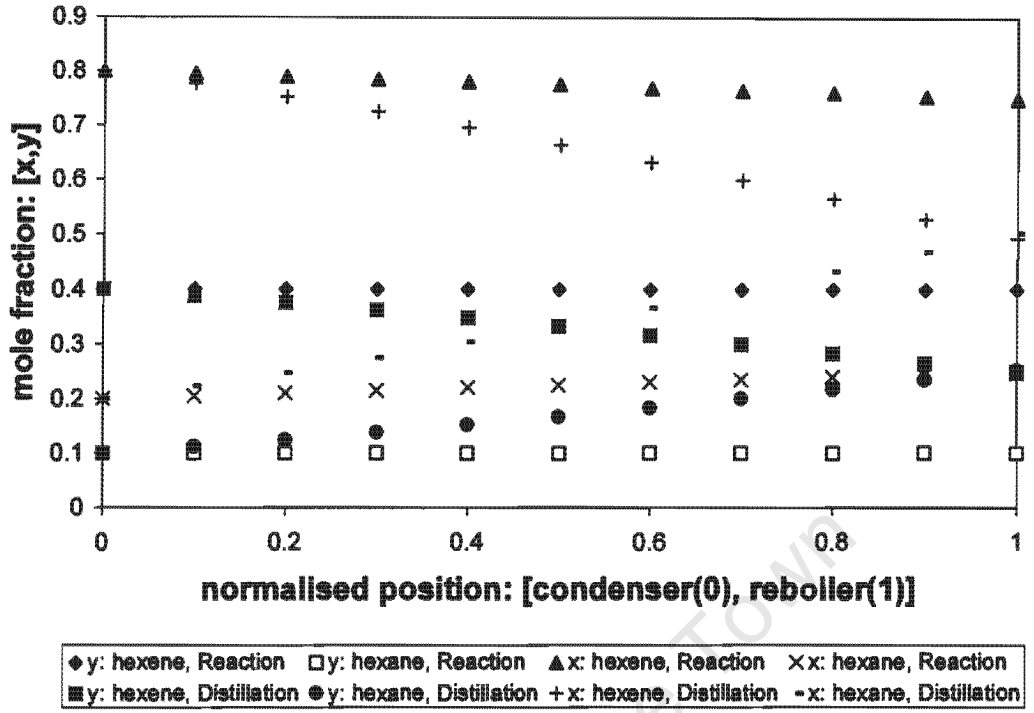

Fig 3.3: Comparison of composition profiles along the length of the column for distillation with no hydrogenation reaction, and hydrogenation reaction without distillation.

Fig 3.3 shows that the reaction only condition also proceeds normally, with the 1-hexene (x_1) concentration highest at the top and the gas phase not changing at all. In this case the reboiler concentration will be substantially higher as for no reaction. The reaction rate is negative as expected and is given by $-By_H$.

Fig 3.4 shows the comparison of composition profiles along the length of the column for distillation and hydrogenation reaction and distillation without reaction.

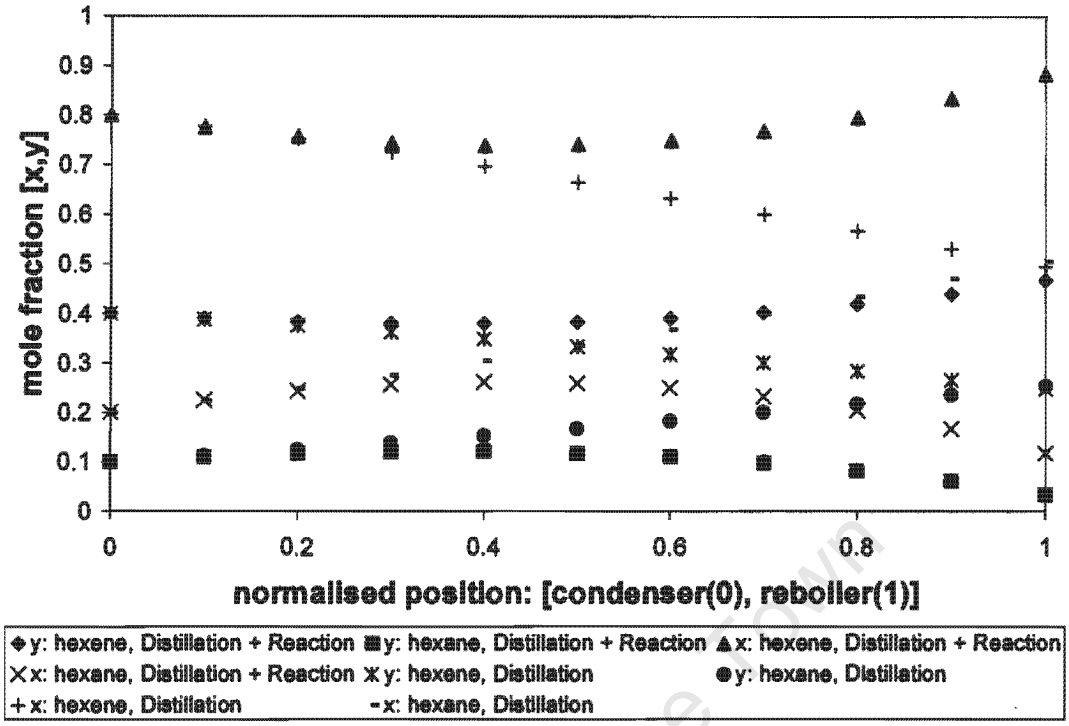

Fig 3.4: Comparison of composition profiles along the length of the column for distillation and hydrogenation reaction, and distillation without reaction.

Fig 3.4 shows what happens when both distillation and reaction phenomena within the column are combined. These curves, even though they obey all the boundary conditions, are rather unexpected as they indicate an increase in the light component in the reboiler even though distillation is occurring. This behaviour may be explained by considering the overall mass balance from the top to some point z in the column:

$$y = \frac{L}{V}x - \frac{L}{V}x_0 + y_0 + R_i^* z \tag{3.59}$$

$$y' = \frac{y}{1 - y_H} = x + \frac{R_i^* z}{V} \tag{3.60}$$

$$A_{in} = A_{out} + A_{reacted} \tag{3.61}$$

where Equation (3.61) arises from the total reflux column operation condition that $x_0 = y_0$, $L = V$ and R_i^* is the rate of consumption of A, where the zero order reaction $A \rightarrow B$ takes place, A being the light component. When there is no reaction, then $y' = x$, i.e. the operating line lies along the $y = x$ line at

total reflux (Seader and Henley, 1998). When a reaction takes place $y' > x$, and thus the difference in flow of hexene out the bottom of the column is accounted for by the reaction.

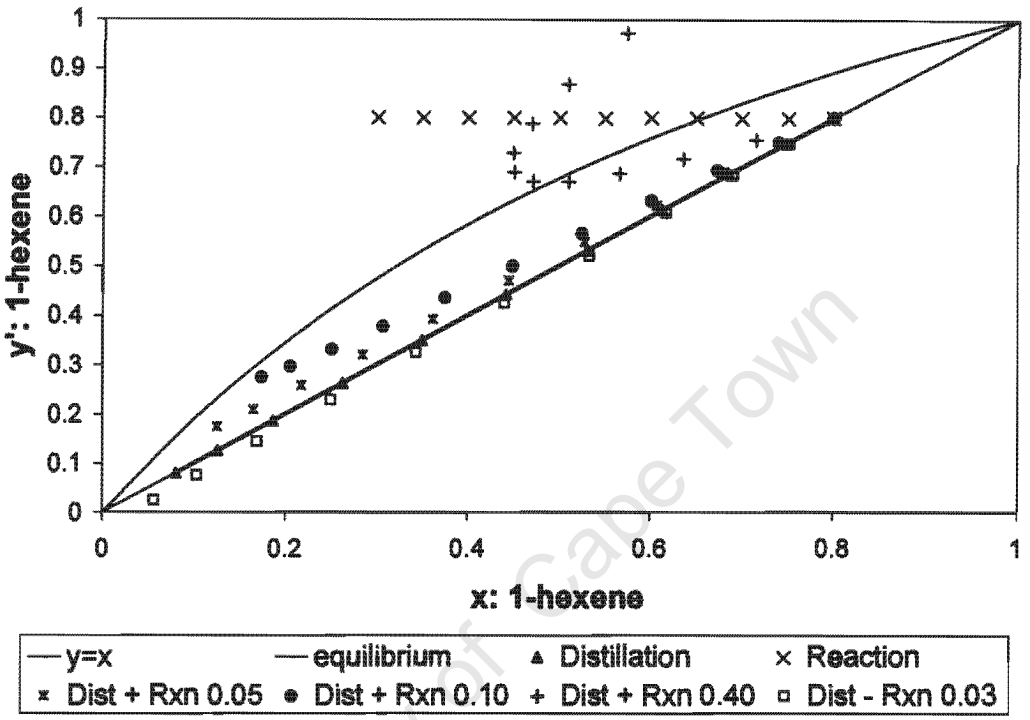

Fig 3.5: Effect of hydrogenation reaction on McCabe-Thiele diagram. Here the reaction numbers represent the values of parameter A.

Fig 3.5 is then generated using α = 2.1, to make it easier to see the trends. No reaction follows the $y = x$ line as expected for total reflux. Reaction only follows the y = constant line, because there is no mass transfer to the gas phase. The combination must lie somewhere between the two limiting cases. But as the reaction rate is increased the equilibrium line is crossed. This can only happen when reaction takes place and seems to be a feature of reactive distillation. When no reaction occurs, the model can be made to approach the equilibrium line by changing the reflux ratio but it cannot cross the equilibrium line, as expected. Because 1-hexene is the light component the distillation column operates as a stripper, in which case the 1-hexene is being stripped from the n-hexane. Reaction produces the same effect, by also removing 1-

hexene from the liquid, thus reducing the driving force for mass transfer, which in turn reduced the effective mass transfer coefficient and the system would tend to pinch. However, after sufficient reaction has taken place, the mass transfer driving force will reverse and 1-hexene will start to condense, and this is where it crosses the equilibrium line and heads the other way. This can only happen when reaction is present and counteracts the effect of mass transfer, i.e. this is a situation where the mass transfer rate is adversely affected by the reaction. The composition reaching unity is an artefact of the zero order reaction. The same trend is observed for $L < V$.

Reversing the reaction ($B \rightarrow A$), increases the 1-hexene in the liquid phase, increasing the driving force for stripping (i.e. enhancing mass transfer), hence a more efficient column, and for this case $y < x$. This is the same as reaction enhanced absorption except that it is applied to stripping. The strange features are also a result of batch distillation operation and steady state assumptions. If integration proceeded the other way, the same result would be obtained, but iteration would be necessary to meet the $y_0 = x_0$ reflux condition.

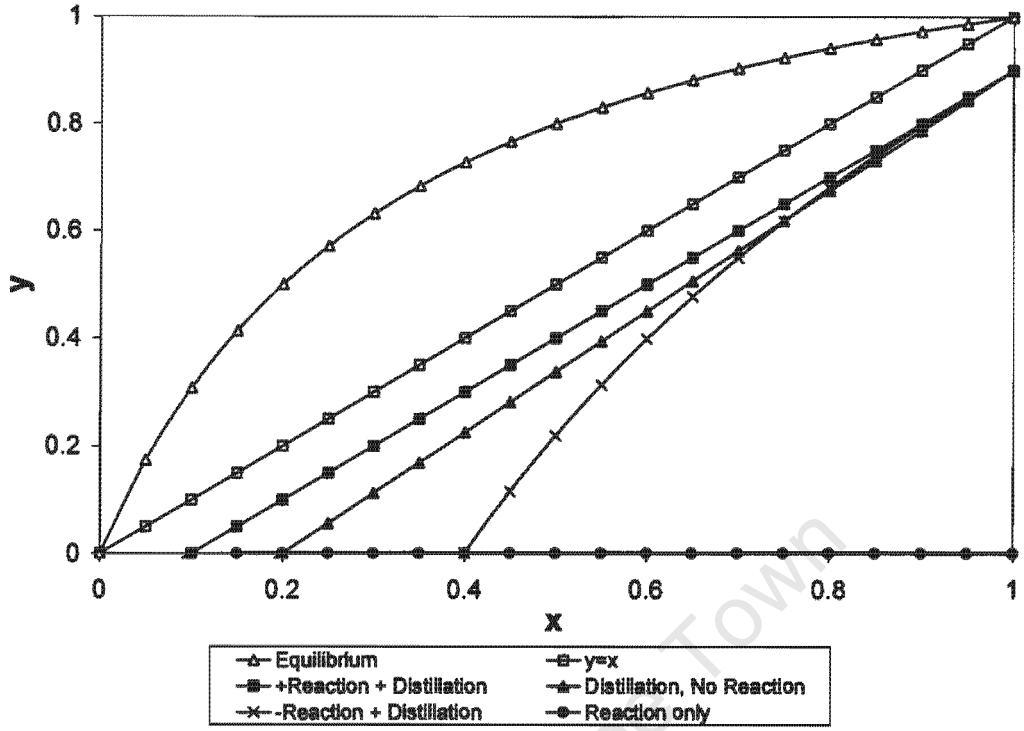

Fig 3.6: General representation of the effect of heterogeneous chemical reaction on a stripper.

The same argument can be applied to a stripping column assuming $L = V = 1$ as shown in Fig 3.6 where x = 1 is pure A and $y = 0$ is pure B, and A is the light component. For no reaction, applying the mass balance as above gives x = 0.05. When $A \rightarrow B$, $x = 0.05 - R_i^*$, i.e. x gets smaller (the reaction curve) which is consistent with less A exiting because it has reacted to B. The opposite is true if the reaction is reversed, i.e. $x = 0.05 + R_i^*$, x increases as more A exits in the liquid because it is produced (-reaction curve). These results are a consequence of holding y_0 and y constant causing x to reflect the effect of reaction. The no stripping and reaction only curve means that no A is transferred ($y_0 = 0$) and the curves creeps along the x-axis to lower x values as the reaction proceeds.

Referring back to Fig 3.4, at the top of the column, the curve starts out by following the normal distillation curve, until about $z = 0.4$ where reaction starts to dominate and the curve crosses the equilibrium line and produces very high

values of 1-hexene in the reboiler. The consequence of this is that for the conditions chosen, the concentration of 1-hexene in the reboiler is much higher than the concentration in the condenser, suggesting that a batch distillation system is not well suited for this reaction. This seems to suggest that in a real distillation column it might be reasonable to place the catalyst below the feed where 1-hexene absorption will be promoted so that it will react, but this needs to be checked. However, this was not part of the scope of this work, and therefore it seems that this batch system might be useful to get mass transfer coefficients using this model by measuring reboiler and condenser composition as a function of time.

Of particular interest is whether distillation continues after the operating line crosses the equilibrium curve or whether the system behaves more like a gas-liquid absorber. No heat effects are included in the preceding calculations and these effects could well be critical in determining the behaviour of the system and the crossing of the equilibrium line may well suggest that distillation has ended. If reflux is assumed to be high, then the reaction rate for the catalytic section (i.e. formation of B) will be small and distillation will dominate and the equilibrium curve will never be crossed. For this situation it may be assumed that the system obeys the distillation equilibrium curve. The pre-requisite for distillation to occur is that the operating lines remain within the Txy diagram boundaries. Changing the x composition without changing the temperature will move the system from the liquid equilibrium line. To achieve vapour-liquid equilibrium, temperature must then change. For a reactive distillation system though the operating lines may not lie within the Txy diagram boundaries. In addition when proper distillation no longer takes place, the condition $L = V$ may no longer hold, and this is especially true when heat of reaction causes evaporation of liquid. If heat effects are important, this rather simple system becomes very complicated to analyse.

(f) Simulations using typical model parameters

In the following simulations assume that L and V are large and "conversion per pass" is small, so that heat effects can be neglected. This analysis

attempts not to cross the equilibrium line by keeping the 1-hexene conversion low since the equilibrium envelope is narrow. Three sections of equal length, with the middle section containing the catalyst, was simulated under conditions of equal constant liquid and vapour flow rate (based on packed diameter) using the parameters shown in Table 3.2 below. The relative volatility between the two components was taken to be constant at a value of 1.1 at the average column temperature.

Table 3.2: Parameters used and values obtained for Fig 3.7a - f

Comment	A	B	y_H	x_{01}	x_{R1}
No reaction, Fig 3.7(a)	30	0.00	0.50	0.80	0.47
Reaction, Fig 3.7(b)	30	0.10	0.30	0.70	0.31
Reaction, Fig 3.7(c)	30	0.10	0.10	0.70	0.17
Reaction, Fig 3.7(d)	30	0.10	0.20	0.70	0.24
Reaction, Fig 3.7(e)	30	0.10	0.40	0.70	0.39
Reaction, Fig 3.7(f)	30	0.10	0.50	0.70	0.46

Fig 3.7 (a, b) show that the addition of the reaction term to the model reduces the separation efficiency of the column (similar x_{R1} with different y_1). Fig 3.7 (b – f) show that the separation improves as the reaction rate is reduced. This is due to two factors, namely,

(i) The reduced mass transfer rate caused by the presence of non-condensable H_2 and,

(ii) The counter effect of the reaction on the evaporation of 1-hexene.

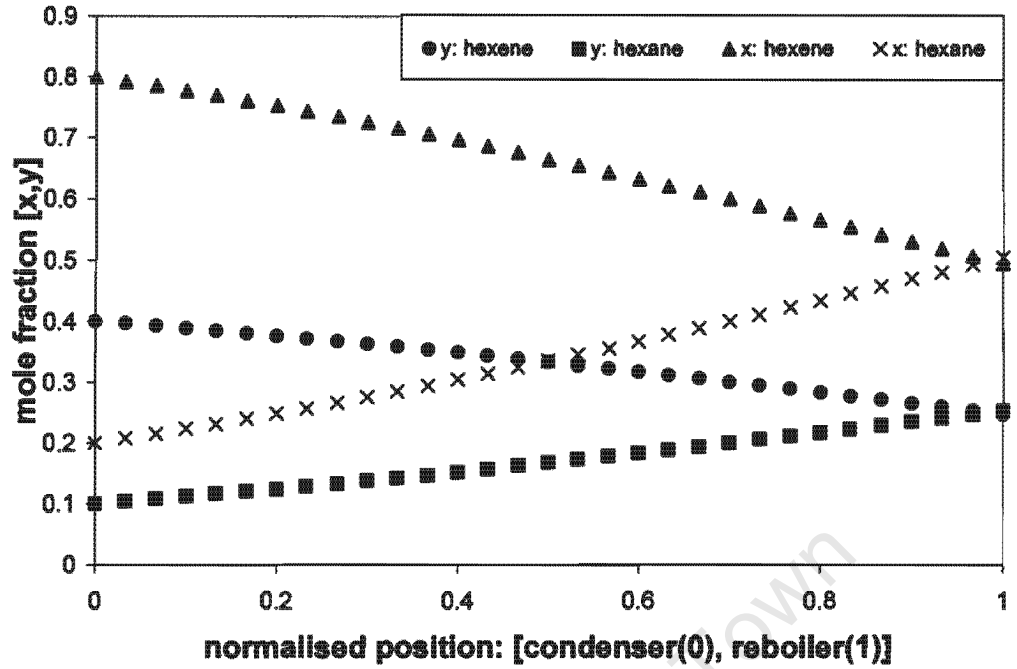

Fig 3.7 (a): Mole fraction profiles of the three region model, in the absence of chemical reaction, for yH=0.5.

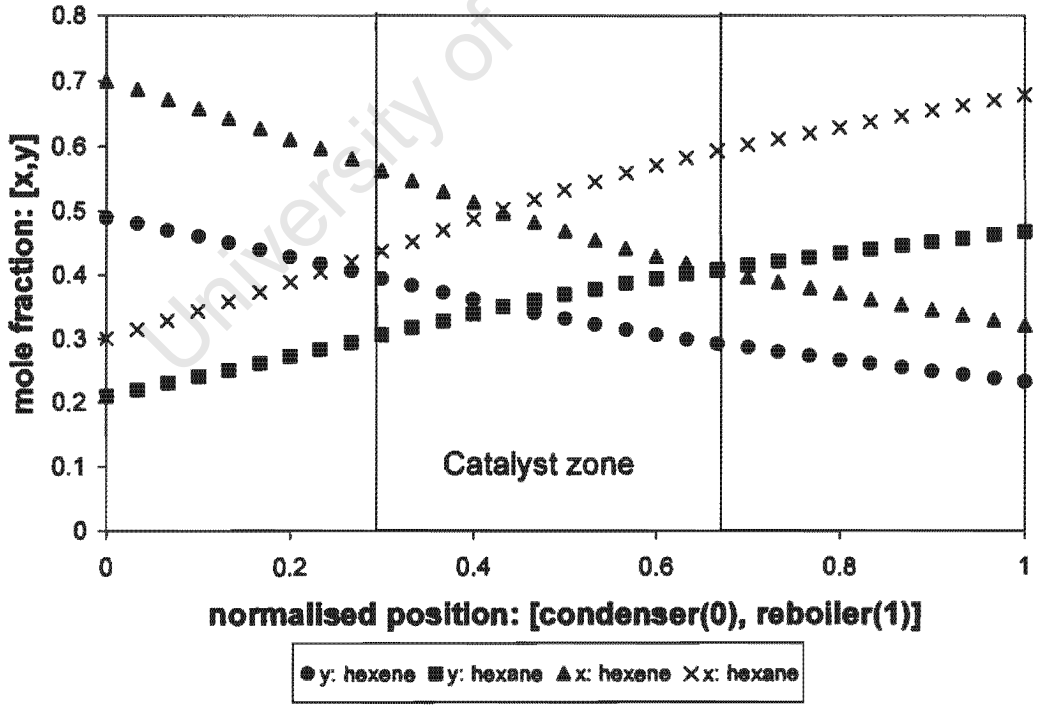

Fig 3.7(b): Mole fraction profiles of the three region model, with the catalyst zone located between z=0.33 and z=0.67, for yH=0.3.

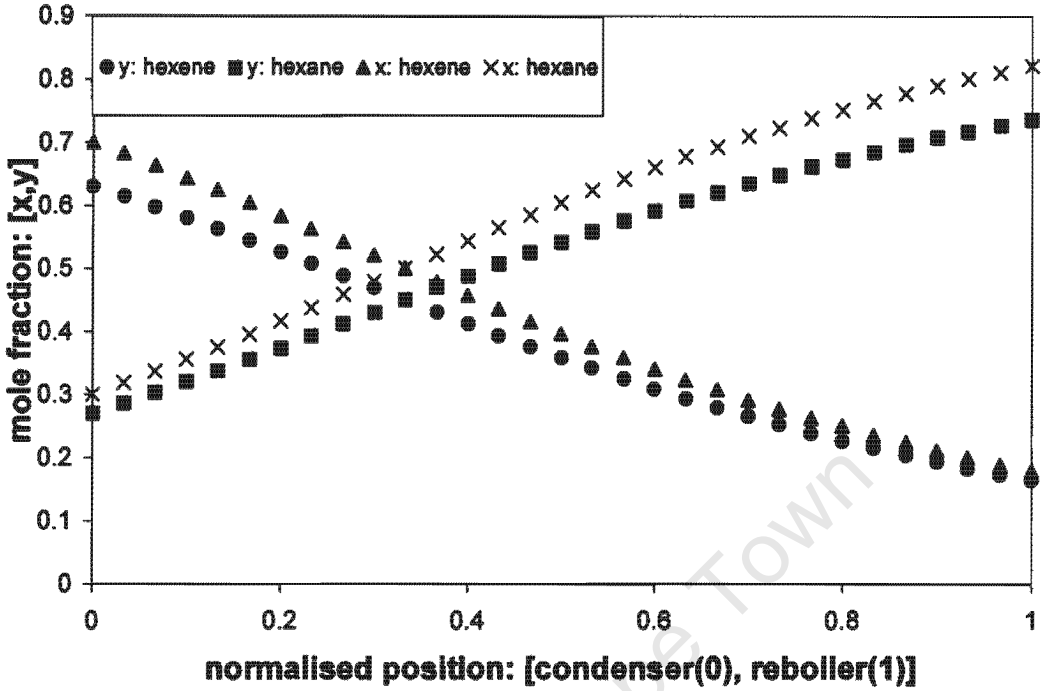

Fig 3.7(c): Mole fraction profiles of the three region model for yH=0.1.

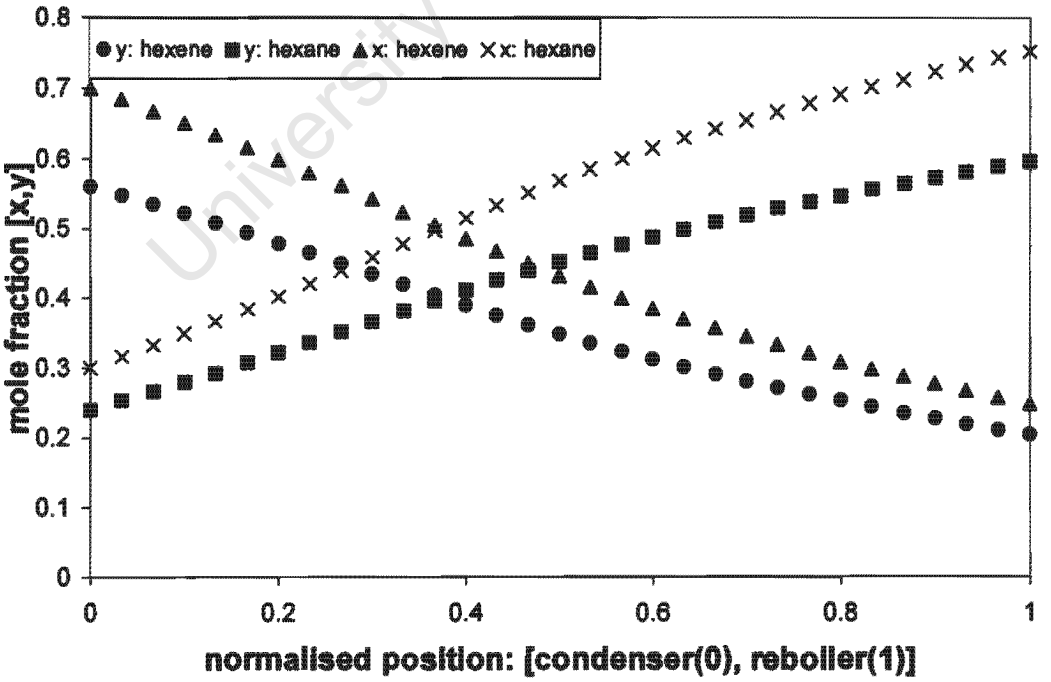

Fig 3.7(d): Mole fraction profiles of the three region model for yH=0.2.

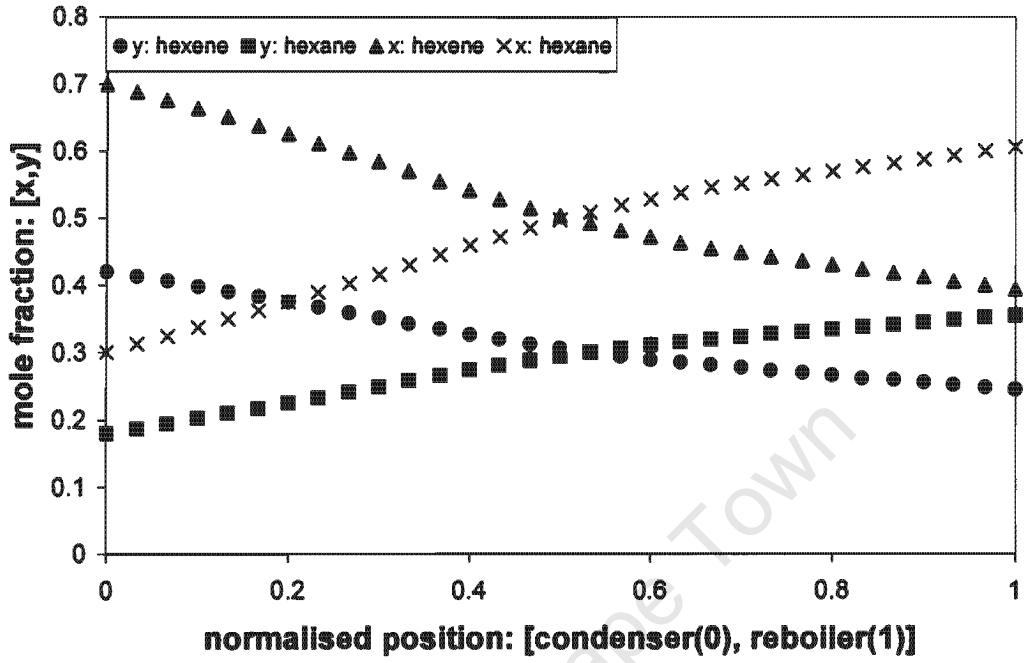

Fig 3.7(e): Mole fraction profiles of the three region model for yH=0.4.

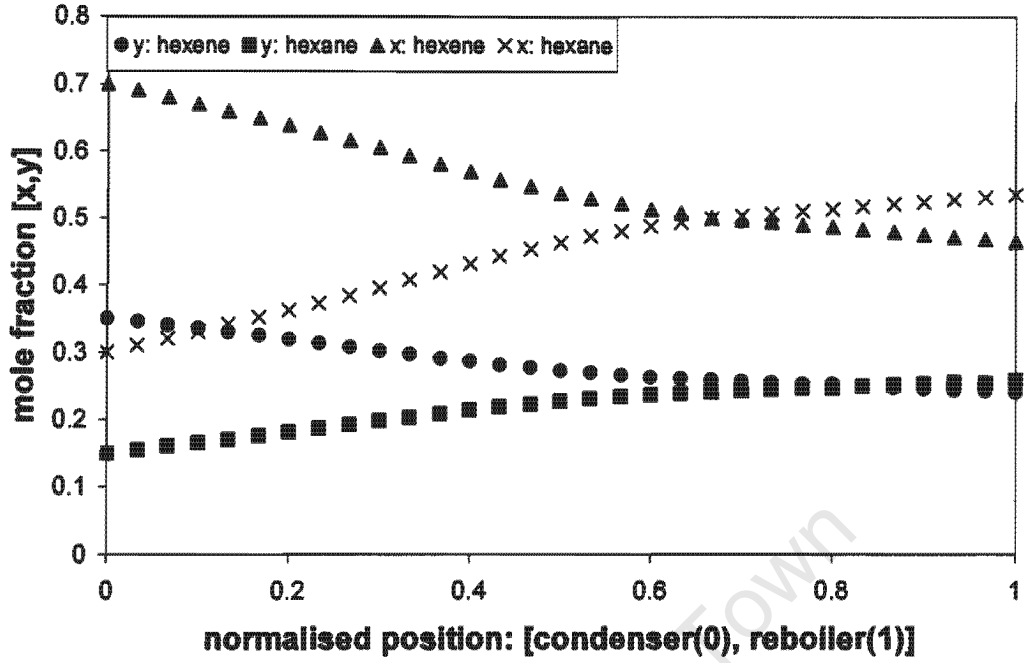

Fig 3.7(f): Mole fraction profiles of the three region model for yH=0.5.

Fig 3.8 shows that these data all fall within the distillation envelope. Notice how it is possible to keep the condenser composition constant even though the reboiler composition is changing, the effect of (i) and (ii). The model is based on fixed composition of the condenser and hence the composition of the reboiler must change to compensate for any deviations in the mass transfer rate as the column length is fixed. Note that low values of 1-hexene would invalidate the first order rate of hydrogenation which assumes excess H_2.

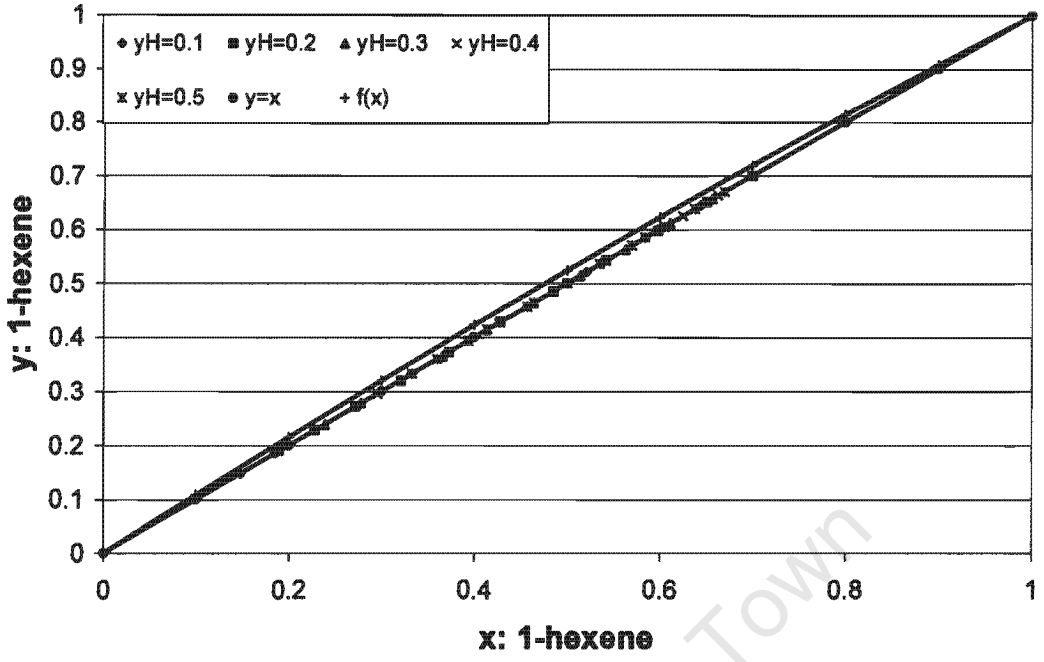

Fig 3.8: McCabe-Thiele diagram for a binary 1-hexene/n-hexane system in which hydrogen is the dissolved gas. The relative volatility is held at a constant value of 1.1.

(g) Uniqueness of the model parameters and parameter estimation using the Levenberg-Marquardt algorithm

It is necessary to verify that the two parameters of this model are indeed independent and unique. This would also provide a test whether the values of A and B can be determined using the measured condenser and reboiler compositions. The simplest and most robust approach is to use the simulated data given in Table 3.2 as "experimental input". The above model can be viewed to operate as follows: given a value of y_1, iterate the values of A and B until the value of x_{R1} is obtained for all data. This can be conveniently arranged into a least squares error routine which minimised the least square errors in the model and experimental values of x_{R1}:

$$\text{error} = \sum_{i=1}^{Ndata} \left(x_{R,\text{exp.}} - x_{R,\text{model}} \right)^2 \qquad (3.62)$$

The Levenberg – Marquardt method (Levenberg, 1944; Marquardt, 1963) is used to determine A and B and the covariance matrix is used to obtain the confidence interval. Table 3.3 gives the values of parameter A and B and their estimated errors.

Table 3.3: Estimated model parameters

Parameter	A	B
Estimated value	30	0.10
Variance	9.78×10^{-3}	1.04×10^{-4}
Estimated value (5% noise)	28.5	7.5×10^{-2}
Variance (5% noise)	0.98	1.20×10^{-2}

The results in Table 3.3 indicate that the model is robust and initial guesses for A and B can vary. The model can even tolerate about 5% noise without too much loss in accuracy.

A simple 2 parameter ideal rate based distillation-reaction model has been developed. It has been shown to conform to all expected behaviour provided that the operating lines remain within the "distillation envelope". The model has been used to extract global 2 parameters: (i) a global reaction rate constant and (ii) a mass transfer coefficient from measured reboiler and condenser compositions as a function of time.

4. RESULTS AND DISCUSSION

4.1 Estimation of gas-phase mass transfer coefficient without reaction.

Fig 4.1 shows variation in the overall gas-phase mass transfer coefficient based on the transfer of 1-hexene with molar vapour flow in an equimolar feed of 1-hexene and n-hexane charged into a batch CD column, measured at 200 kPa and 80 °C:

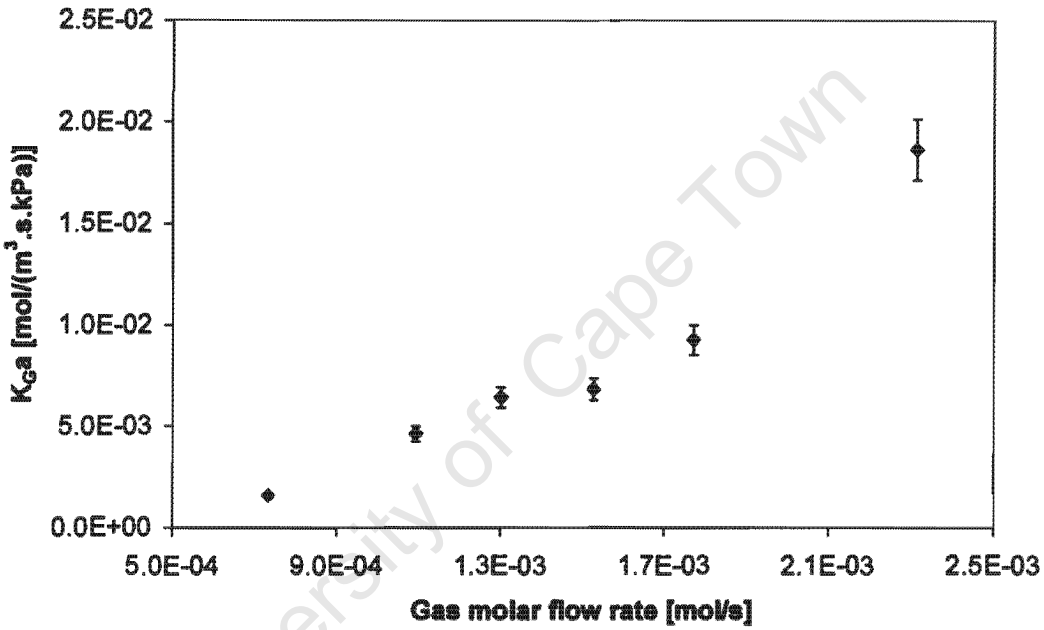

Fig 4.1: Overall gas-phase mass transfer coefficient based on the transfer of 1-hexene at 200 kPa and 80 °C.

The gas-phase mass transfer coefficient, K_Ga, based on reboiler and condenser composition at steady state, was calculated using Equation (3.1). The measured compositions at both the reboiler and condenser outlets are in the liquid phase, and at the condenser the liquid and gas compositions are equal. At the reboiler, it is assumed that the liquid phase is well mixed and the gas phase composition was estimated using the equilibrium relation in Equation (3.3). The mass velocity of gas, also known as mass flux, is based on a cross sectional area of an empty column. The relative volatility in the column used in Equation (3.2) was assumed to be constant across the length

of the column. This is validated by the fact that the temperature variation across the column length is not too large.

The packing in the column is not uniform since the reactive zone is packed with catalyst bags in a form of bales and the non-reactive zones with the metallic Sulzer-BX packing. Therefore it was expected that their performance in terms of mass transfer would be different. However, the gas-phase mass transfer in these different sections is not known since only the exiting compositions were measured.

The column pressure was kept at 2 bar (g) by adjusting the cooling water rate through the condenser. By assuming application of Raoult's and Dalton's laws, the relative volatility is calculated from the ratio of vapour pressures, with the vapour pressures calculated from the Antoine equation:

$$\alpha = \frac{P_A^{vap}}{P_B^{vap}} \tag{4.1}$$

The vapour pressure of 1-hexene and n-hexane were estimated using Antoine's Equation:

$$P_i^{vap} = \exp\left(A - \frac{B}{T + C}\right) \tag{4.2}$$

where the constants A, B, and C are specific to components used.

Fig 4.1 indicates that the overall vapour-liquid mass transfer increases with increasing gas molar flow rate. This is consistent with the work of other investigators (Bravo *et al.*, 1985; Zheng and Xu, 1992; Dudukovic, 1996; Subawalla *et al.*, 1997; Huang *et al.*, 1998a; Van Baten and Krishna, 2002) and/or Equation (1.15), (1.19) and (1.24).

4.1.1 Reproducibility of mass transfer coefficients data

Fig 4.2 gives the 95% confidence limits on the line fitted through the data presented in Fig 4.1. The significance of the line fitted through the data in Fig 4.1 is that most mass transfer coefficient data in literature (Bravo *et al.*, 1985; Zheng and Xu, 1992; Dudukovic, 1996; Subawalla *et al.*, 1997; Huang *et al.*,

1998; Van Baten and Krishna, 2002) shows an almost linear relationship between the coefficient and the liquid/gas molar flow rate. Fig 4.2 indicates that we are 95% sure that the real regression line is between the two bounds indicated. Therefore, we can conclude that the linear relationship between the overall gas phase mass transfer coefficient and gas flow rate is statistically significant, i.e. it is not by coincidence.

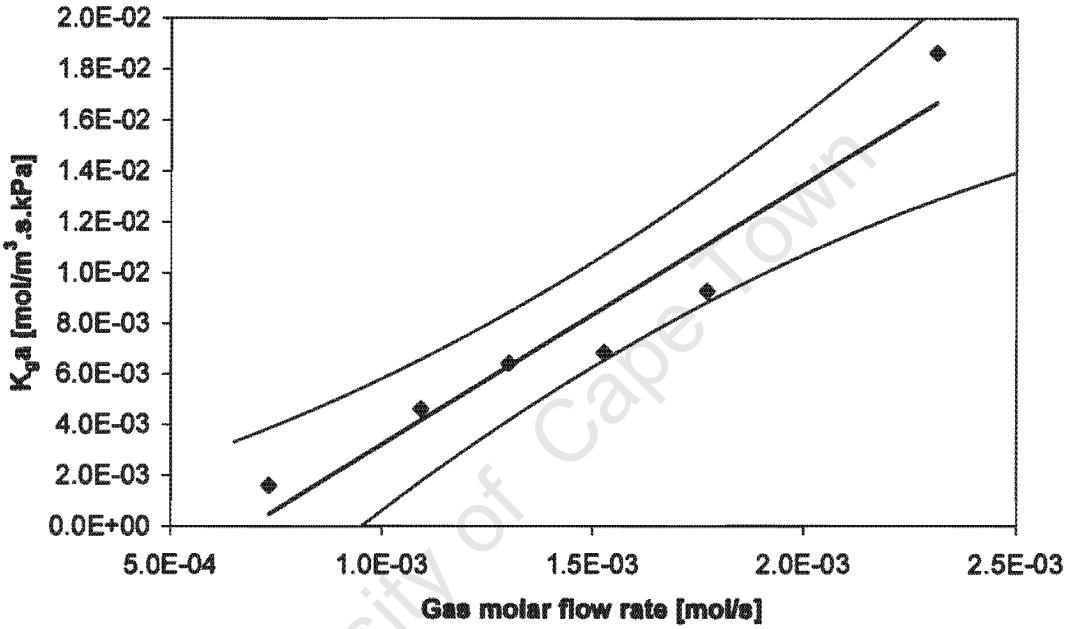

Fig 4.2: 95% confidence limits on the regression line between mass transfer coefficient and gas molar flow rate.

Fig 4.3 presents the limits on the predicted value of $K_g a$ for any given value of gas flow rate for a confidence level of 95%. This means that 95% of the data should fall within the two limits indicated. The significance for this Figure is that it shows that the experimental data obtained fall within the bounds, and hence the data obtained is statistically significant.

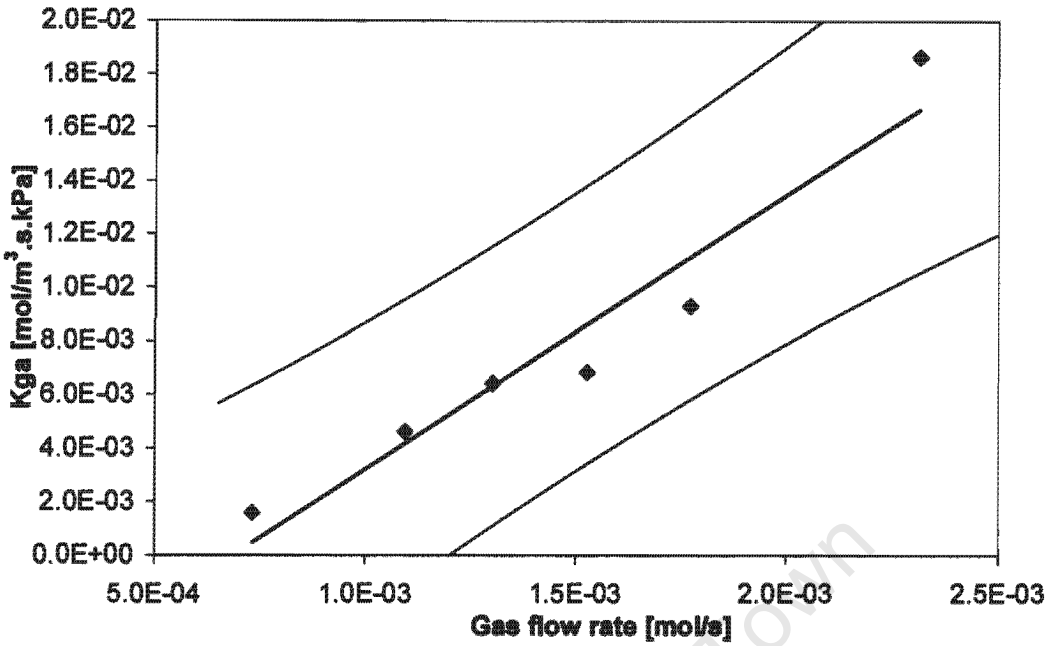

Fig 4.3: The limits on the predicted value of overall gas phase mass transfer coefficient for any given value of gas flow rate for a 95% confidence level.

Table 4.1 gives the gas phase mass transfer coefficients evaluated in the absence of the reaction at the same gas molar flow rate and keeping all other experimental conditions in order to determine the reproducibility of the experimental data.

Table 4.1: Reproducibility of the gas phase mass transfer coefficient

Flow rate [mmol/s]	Column pressure [kPa]	K_Ga [mmol/(m^3.s.kPa)]	K_ya [mmol/(m^3.s)]
1.30	220	6.96	1.53
1.30	225	6.41	1.36

The reproducibility of the experiments is determined by the relative error between the two mass transfer coefficients. From Table 4.1, it is clear that the % relative error expressed in terms of K_ya is 11.2%, while in terms of K_Ga it is 7.9%. The discrepancy between these relative errors is brought about by amongst others, sampling error, boilup rate error and pressure reading error. These relative errors are acceptable considering the experimental difficulties. Huang *et al.* (1998) reported relative errors of about 10%.

4.2. Isomerization of 1-hexene over the Nickel/alumina catalyst.

Ideally, no side reaction should take place so that only one product, i.e. n-hexane is formed. Fig 4.4 shows the change in composition of the feed as a result of isomerization reaction over a Nickel/Alumina catalyst at 200 kPa and 80 °C for a flow rate of 1.3 kmol/s.

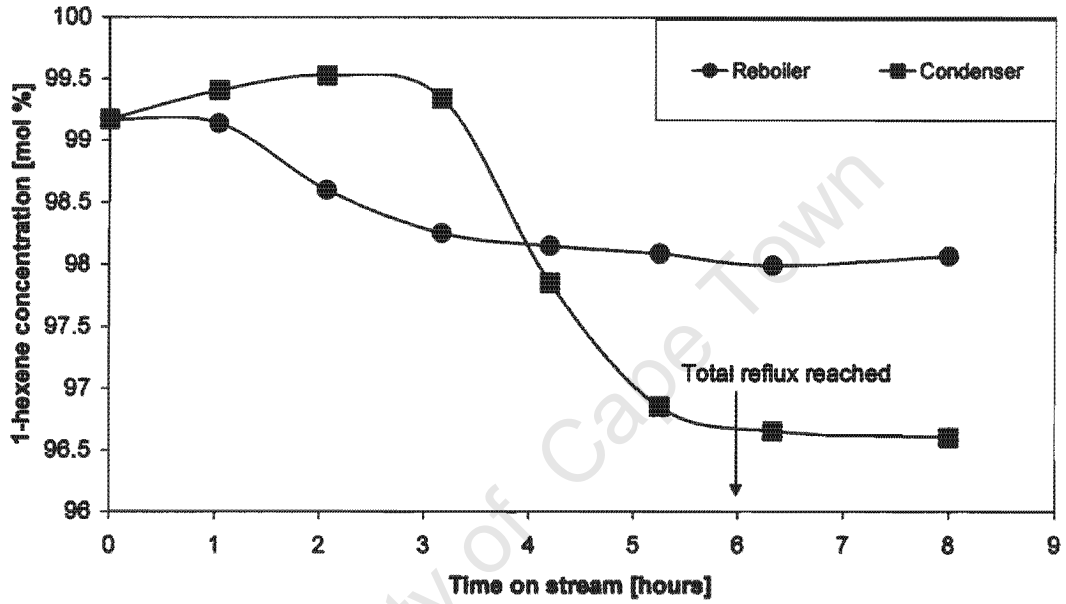

Fig 4.4: Isomerization of the feed over a Nickel/Alumina catalyst at 200 kPa and 80 °C for a flow rate of 1.3 kmol/s.

The unexpected lower amount of 1-hexene in the condenser than in the reboiler as shown in Fig 4.4 is due to its isomerization to other products and the side reactions (i.e. 1-hexene gets converted in the packed section of the column on its way to the condenser), such as cracking and oligomerization, which were observed. The decrease in the amount of 1-hexene in the reboiler is primarily attributable to the separation taking place in the column.

It is clear from Fig 4.4, 4.5 and 4.6 that the isomerization reaction is slow. It was also observed that total reflux condition in the column was achieved after about 6 hours. This occurs when the column temperatures and pressures reach steady state, i.e. stop increasing. The hydrogenation reaction can

therefore begin after 6 hours have elapsed. Therefore, isomerization reaction would not affect the main hydrogenation reaction.

Fig 4.4 indicates the products formed through isomerization reaction over a Ni/Al_2O_3 catalyst for a vapour flow rate of 1.30 mmol/s, while Fig 4.5 and Fig 4.6 shows the products formed in the reboiler and condenser over time respectively (excluding the feed 1-hexene and the main product n-hexane). It is worth noting that the composition of the products does not change much after about 6 hours, which is consistent with the results of Fig 4.4. It is clear that trans-3-hexene, cis-3-hexene and other internal olefins dominate the products formed in the reboiler. These products are the result of double bond migration on the 1-hexene compound. These observations are consistent with the results of Sanchez-Delgado et al. (1981).

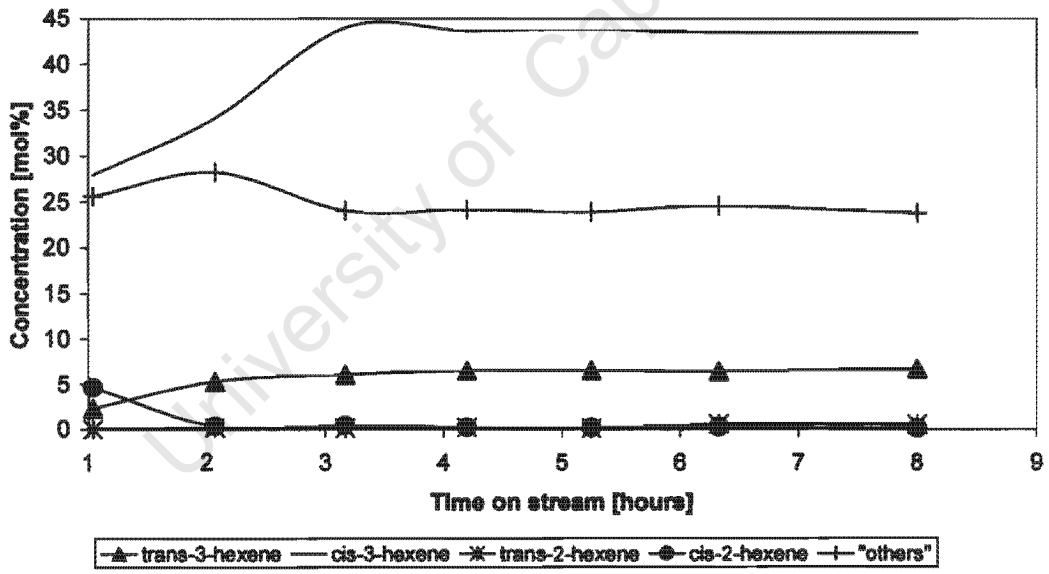

Fig 4.5: Reboiler composition of the isomerization reaction over the Nickel/Alumina catalyst on a 1-hexene free basis at 200 kPa and 80 °C.

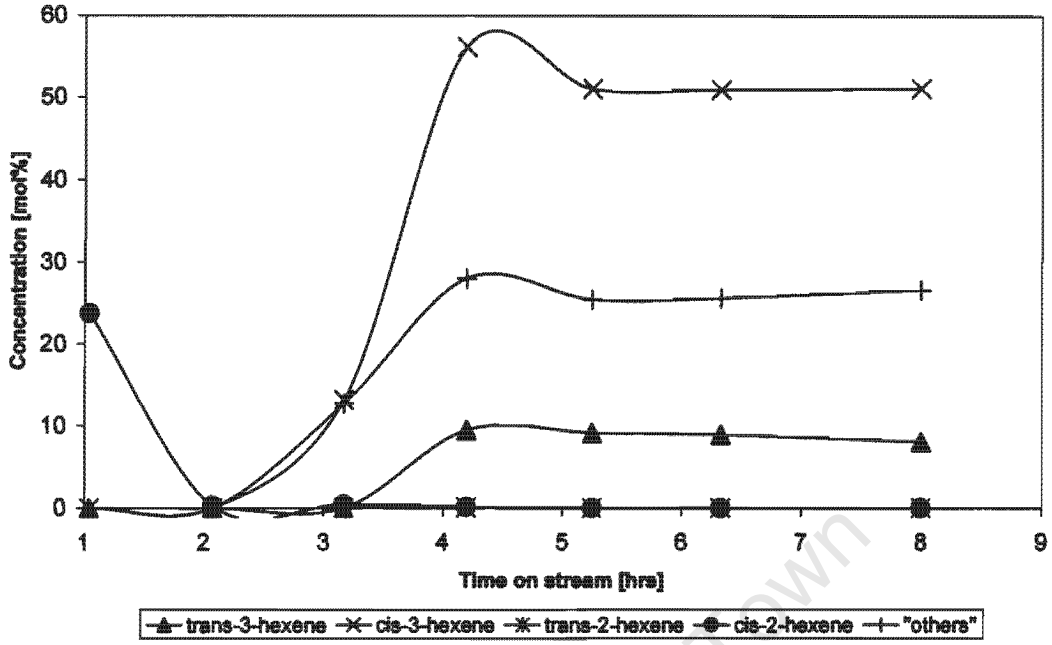

Fig 4.6: Condenser composition of the isomerization reaction over the Nickel/Alumina catalyst on a 1-hexene free basis at 200 kPa and 80 °C.

Fig 4.7 indicates the observed column pressure during isomerization of the feed over the Nickel/Alumina catalyst. The initial increase in column pressure is attributable to the increase in the composition of 1-hexene in the overhead condenser. Steady state is reached when total reflux conditions have been established, which is approximately after 6 hours of distillation time.

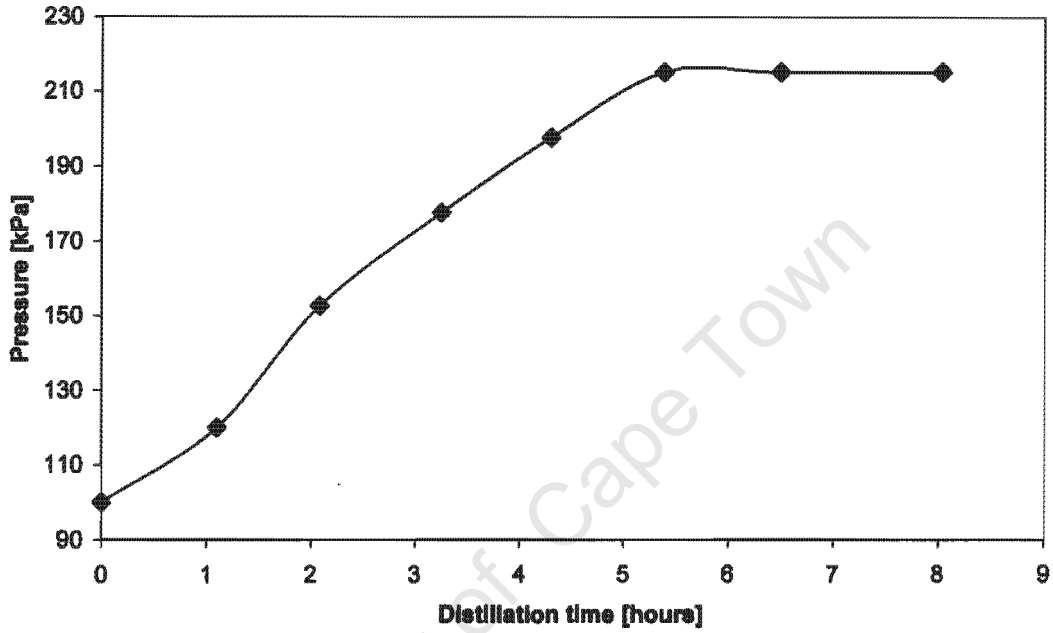

Fig 4.7: Column pressure for isomerization of the feed over the Nickel/Alumina catalyst.

Fig 4.8 indicates the column temperature profile for the isomerization of the feed over the Nickel/Alumina catalyst at 200 kPa.

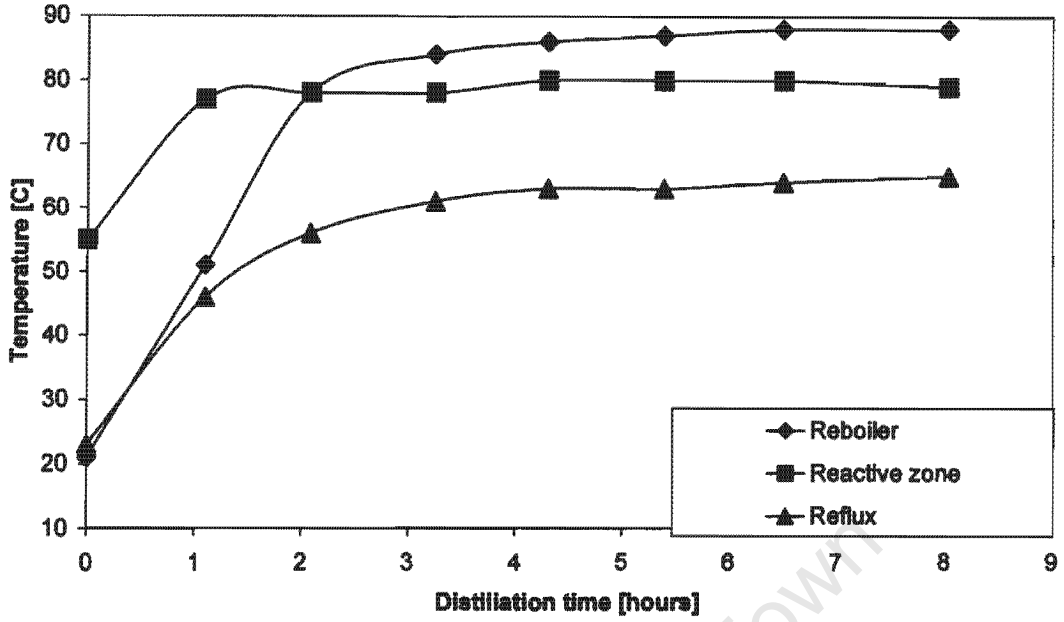

Fig 4.8: Column temperature profile for the isomerization of the feed over the Nickel/Alumina catalyst at 200 kPa.

As expected Fig 4.8 seemingly supports Fig 4.4, 4.5, 4.6 and 4.7 in the assertion that steady state is reached after 6 hours.

4.3 Validation of the model with experimental data

To validate the simple simulation model described in the previous chapter, reboiler composition of 1-hexene obtained experimentally was compared with that predicted by the model. In the model, the composition at the condenser is set to be the same as the experimentally determined value and then the ordinary differential and algebraic equations describing the operation are solved using a DDASAC method (Caracotsis and Stewart, 1985) in FORTRAN to obtain the reboiler composition. Table 4.2 gives the results of pseudo steady state composition of 1-hexene obtained for a case of the absence of hydrogenation reaction, i.e. distillation alone:

Table 4.2: Comparison between measured and predicted reboiler composition of 1-hexene in the reboiler

Gas flow rate [mmol/s]	Measured composition	Predicted composition	AARE %
0.732	0.545	0.548	0.60
1.09	0.536	0.544	3.12
1.30	0.543	0.551	1.44
1.52	0.537	0.545	1.49
1.77	0.538	0.549	2.04
2.31	0.535	0.565	5.35

In Table 4.2 the average absolute relative error percentage between the measured and predicted values is defined as:

$$\text{AARE \%} = 100\left(\frac{1}{N}\right)\sum_{i=1}^{N}\left|\frac{\left(y_{calc,i} - y_{exp,i}\right)}{y_{calc,i}}\right| \tag{4.3}$$

The significance of AARE % is that it shows that the predicted values are very close to the measured values, especially considering experimental error in obtaining the latter. Therefore, the model can be considered to be accurate enough in describing the distillation process taking place in the packed section of the column in the absence of hydrogenation reaction.

Fig 4.9 shows the liquid concentration profile over the CD column length as a function of the boilup rate in the absence of hydrogenation reaction. As expected, for all flow rates, the mole fraction of the more volatile component, 1-hexene, is the highest at the reboiler than in the condenser. In addition, as the boilup rate increases, the top concentration increases. Due to low flow rate and small column length, the concentration change over the entire column length is too small. Nonetheless, there is a clear trend among all the flow rates investigated. Unfortunately, higher flow rates and longer column height was not possible.

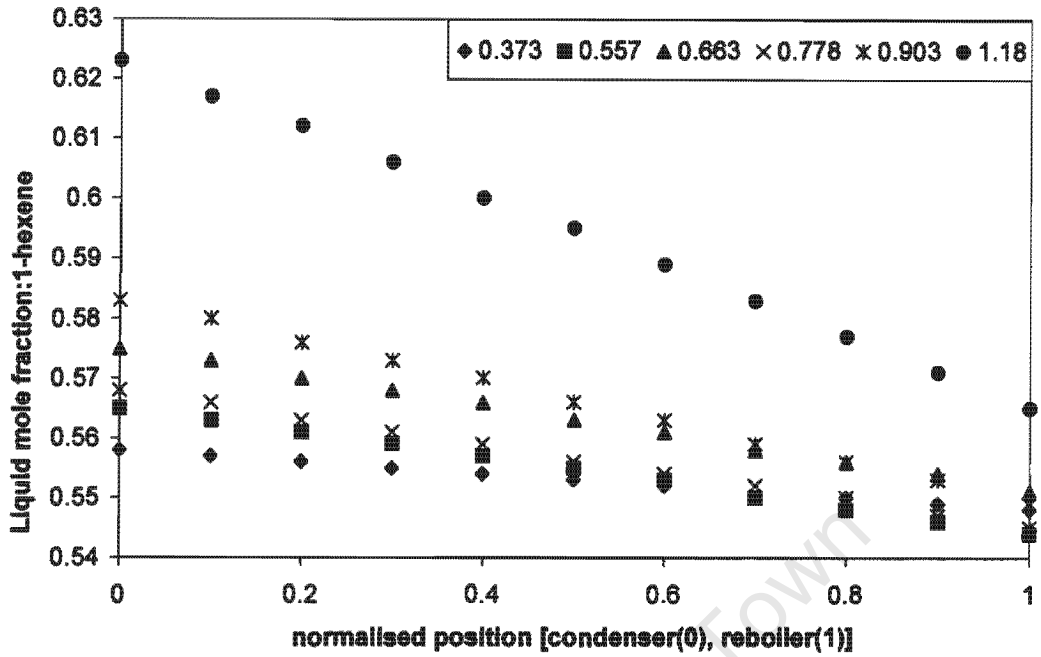

Fig 4.9: Liquid concentration profile of 1-hexene across the height of the column, plotted as a function of liquid mole flux, for distillation in the absence of hydrogenation reaction.

The presence of reaction will obviously influence the dynamics of the column, and hence different results from those listed in Table 4.2 will be obtained. With the presence of reaction, $k_y a$ in Equation (3.55) is unkown. To facilitate the solution, it is assumed that the presence of reaction does not significantly affect the value of $k_y a$. The number of moles of hydrogen and 1-hexene/n-hexane mixture in the vapour phase is determined using the ideal gas law. The liquid mixture concentration in the reboiler and condenser were estimated, and the average value of these was used in Equation (3.30) to determine K_A. The liquid densities used for determining the liquid mixture concentration were estimated using the DIPPR Equation:

$$\rho_{L,i} = \frac{M_i A}{B^{\left[1+(1-T/C)^D\right]}} \tag{4.4}$$

Where A, B, C, and D are constants which are specific to a chemical component and M_i is the molar mass of species i. The Henry's constant

used in Equation (3.30) was obtained by extrapolating the data presented by Orentlicher and Prausnitz (1964). The liquid side mass transfer coefficient of 1-hexene was determined using the Equation presented by Huang *et al.* (1998):

$$K_X a = m\frac{L}{V}K_Y a \tag{4.5}$$

where the gas side mass transfer coefficient, $K_Y a$, has been experimentally determined, and the equilibrium constant, m, is taken to equal to the ratio of vapour pressures of 1-hexene and n-hexane defined in Equation (4.2). The gas and liquid molar flow rates used in Equation (3.37) and (3.38) were based on the area of an empty column as opposed to a packed column area.

To test the validity of the model in the presence of hydrogenation reaction, the measured condenser composition of 1-hexene was used in the model to predict the reboiler composition. The results listed in Table 4.3 indicate the pseudo steady state composition of 1-hexene in the reboiler. The measured composition of 1-hexene is on a hydrogen free basis. The molar fraction of hydrogen is estimated using the ideal gas equation. In the ideal gas equation, the temperature used is the average of the temperatures along the column packing.

Table 4.3: Comparison between measured and predicted 1-hexene composition in the reboiler

Gas flow rate [mmol/s]	Measured composition	Predicted composition	AARE %
0.732	0.305	0.373	18.5
1.09	0.236	0.325	27.5
1.30	0.211	0.368	42.8
1.52	0.403	0.425	5.18
1.77	0.264	0.293	9.78

The values of the measured composition were estimated in the presence of hydrogen. The hydrogen mole fraction in the vapour phase is estimated using

the ideal gas law. In the simulation code, it is necessary to estimate the liquid flow rate since it is not equal to the boil up rate when the reaction is present. The liquid rate was estimated using the molar flux rate in the condenser. The Hirschfelder, Bird and Spotz correlation is used to estimate the binary diffusivity between 1-hexene and n-hexane in the condenser. It is assumed that the non-condensable hydrogen in the condenser has negligible effect on the condensable composition of the hydrocarbons.

As the values of AARE % at each flow rate indicate, there is discrepancy between the measured and predicted composition values. However, the AARE % values are not too large considering the assumptions made in the evaluation of the predicted composition values. Hence, the model can be considered to be valid with respect to taking into account the effect of hydrogenation reaction. In literature there is no correlations of liquid phase mass transfer coefficient of hydrogen through a hydrocarbon liquid phase measured in a CD environment. Most liquid phase mass transfer coefficients found in literature so far were measured in the absence of hydrogen, or at least some noncondensable gas, and therefore are inapplicable in this case. Therefore, one of the key assumptions made in obtaining the values listed in Table 4.3 is that the liquid phase mass transfer coefficient of hydrogen as required in Equation (3.27) through to (3.30) is equal to the liquid phase mass transfer coefficient of 1-hexene.

Fig 4.10 to 4.14 show the concentration profile of 1-hexene over the CD column length for the dual effect of distillation and hydrogenation reaction for all the boil up rates investigated.

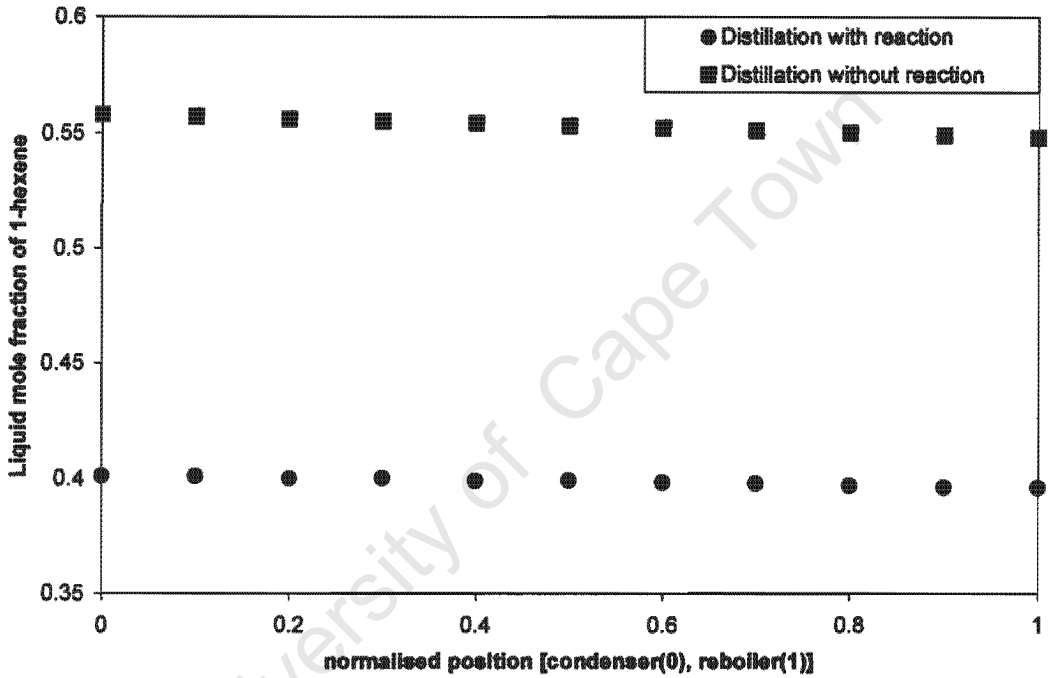

Fig 4.10: Liquid concentration profile due to the combined effect of distillation and hydrogenation reaction for boilup flow rate of 0.377 mol/m^2.s.

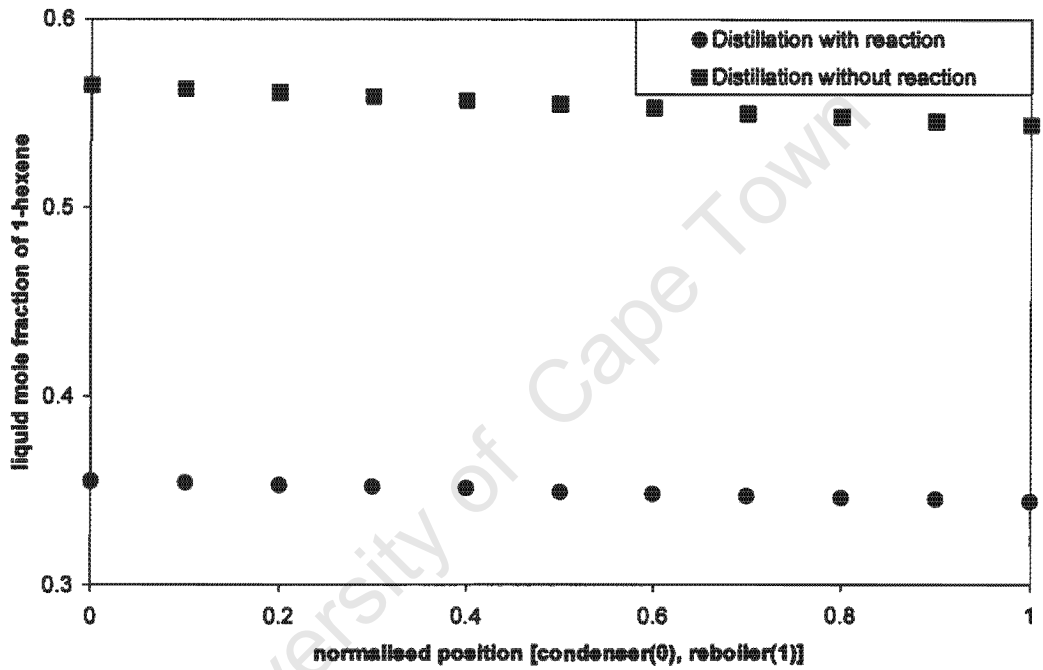

Fig 4.11: Liquid concentration profile due to the combined effect of distillation and hydrogenation reaction for boilup flow rate of 0.560 mol/m^2.s.

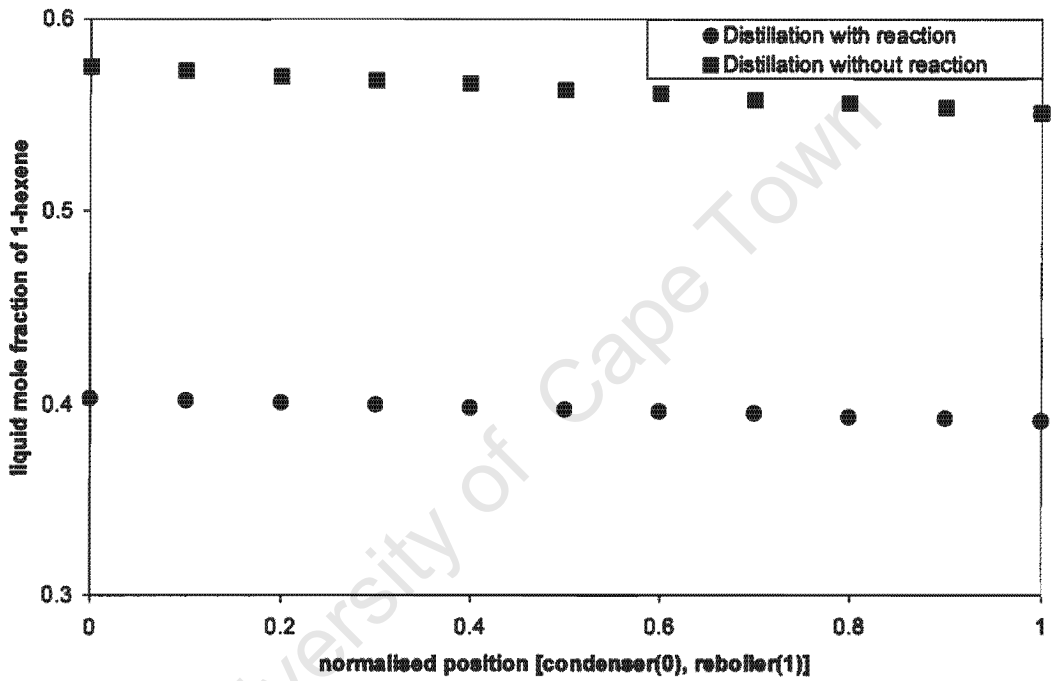

Fig 4.12: Liquid concentration profile due to the combined effect of distillation and hydrogenation reaction for boilup flow rate of 0.669 mol/m^2.s.

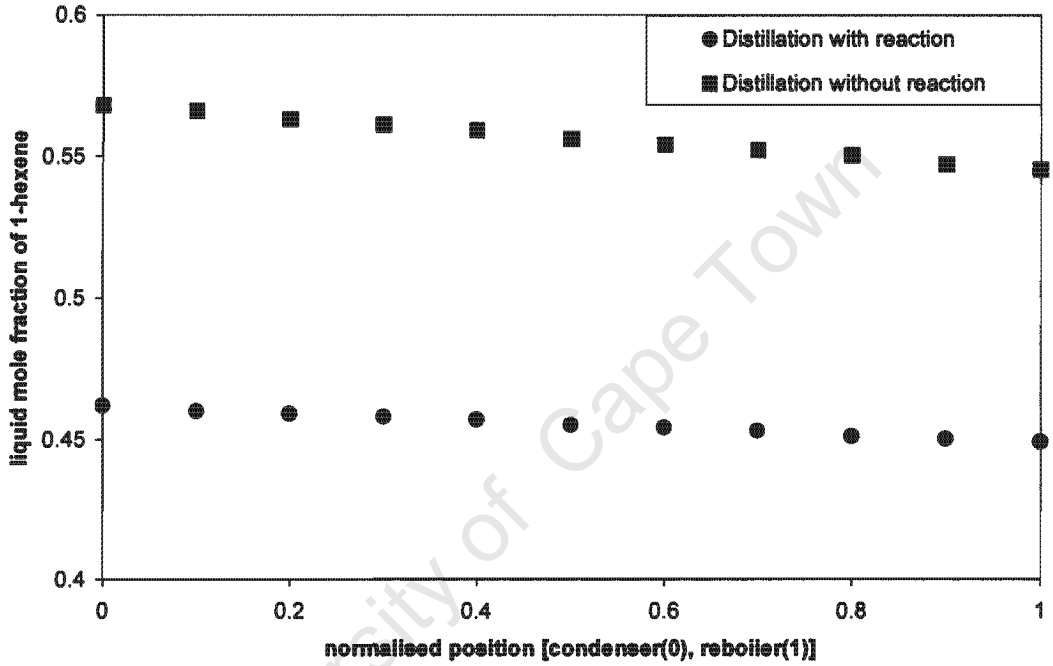

Fig 4.13: Liquid concentration profile due to the combined effect of distillation and hydrogenation reaction for boilup flow rate of 0.783 mol/m^2.s.

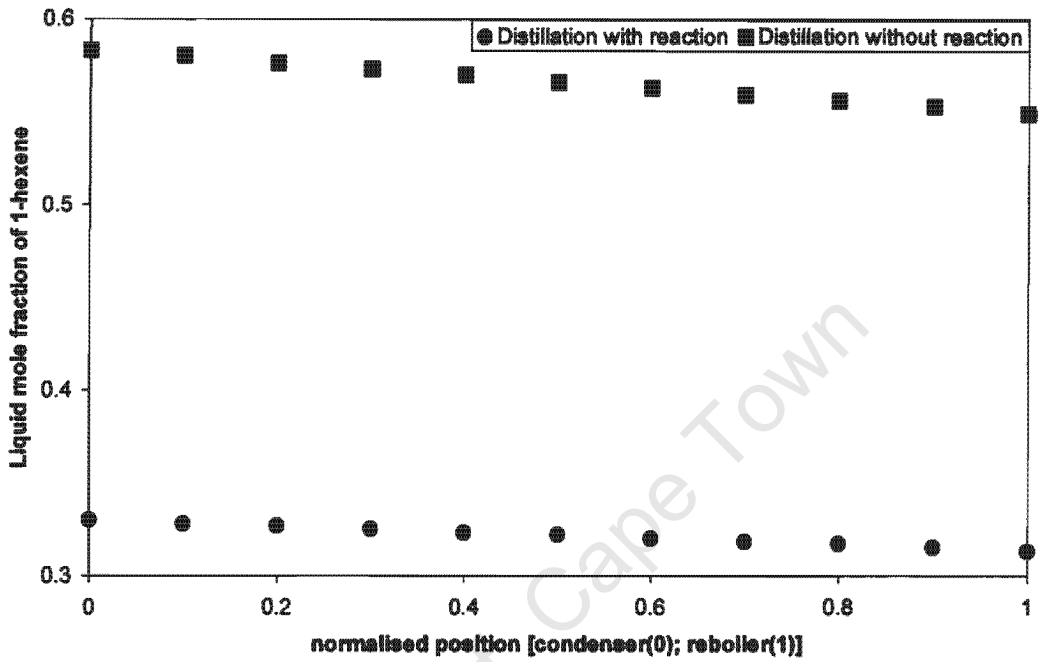

Fig 4.14: Liquid concentration profile due to the combined effect of distillation and hydrogenation reaction for boilup flow rate of 0.908 mol/m^2.s.

Fig 4.10 to 4.14 clearly indicate that the presence of hydrogenation reaction results in the expected decrease in concentration of 1-hexene over the column length.

Fig 4.15 shows y-x plot, also known as McCabe-Thiele plot, for distillation without reaction. It is clear from Fig 4.15 that the experimental data points investigated obey the distillation equilibrium curve.

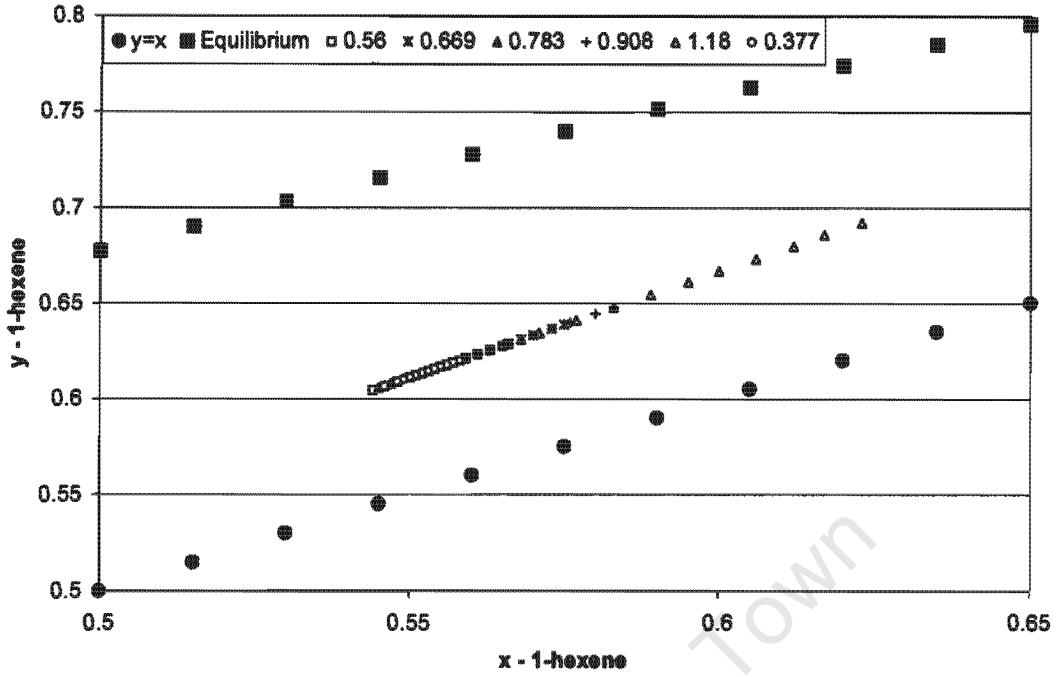

Fig 4.15: McCabe-Thiele plot for the distillation of the 1-hexene/n-hexane mixture without hydrogenation reaction.

Fig 4.16 to 4.20 illustrate the effect of hydrogenation reaction on McCabe-Thiele plot for the boilup rates investigated. It is clear from these plots that hydrogenation reaction causes the distillation lines to fall outside the equilibrium curve, which is consistent with the 'theoretical' results illustrated by Fig 3.5. Although this behaviour looks at first unusual it can be explained. Barbosa and Doherty (1988) studied the effect of equilibrium chemical reactions on vapour-liquid equilibrium and distillation processes by using reactive-phase diagrams and residue curve maps, whereby it was shown that equilibrium chemical reactions can create or break distillation boundaries. It is understood here that similar reasoning can be applied. Therefore, it can be concluded that the presence of irreversible reaction, as investigated experimentally here, can result in the elimination of distillation boundaries.

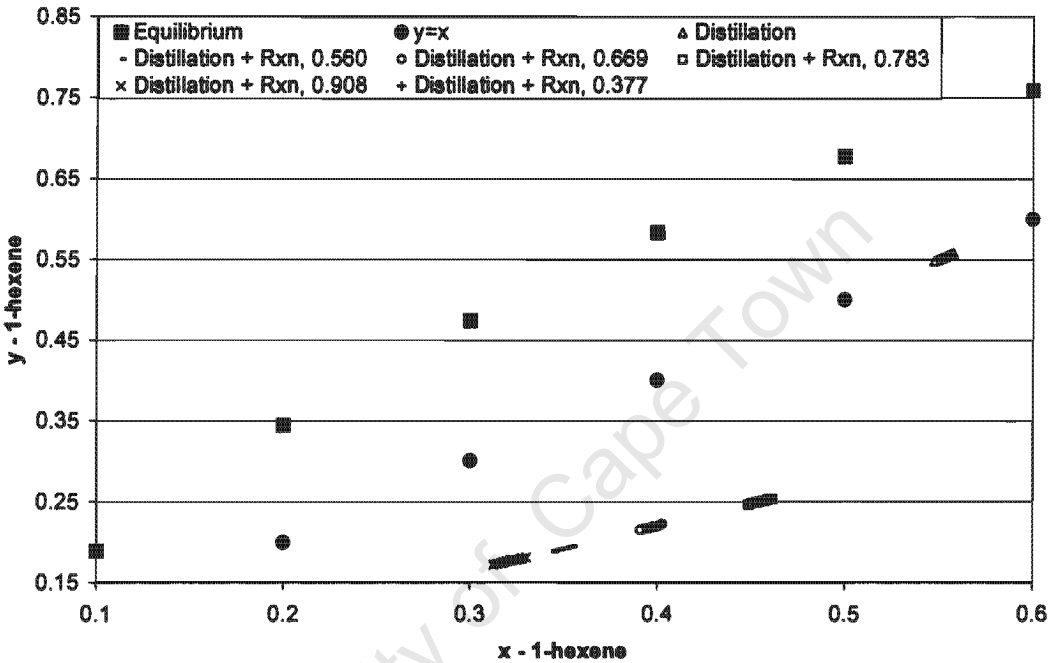

Fig 4.16: Effect of hydrogenation reaction on McCabe-Thiele plot for the 1-hexene/n-hexane/hydrogen mixture. The distillation case is for boilup rate of 0.377 mol/m^2.s.

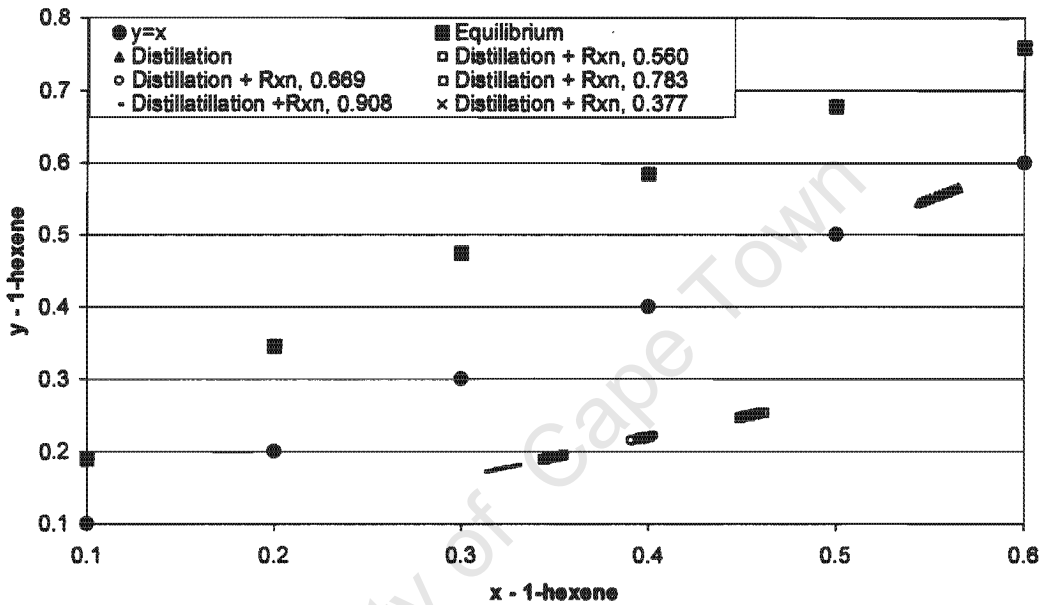

Fig 4.17: Effect of hydrogenation reaction on McCabe-Thiele plot for the 1-hexene/n-hexane/hydrogen mixture. The distillation case is for the flow rate of 0.560 mol/m^2.s.

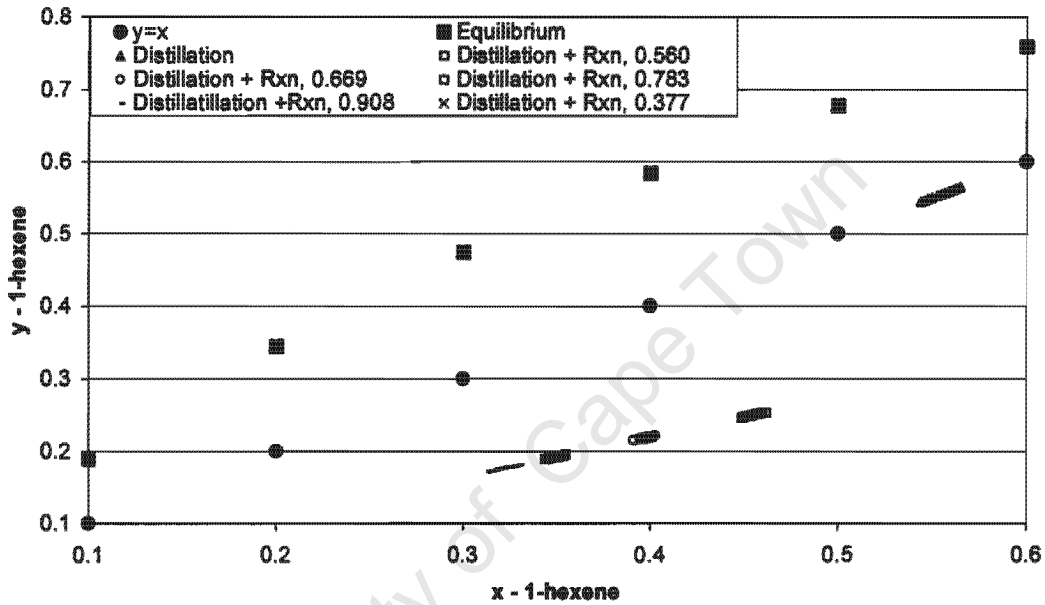

Fig 4.18: Effect of hydrogenation reaction on McCabe-Thiele plot for the 1-hexene/n-hexane/hydrogen mixture. The distillation case is for the flow rate of 0.669 mol/m^2.s.

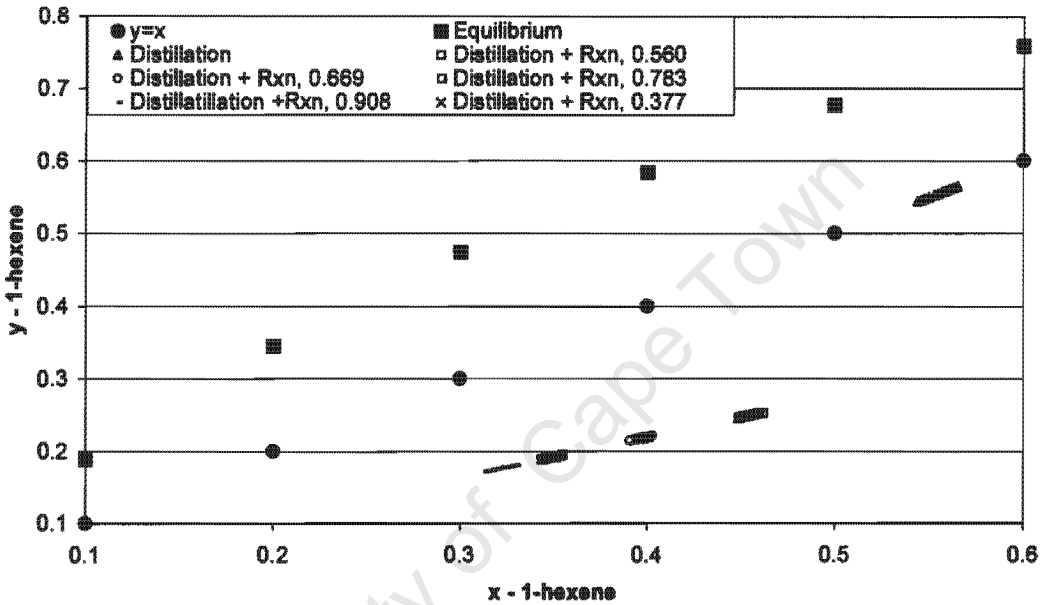

Fig 4.19: Effect of hydrogenation reaction on McCabe-Thiele plot for the 1-hexene/n-hexane/hydrogen mixture. The distillation case is for the flow rate of 0.783 mol/m^2.s.

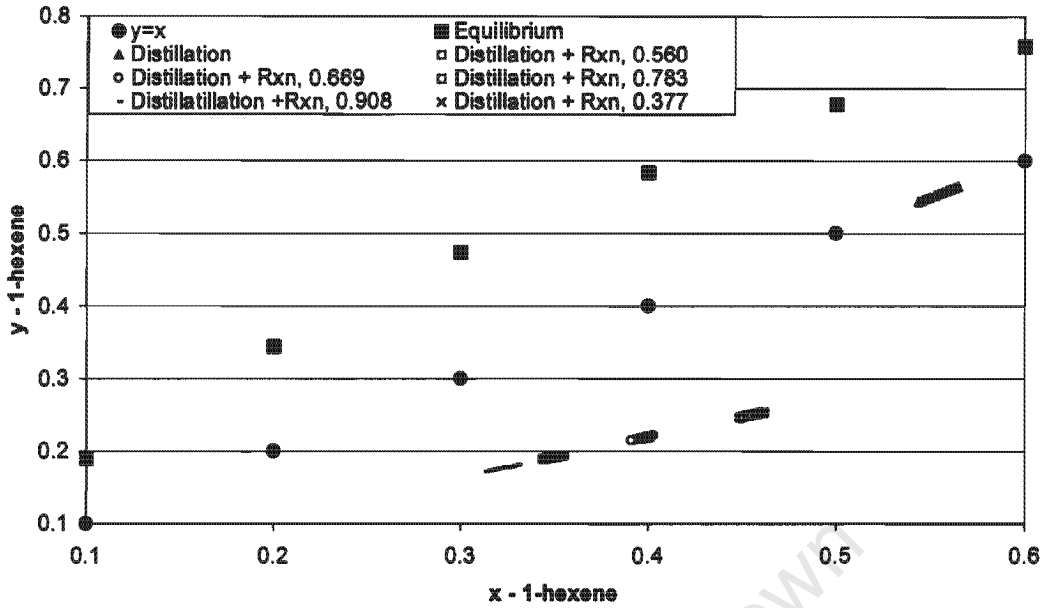

Fig 4.20: Effect of hydrogenation reaction on McCabe-Thiele plot for the 1-hexene/n-hexane/hydrogen mixture. The distillation case is for the flow rate of 0.908 mol/m^2.s.

4.4 Effect of hydrogen on the reboiler composition

Fig 4.21 to 4.25 show the effect of hydrogen on concentration profile of 1-hexene over the distillation column height. In all cases investigated, the liquid concentration of 1-hexene in the reboiler increases with increasing concentration of hydrogen. This is rather surprising since the reaction rate of hydrogen, and similarly that of 1-hexene, should increase with increasing amount of hydrogen. However, this depends on among other factors, column pressure and temperature.

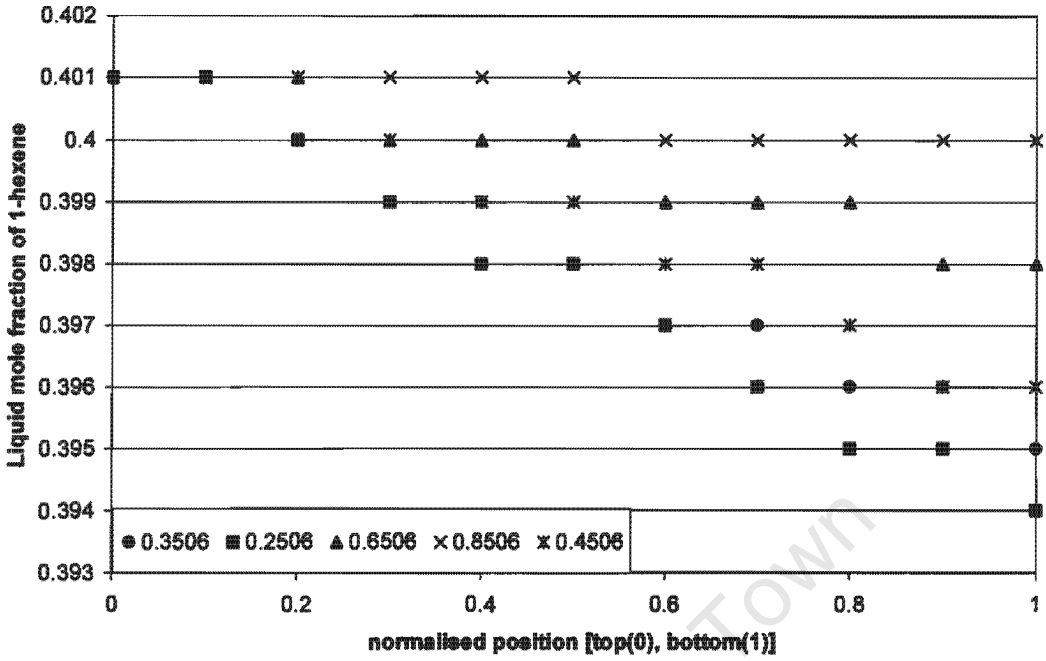

Fig 4.21: Effect of hydrogen on concentration profile of 1-hexene for a boilup rate of 0.377 mol/m^2.s.

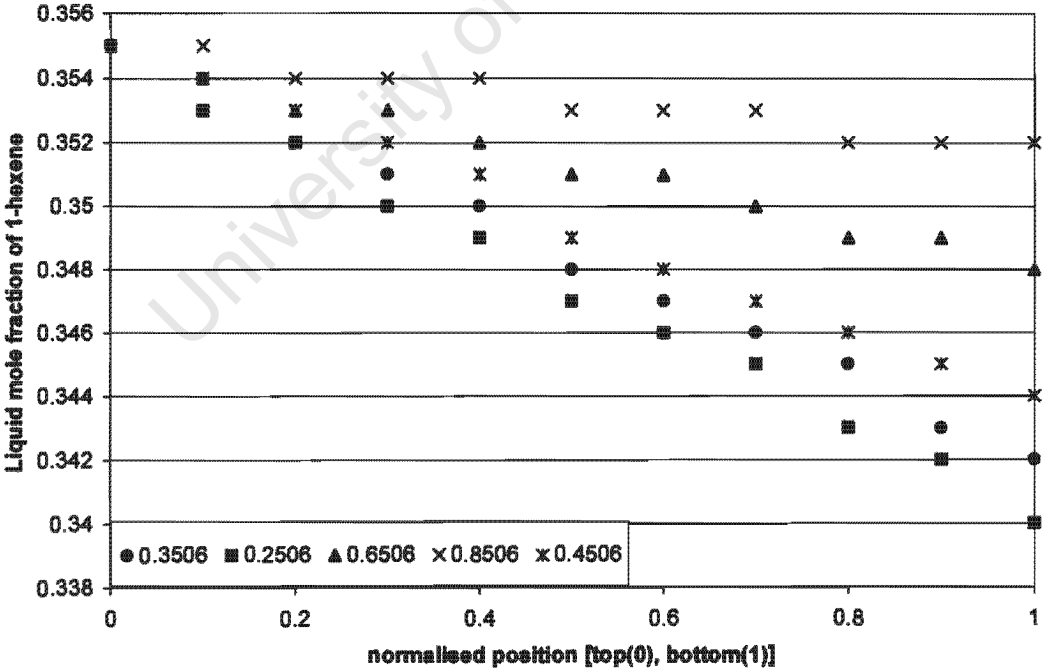

Fig 4.22: Effect of hydrogen on concentration profile of 1-hexene for a boilup rate of 0.560 mol/m^2.s.

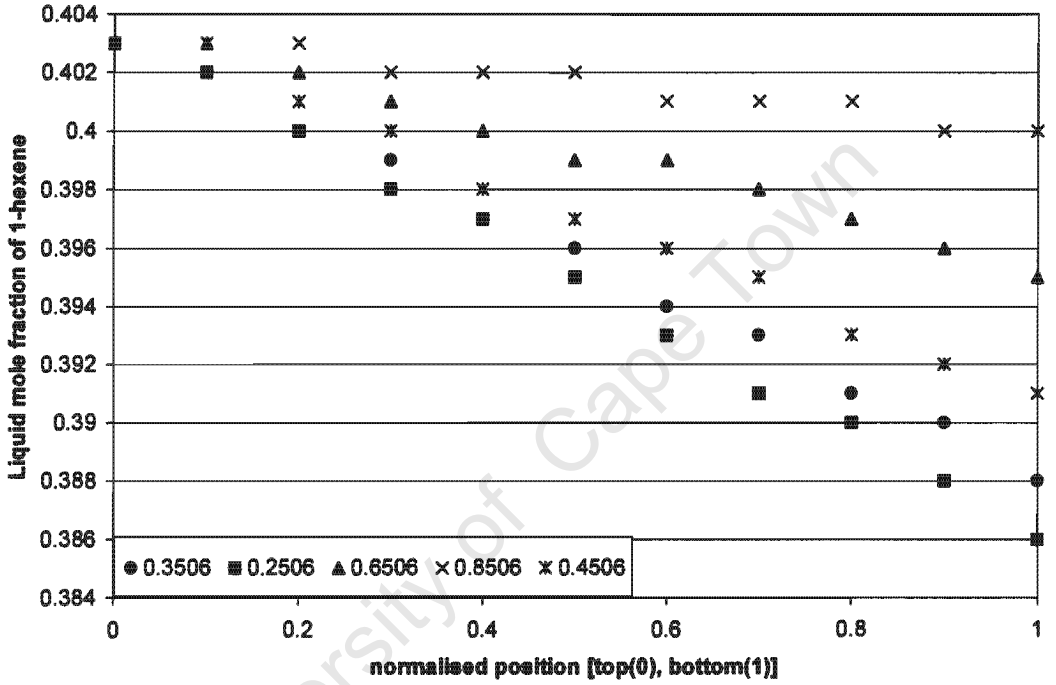

Fig 4.23: Effect of hydrogen on concentration profile of 1-hexene for a boilup rate of 0.669 mol/m^2.s.

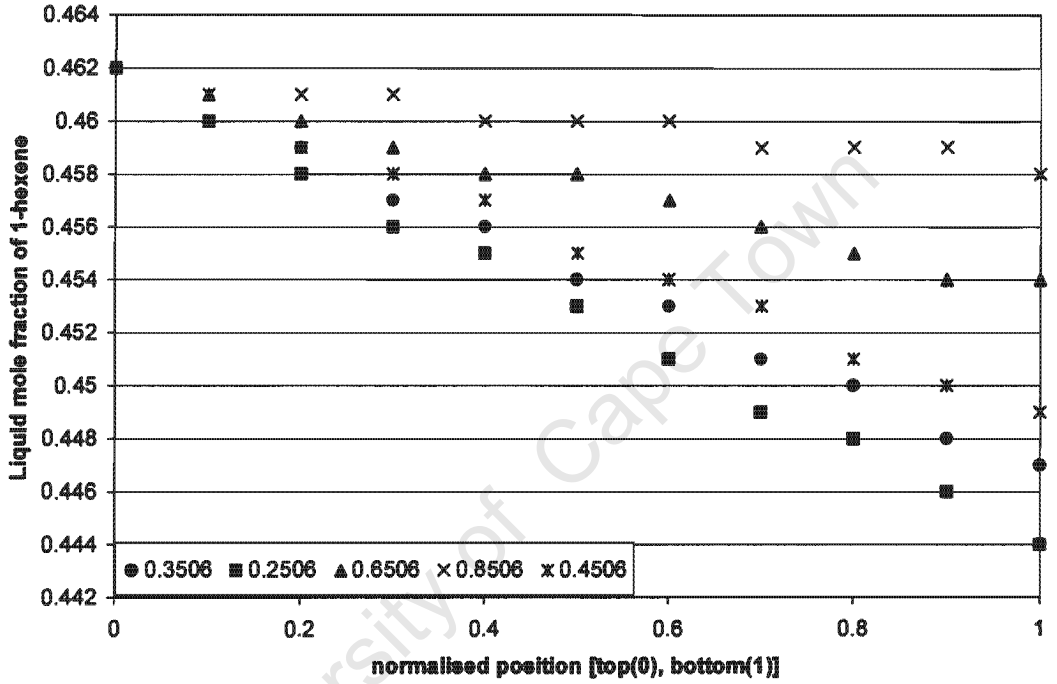

Fig 4.24: Effect of hydrogen on concentration profile of 1-hexene for a boilup rate of 0.783 mol/m^2.s.

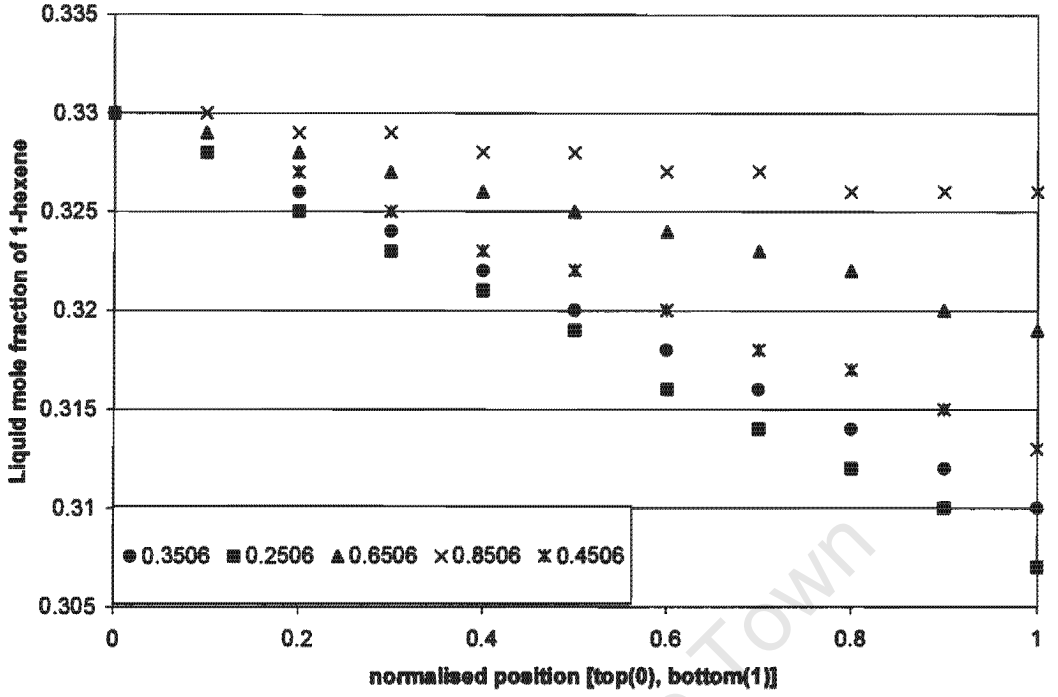

Fig 4.25: Effect of hydrogen on concentration profile of 1-hexene for a boilup rate of 0.908 mol/m^2.s.

4.5 Analysis of the modeling results

The slight disagreement between the experimental and modeling composition results listed in Table 4.3 can be accounted by the following facts:

- Hydrogenation of 1-hexene is an exothermic reaction, and therefore there are concentration gradients between the catalyst surface and the bulk conditions. Therefore the usage of bulk concentration in the determination of C_i (in Equation (3.21) is not accurate.
- Determination of condenser compositions is slightly inaccurate because the amount of hydrogen that escapes during sampling cannot be accounted for.
- Vapour-liquid equilibrium should strictly be considered to be ternary to improve the results.
- A correlation for determining the liquid phase mass transfer for hydrogen in Equation (3.31) is needed to improve the results.

- The range of boilup rates is narrow. It would have been preferable to carry out experiments on a wide range of boilup rates.

Nonetheless, the model provides adequate description of the distillation process in the absence or presence of chemical reaction. Therefore, given enough data to describe the additional correlations required by the CD process, the model shows promise.

5. CONCLUSIONS AND RECOMMENDATIONS

As set out in the introduction, there were two aims for this study, viz evaluating the effect of irreversible catalytic chemical reaction on the gas phase mass transfer coefficient through the use of y-x diagrams, and secondly to experimentally evaluate the overall gas phase mass transfer coefficient.

As shown in Fig 4.1 the gas phase mass transfer coefficient increases with increasing gas/liquid flow rate in the column. This result confirmed the hypothesis made in Chapter 1, and agreed with the studies carried out by Bravo *et al.*(1985), Zheng and Xu (1992), Dudukovic (1996), Subawalla *et al.* (1997), Huang *et al.* (1998a) and Van Baten and Krishna (2002). The results in Table 4.2 and 4.3 confirmed that the model developed in Chapter 3 was indeed valid when compared with the experimental data.

As shown in Fig 4.16 to 4.20, the hydrogenation reaction broke the distillation boundaries established in Fig 4.15. This result agrees with the work of Barbosa and Doherty (1988) in which they found that an equilibrium chemical reaction could break distillation boundaries.

So the two hypotheses set out in Chapter 1 have been fulfilled. Nevertheless there are few improvements that could be made to further enhance the results of this study. Firstly, a wide range of gas/liquid flow rates could be investigated to establish clear trends in Fig 4.16 to 4.20. A catalyst with a support other than alumina, Al_2O_3, for example charcoal, could be used to avoid isomerization. The distillation column setup used in this study could be re-designed, such that a pump is introduced to pump the unreacted hydrogen gas back to the reactive zone. This will eliminate the problem of insufficient diffusion of n-hexane through the hydrogen gas. The reaction rate of hydrogenation of 1-hexene could be measured in a classical reaction engineering reactor, such as a CSTR, so that a true rate can be obtained. A full dynamic simulation for the simple model developed in Chapter 3 could be carried out to evaluate the transient behaviour of the process. Finally, the

liquid-solid mass transfer coefficient could be experimentally measured, and its effect on the global reaction rate can then be evaluated.

References

1) Agreda, V.H., Partin, L.R., Heise, W.H., "*High-purity methyl acetate via reactive distillation*", Chemical Engineering Progress, 1990, **54**, 1299-1305.
2) Aiouache, F, Goto, S, "*Reactive distillation–pervaporation hybrid column for tert-amyl alcohol etherification with ethanol*", Chemical Engineering Science, 58(12), 2003, 2465-2477.
3) Al-Dahhan, M., Highfill, W., Ong, B., "*Drawbacks of the dissolution method for the measurement of liquid-solid mass transfer coefficients in two-phase flow packed-bed reactors operated at low and high pressures*", Industrial and Engineering Chemistry Research, 2000, **39**(8), 3102-3107.
4) Astarita, G., "*Mass transfer with chemical reaction*", 1967, Amsterdam: London Elsevier
5) Augustine, R.L., "*Catalytic hydrogenation: techniques and application in synthesis*", 1965, Dekker, New York.
6) Barbosa, D, Doherty, M.F., "*The influence of equilibrium chemical reactions on vapour-liquid phase diagrams*", Chemical Engineering Science, 1988, **43**(3), 529-540.
7) Baur, R.; Taylor, R., Krishna, R., "*Dynamic behaviour of reactive distillation tray columns described with a nonequilibrium cell model*", Chemical Engineering Science, 2001*a*, **56**(4), 1721-1729.
8) Baur, R.; Taylor, R., Krishna, R., "*Dynamic behaviour of reactive distillation columns described by a nonequilibrium stage model*", Chemical Engineering Science, 2001*b*, **56**(6), 2085-2102.
9) Baur, R.; Taylor, R., Krishna, R., "*Development of a dynamic nonequilibrium cell model for reactive distillation tray columns*", Chemical Engineering Science, 2000*a*, **55**(24), 9139-6154.
10) Baur, R; Higler, A.P., Taylor, R; Krishna, R, "*Comparison of equilibrium stage and nonequilibrium stage models for reactive distillation*", Chemical Engineering Journal, 2000*b*, **76**(1), 33-47.
11) Bhaskar, M., Valavarasu, G., Meenakshisundaram, A., Balaraman, K.S., "*Application of a three phase heterogeneous model to analyse the*

performance of a pilot plant trickle bed reactor", Petroleum Science and Technology, 2002, **20**(3-4), 251-268.

12) Billet, R. and Schultes, "*Predicting mass transfer in packed columns*", Chemical Engineering Technology, 1993, **16**, 1-9.

13) Bird, R.B., Stewart, W.E., Lightfoot, E.N., "*Transport phenomena*", 2nd edition, 2002, John Wiley and Sons Inc.

14) Bond, G.C., "Catalysis by metals, 1962, Academic, London and New York.

15) Boutonnet, M., Andersson, C., Larsson, R., "*Liquid-phase hydrogenation of 1-hexene and 2-hexene with 30 Å platinum particles on alumina support*", Acta Chemica Scandinavica, 1980, **34**, 639-644.

16) Bravo, J.L, Rocha, J.A, Fair, J.R, "*Mass transfer in gauze packings*", Hydrocarbon processing, 1985, 1, 91-95.

17) Brian, P.L.T., Hales, H.B., "*Effects of transpiration and changing diameter on heat and mass transfer to spheres*", American Institute of Chemical Engineers, 1969, **15**(3), 419-425.

18) Caracotsis, M.; Stewart, W.E, "*Sensitivity analysis of initial value problem with mixed ODEs and algebraic equations*", Computers and Chemical Engineering, 1985, **9**(4), 359-365.

19) Carturan, G., Scrivanti, A., "*Hydrogenation of 1-hexene catalyzed by saline hydride-reduced palladium*", Journal of Molecular Catalysis, 1979, **5**, 139-146.

20) Chen, G.X. and Chuang, K.T., "*Determining the number of gas-phase and liquid-phase transfer units from point efficiencies in distillation*", Industrial Engineering and Chemistry Research, 1994, **33**, 907-913.

21) Chen, G.X. and Chuang, K.T., "*Liquid-phase resistance to mass transfer on distillation trays*", Industrial Engineering and Chemistry Research, 1995, **34**, 3078-3082.

22) Chilton, T. H. and Colburn, A. P., "*Distillation and absorption in packed columns*", Industrial and Engineering Chemistry, 1935, No. 3, 255-260.

23) Chou, S., Chen, S., Tan, C., "*Hydrogenation of dicyclopentadiene in a trickle bed reactor*", Journal of the Chinese Institute of Chemical Engineers, 1997, **28**(3), 175 – 183.

24) Danckwerts, P. V., Industrial and Engineering Chemistry, 1951, **43**, 1460-1467.

25) Fair, J.R., Bravo, J.L., "*Distillation columns containing structured packing*", Chemical Engineering Progress, 1990, **1**, 19-29.

26) Frank, M.J.W., Kuipers, J.A.M., Versteeg, G.F., Van Swaaij, W.P.M, "*Modelling of simultaneous mass and heat transfer with chemical reaction using the Maxwell-Stefan theory – Model development and isothermal study*", Chemical Engineering Science, 1995; **50**(10), 1645-1659.

27) Henley, J. E. and Seader, J. D.," *Separation process principles*, John Wiley and Sons Inc., 1998, 90-154.

28) Herskowitz, M., "*Wetting efficiency in trickle bed reactors: The overall effectiveness factor of partially wetted catalyst particles*", Chemical Engineering Science, 1981, **36**(10), 1665-1671.

29) Herskowitz, M., Abuelhaija, M., "*Liquid-solid mass transfer in a trickle bed reactor measured by a means of a catalytic reaction*", Annual meeting of American Institute of Chemical Engineers, New York, 1985, 79E.

30) Higbie, R., Transactions of American Institute of Chemical Engineers, 1935, **31**, 365-389.

31) Higler, A.P., Taylor, R., Krishna, R., "*Nonequilibrium modelling of reactive distillation: a dusty fluid model for heterogeneously catalyzed process*", Industrial and Engineering Chemistry Research, 2000, **39**(6), 1596-1607.

32) Higler, A.P., Taylor, R., Krishna, R., "*Influence of mass transfer and mixing on the performance of a tray column for reactive distillation*", Chemical Engineering Science, 1999, **54**(13), 2873-2881.

33) Highfill, W, Al-Dahhan, M.,"*Liquid-solid mass transfer coefficient in high pressure trickle bed reactors*", Chemical Engineering Research and Design, 2001, **79**(6), 631-640.

34) Huang, C., Kuo, C., "*Mathematical models for mass transfer accompanied by reversible chemical reaction*", American Institute of Chemical Engineers Journal, 1965, **11**(5), 901-910.

35) Huang, C, Ng, F.T.T., Rempel, G.L, " *Application of catalytic distillation for the aldol condensation of acetone: the effect of mass transfer and kinetic rates on the yield and selectivity*", Chemical Engineering Science, 2000, **55**(23), 5919-5931.

36) Huang, C, Yang, L., Ng, F.T.T, Rempel, G.L, "*Application of catalytic distillation for the aldol condensation of acetone: a rate-based model in simulating the catalytic distillation performance under steady-state operations*", Chemical Engineering Science, 1998*a*, **53**(19), 3489-3499.

37) Huang, C., Podrebarac, G. G. and Rempel, G. L., "*A study of mass transfer behaviour in a catalytic distillation column*", The Canadian Journal of Chemical Engineering, 1998*b*, **76**, 323-330.

38) Irandoust, S. and Andersson, B., "*Concentration-dependent diffusivity of benzoic acid in water and its influence on the liquid-sold mass transfer*", The Canadian Journal of Chemical Engineering, 1986, **64**, 954-959.

39) Johnson, A.I., Akehata, T., "*Reaction accompanied mass transfer from fluid and solid spheres at low Reynolds numbers*", The Canadian Journal of Chemical Engineering, 1965, **43**, 10-15.

40) Johnstone, H.F, Pigford, R.L., Transactions of American Institute of Chemical engineers, **38**, 1942, 25-30.

41) Kelkar, C. P.; Akyurtlu, J. F.; Akyurtlu, A.; Hamrin, C. E., "*Performance of an annular catalytic three phase reactor for a second order reaction*", Chemical Engineering Communications, 1992, **117**, 101-109.

42) Kieboom, A. P. G., *Hydrogenation and hydrogenolysis in synthetic organic chemistry*, Delft University Press, 1977.

43) Knudsen, J. G., Hottel, H. C., Sarofin, A.F., Wankat, P.C and Knaebel, K.S., "*Heat and mass transfer in Perry's chemical engineers' handbook*", McGraw-Hill international Series, 1998, **7th ed.**, 5-54 – 5-79.

44) Kolodziej, A., Jaroszynski, M., Hoffman, A, GoraK, A., "*Determination of catalytic packing characteristics for reactive distillation*", Catalysis Today, 2001, 75-85

45) Krishna, R., "*Reactive separations: more ways to skin a cat*", Chemical Engineering Science, 2002, **57**, 1491-1504.

46) Krishna, R. and Standart, G. L.," *Mass and energy transfer in multicomponent systems*", Chemical Engineering Communications, 1979, **3**, 201-275.

47) Larachi, F., Laurent, A., Wild, G. and Midoux, N., "*Pressure effects on gas-liquid interfacial areas in cocurrent trickle-flow reactors*", Chemical Engineering Science, 1992, **47**, 2325-2330.

48) Lara-Marquez, A., Larachi, F., Wild, G. and Laurent, A., "*Mass transfer characteristics of fixed beds with cocurrent upflow and downflow. A special reference to the effect of pressure*", Chemical Engineering Science, 1992, **47**, 3485-3490.

49) Levenberg, K., Quart. Appl. Math, 1944, **2**, 164.

50) Levich, V.G., "*Physicochemical hydrodynamics*", 1962, Englewood Cliffs: Prentice-Hall, 1962.

51) Li, K.Y., Chiang, C.L., Hopper, J.R., "*New mass transfer model for partially wetted trickle bed reactor*", Annual meeting of American Institute of Chemical Engineers, New York, 1985, 131B.

52) Linton, W.H., Sherwood, T.K., Ibid., 1950, **46**, 258-268.

53) Marquardt, D.W, "*An algorithm for least squares estimation on nonlinear parameters*", SIAM J. Appl. Math, 1963, **11**, 431-441.

54) McCune, L.K., Wilhelm, R.H., "*Mass and momentum transfer in solid-liquid system*", Industrial and Engineering Chemistry, 1949, **41**(6), 1124-1134.

55) Mills, P. L., Beaudry, E.G and Dudukovic, M. P., "*Comparison and prediction of reactor performance for packed beds with two-phase flow: Downflow, upflow and countercurrent flow*", Institution of Chemical Engineers Symposium Series, 1984, **87**, 527-534.

56) Nerst, W., Journal of Physical Chemistry, 1904, **47**, 52-60.

57) Nishimura, Y., Ishii, T., "*An analysis of transport phenomena of multi-solid particle systems at higher Reynolds numbers by a standard Karman-Pohlhausen method-II*", Chemical Engineering Science, 1980, **35**(1), 1205-1209.

58) Onda, K., Takeuchi, H. and Okumoto, Y., "*Mass transfer coefficients between gas and liquid phases in packed columns*", Journal of Chemical Engineering of Japan, 1968, **1(1)**, 56-62.

59) Paludetto, R., Paret, G., Donati, G., "*Multicomponent distillation with chemical reaction: mathematical model analysis*", Chemical Engineering Science, 1992, **47**(9-11), 2891-2896.

60) Podrebarac, G. G., NG, F.T.T. and Rempel G. L., "*More uses for catalytic distillation*", Chemtech, 1997, No. **5**, 37-45.

61) Podrebarac, G.G., "*The dimerization of 1-butene using catalytic distillation*", M.A.Sc. Thesis, University of Waterloo, Waterloo, ON, 1992.

62) Rajashekaram, M.V., Jaganathan, R., Chaudhari, "*Trickle-bed reactor model for hydrogenation of 2,4 dinitrotoluene: experimental verification*", Chemical Engineering Science, **53**(4), 1998, 787-805.

63) Reid, R. C., Prausnitz, J.M., Poling, B.E., "*The properties of gases and liquids*", 1987, McGraw-Hill, New York.

64) Rock, K., Gildert, G.R. and McGuirk, T., "*Catalytic distillation extends its reach*", Chemical Engineering, 1997, No. **7**, 78-84.

65) Rode, S., Midoux, N., Latifi, M.A., Storck, A., "*Hydrodynamics and liquid-solid mass transfer mechanisms in packed beds operating in cocurrent gas-liquid downflow: An experimental study using electrochemical shear rate sensors*", Chemical Engineering Science, 1994, **49**(9), 1383-1401.

66) Roizard, C., Wild, G., "*Mass transfer with chemical reaction: the slow reaction regime revisited*", Chemical Engineering Science, 2002, **57**(16), 3479-3484.

67) Sakornwimon, W., Sylvester-Nicholas, D., "*Effectiveness factor for partially wetted catalysts in trickle bed reactors*", Industrial and Engineering Chemistry Process Design and Development, 1982, **21**(1), 16-25.

68) Satterfield, C.N., Van Eek, M.W. and Bliss, G.S., "*Liquid-solid mass transfer in packed beds with downward concurrent gas-liquid flow*", American Institute of Chemical Engineers Journal, 1978, **24**(4), 709-717.

69) Satterfield, C.N., "*Trickle-bed reactors*", American Institute of Chemical Engineers Journal, 1975, **21**, 209-220.

70) Savkovic-Stevanovic, J., "*Modelling of mass transfer phenomena of associated systems in packed distillation columns*", Chemical Engineering Technology, 1992, **15**, 453-440.

71) Schlichting, H., "*Boundary layer theory*", 1979, McGraw-Hill, New York.

72) Sherwood, T.K, Pigford, R.L. and Wilke C.R, "*Mass transfer*", McGraw-Hill International Series, 1975, 301-385.

73) Sims, W.B., Schulz, F.G. and Luss, D., "*Solid-liquid mass transfer to hollow pellets in a trickle bed*", Industrial Engineering and Chemistry Research, 1993, **32**, 1895-1903.

74) Skelland, A.H.P., "*Diffusional mass transfer*", 1974, John Wiley and Sons Inc, New York.

75) Subawalla, H., Gonzalez, J.C., Seibert, A.F., Fair, J.R., "*Capacity and efficiency of reactive distillation bale packing: modelling and experimental validation*", Industrial and Engineering Chemistry Research, 1997, **36**, 3821-3832.

76) Sundmacher, K. and Hoffmann, "*Development of a new catalytic distillation process for fuel ethers via a detailed nonequilibrium model*" Chemical Engineering Science, 1996, **51**(10), 2359-2368

77) Trambouze, P., "*Countercurrent two-phase flow in fixed bed reactors*", Chemical Engineering Science", 1990, **45**(8), 2269-2275.

78) Toor, H. L. and Marchello, J. M., American Institute of Chemical Engineers Journal, 1958, **4**, 97-101.

79) Toppinnen, S., Aittamaa, J., Salmi, T., "*Interfacial mass transfer in trickle bed reactor modelling*", Chemical Engineering Science, 1996, **51**(18), 4335-4345.

80) Turek, F., Lange, R, "*Mass transfer in trickle bed reactors at low Reynolds numbers*", Chemical Engineering Science, 1981, **36**(3), 569-579.

81) Uchytil, J., Kocova, E. and Kraus, M., "*Hydrogenation of alkenes on a nickel-tungsten-alumina catalyst*", Collection Czechoslovak Chemical Communication, 1981, **46**, 2076-282.

82) Van Krevelen, D. W., Krekels, J. T. C., "*Rate of dissolution of solid substances*", Recl. Trav. Chim. Pays-Bas, 1948, **14**, 1.

83) Versteeg, G.F., Visser, J.B.M., Van-Dierendonck, L.L., Kuipers, J.A.M., "*Absorption accompanied with chemical reaction in trickle bed reactors*", Chemical Engineering Science, 1997, **52**(21-22), 4057-4067.

84) Wammes, W. J., Middelkamp, J., Huisman, W. J., de Baas, C. M. and Westerterp, K. R., "*Hydrodynamics in a cocurrent gas-liquid trickle-bed at elevated pressure*", American Institute of Chemical Engineers Journal, 1991b, **37**, 1849-1855.

85) Welty, J. R., Wicks, C. E. and Wilson, R. E., "*Fundamentals of momentum, heat and mass transfer*", John Wiley & Sons, 1984, **3rd ed.**, 629-641.

86) Whitney, J. S and Vivian, K. N., Chemical Engineering Progress, 1949, **45**, 323-326.

87) Wild, G., Larachi, F. and Charpentier, J. C., " *Heat and Mass transfer in gas-liquid solid fixed bed reactors – heat and mass transfer in porous media*", Elsevier, Amsterdam, Netherlands, 1992, 616-680.

88) Williamson, J.E., Bazaire, K.E., Geankoplis, C.J., "*Liquid-phase mass transfer at low Reynolds numbers*", Industrial Engineering and Chemistry fundamentals, 1963, **2**(2), 126-129.

89) Zheng, Y. and Xu, X., "*Study on catalytic distillation processes, Part I: Mass transfer characteristics in catalyst bed within the column*", Transactions of The Institution of Chemical Engineers, 1992*a*, **70**(Part A), 459-464.

90) Zheng, Y, Ng, F.T.T., Rempel, G.L., "*A three phase nonequilibrium model for the simulation of the aldol condensation of acetone*", Industrial and Engineering Chemistry Research, 2001, **40**(23), 5342-5349.

91) Zhukova, T. B., Pisarenko, V. N. and Kafarov, V. V., "*Modelling and design of industrial reactors with a stationary bed of catalyst and two-phase gas-liquid flow: A review*", International Chemical Engineering Journal, 1990, **30(1)**, 57-102.

Appendix A - Sample Spreadsheet for calculation of Gas Phase Mass Transfer Coefficients

Sample of Spreadsheet to calculate the overall gas phase mass transfer coefficients

Column ID [m]	0.05
Nonreactive packing height [m]	0.16
Reactive packing height [m]	0.17
Catalyst bag ID [m]	0.02

Pseudo-steady state composition

	1-hexene composition							
Gas flow rate mol/s	Xreb, initial	Xreb	Xcond	Pressure kPa	NTU	Kga mol/m3/s/kPa	Kga, LLMT	Kga, ULMT
7.32E-04	0.509	0.506	0.520	205	0.358	1.57E-03	1.44E-03	1.70E-03
1.09E-03	0.503	0.499	0.527	215	0.739	4.62E-03	4.25E-03	4.98E-03
1.30E-03	0.502	0.504	0.537	212	0.851	6.41E-03	5.90E-03	6.93E-03
1.53E-03	0.502	0.498	0.530	225	0.820	6.83E-03	6.28E-03	7.38E-03
1.77E-03	0.503	0.499	0.545	220	1.204	9.27E-03	8.53E-03	1.00E-02
2.31E-03	0.501	0.496	0.586	230	2.363	1.86E-02	1.72E-02	2.01E-02

Appendix B - Sample Data: Distillation with Hydrogenation Reaction

Sample of the spreadsheet for outlet concentrations obtained experimentally

Experiment 10 29 April, 2002

Mass of Nickel/Alumina catalyst 50 g

		mol %			mol %				
		Reboiler			Condenser				
Sample #	Time [hrs]	Hexene	Hexane	Others	Hexene	Hexane	Others	Pcolumn [bar]	Treaction [K]
1	0	95.8	3.163	1.037	90.473	5.48	4.047	7.05	379
2	0	95.828	3.111	1.061	90.585	5.411	4.004	4.93	393
3	3.03	97.477	1.875	0.648	80.659	9.082	10.259	4.45	376
4	7.47	97.246	1.919	0.835	78.55	9.559	11.891	4.3	361
5	23.25	96.761	2.044	1.195	77.19	9.816	12.994	4.1	350
6	31.93	96.233	2.122	1.645	76.37	9.748	13.882	3.93	349
7	48.77	95.134	2.321	2.545	75.268	9.496	15.236	3.8	357
8	51.20	95.014	2.412	2.574	74.474	9.315	16.211	3.68	360

Note: Sample 1 is the initial sample and 2 is the total reflux condition
Other components include branched alkanes and alkenes in small and negligible quantities

Sample of spreadsheet for outlet concentrations obtained experimentally

Hydrogenation reaction

Experiment 7 25 July, 2002

Mass of Nickel/Alumina catalyst 50 g

Boil up flow rate [kmol/s] 1.3

		mol % Reboiler		mol % Condenser			
Sample #	Time [hrs]	Hexene	Hexane	Hexene	Hexane	Pcolumn [kPa, abs]	T, reaction zone [K]
1	0	98.944	1.056	-	-	550	79.5
2	3	98.716	1.284	99.566	0.434	525	79
3	4.12	97.797	2.203	93.91	6.09	507.5	79
4	7.33	97.569	2.431	84.876	15.124	452.5	79
5	20.2	97.357	2.643	59.067	40.933	235	78.5
6	25.29	96.673	3.327	55.511	44.489	155	79
7	27.49	96.231	3.769	44.247	55.753	152	80.5
8	34.36	95.581	4.419	43.221	56.779	150	80.5
9	37.33	93.86	6.14	40.14	59.86	150	80

Sample 1 is the initial reboiler charge before heating commenced
Sample 2 is taken at total reflux before putting Hydrogen on-stream

Appendix C - Effect of Isomerization Reaction

Sample of the spreadsheet for outlet concentrations obtained experimentally

Isomerization experiment

Experiment 10 29 April, 2002

Mass of Nickel/Alumina catalyst 50 g

Boil up flow rate [kmol/s] 1.3

		mol % Reboiler		mol % Condenser			
Sample #	Time [hrs]	Hexene	Hexane	Hexene	Hexane	Pcolumn [kPa, abs]	T, reaction zone [K]
1	0	99.17	0.83	99.17	0.83	100	328
2	1.04	99.14	0.86	99.4	0.6	120	350
3	2.07	98.6	1.4	99.53	0.47	152.5	351
4	3.17	98.25	1.75	99.34	0.66	177.5	351
5	4.20	98.15	1.85	97.85	2.15	197.5	353
6	5.25	98.09	1.91	96.85	3.15	215	353
7	6.33	97.99	2.01	96.65	3.35	215	353
8	8.00	98.07	1.93	96.6	3.4	215	352

Note: Sample 1 is the initial feed

Therefore, the concentration of 1-hexene drops by just over 1 and 3% in the reboiler and condenser over 8 hours of time on stream

Appendix D - Statistical Analysis of Experimental Data

Sample of the Spreadsheet used to carry out Statistical Analysis of Experimental data

Flow rate, X	Kga, Y
7.32E-04	1.57E-03
1.09E-03	4.62E-03
1.30E-03	6.41E-03
1.53E-03	6.83E-03
1.77E-03	9.27E-03
2.31E-03	1.86E-02

Statistic	Value
N	6
∑X	0.01
Mean X	0.00146
∑Y	0.05
Mean Y	0.00789
∑x^2	1.5E-06
∑y^2	0.00017
∑xy	1.6E-05

Ao =	-0.007	V(Ao) =	5E-06
A1 =	10.2466	V(A1) =	1.9581
R =	0.96467	D.f.(R) =	4
t(R) =	7.3226	p(t{R}) =	0.0019

Analysis of Variance for Regression

Source	D.F	SS	MS	F (p)
Regre	1	0.00016	0.0002	53.62
Residual	4	1.2E-05	3E-06	0.002
Total	5	0.00017	-	

Residual Standard Error	R-square
0.00173	0.9306

Conf. Level %	Prediction of Line			Prediction of Values Y		
95						
Choose X	Pred. Y	Lower Y	Upper Y	Pred. Y	Lower Y	Upper Y
6.50E-04	-3.79E-04	-4.07E-03	3.32E-03	-3.79E-04	-6.43E-03	5.67E-03
7.75E-04	9.02E-04	-2.39E-03	4.20E-03	9.02E-04	-4.91E-03	6.71E-03
9.00E-04	2.18E-03	-7.34E-04	5.10E-03	2.18E-03	-3.43E-03	7.79E-03
1.03E-03	3.46E-03	8.86E-04	6.04E-03	3.46E-03	-1.98E-03	8.90E-03
1.15E-03	4.74E-03	2.45E-03	7.03E-03	4.74E-03	-5.65E-04	1.01E-02
1.28E-03	6.02E-03	3.95E-03	8.10E-03	6.02E-03	8.03E-04	1.12E-02
1.40E-03	7.31E-03	5.34E-03	9.27E-03	7.31E-03	2.13E-03	1.25E-02
1.53E-03	8.59E-03	6.61E-03	1.06E-02	8.59E-03	3.41E-03	1.38E-02
1.65E-03	9.87E-03	7.77E-03	1.20E-02	9.87E-03	4.64E-03	1.51E-02
1.78E-03	1.11E-02	8.84E-03	1.35E-02	1.11E-02	5.83E-03	1.65E-02
1.90E-03	1.24E-02	9.82E-03	1.50E-02	1.24E-02	6.98E-03	1.79E-02
2.03E-03	1.37E-02	1.08E-02	1.67E-02	1.37E-02	8.09E-03	1.93E-02
2.15E-03	1.50E-02	1.17E-02	1.83E-02	1.50E-02	9.16E-03	2.08E-02
2.28E-03	1.63E-02	1.25E-02	2.00E-02	1.63E-02	1.02E-02	2.23E-02
2.40E-03	1.76E-02	1.34E-02	2.17E-02	1.76E-02	1.12E-02	2.39E-02
2.53E-03	1.88E-02	1.42E-02	2.34E-02	1.88E-02	1.22E-02	2.55E-02

Appendix E - FORTRAN Code: Estimation of Parameters A and B

Program CDmodelSSpar

```
c=============================================================
============
c Determine parameters A and B from measured condenser and reboiler
c compositions using the 3 region CD model
c km & GM Jan 2003
c-------------------------------------------------------------
      implicit none
      integer nn,mm
      parameter (nn=2,mm=12)
    INTEGER
i,J,M,N,MAXFEV,MODE,NPRINT,INFO,NFEV,LDFJAC,NWRITE
    INTEGER IPVT(nn)
    DOUBLE PRECISION FTOL,XTOL,GTOL,EPSFCN,FACTOR,FNORM
    DOUBLE                                          PRECISION
X(nn),FVEC(mm),DIAG(nn),FJAC(mm,nn),QTF(nn),
   *          WA1(nn),WA2(nn),WA3(nn),WA4(mm)
    integer ldr,iseed
    double precision tol,r(nn,nn),wa(nn)
    DOUBLE PRECISION ENORM,DPMPAR
      real*8 var,var2exp,rnd,xnoise
    EXTERNAL FCN
c common block
      real*8 alpha,Kya,Kh,L,V,yh,xd(12),xr(12),yh2(12)
      common alpha,Kya,Kh,L,V,yh,xd,xr,yh2

c print device
    DATA NWRITE /7/
C supply exp data
    M = 6 !number of data points
    N = 2 !number of variables
      data xd /0.558,0.565,0.575,0.568,0.583,0.623,6*0/
c     data xr /0.545, 1*0./
      data xr /0.506,0.499,0.504,0.498,0.499,0.496,6*0/  !3 dec places
```

```
c       data xr /0.45,0.38,0.31,0.23,0.16,5*0./    !2 dec places
        data yh2 /12*0/
c       data yh2/0.5,1*0./
c add error to xr data, to see how robust the routine is
        iseed=1
        xrnoise=0.0  !2*xrnoise*100 %
        do i=1,m
          rnd=dble(ran(iseed))
          xr(i)=xr(i)*(1.-xrnoise+2.*xrnoise*rnd)
        end do
c       do 41 i=1,m
c         md = ran(iseed)
c         obs(i)=obs(i)*(1.d0-0.5d0*ynoise+ynoise*dble(rnd))  !5%

C THE FOLLOWING STARTING VALUES PROVIDE A ROUGH FIT.
      X(1) = 3. !initial value for A
      X(2) = 0.0005 !initial value for B
c set minpack parameters
C     SET FTOL AND XTOL TO THE SQUARE ROOT OF THE MACHINE
PRECISION
C     AND GTOL TO ZERO. UNLESS HIGH PRECISION SOLUTIONS ARE
C     REQUIRED, THESE ARE THE RECOMMENDED SETTINGS.
      LDFJAC = mm
      FTOL = DSQRT(DPMPAR(1))
      XTOL = DSQRT(DPMPAR(1))
      GTOL = 0.D0
      MAXFEV = 800
      EPSFCN = 0.D0
      MODE = 1
      FACTOR = 1.D2
      NPRINT = 0
C
      CALL LMDIF(FCN,M,N,X,FVEC,FTOL,XTOL,GTOL,MAXFEV,EPSFCN,
     *           DIAG,MODE,FACTOR,NPRINT,INFO,NFEV,FJAC,LDFJAC,
```

```
     *         IPVT,QTF,WA1,WA2,WA3,WA4)
      FNORM = ENORM(M,FVEC)
      WRITE (NWRITE,1000) FNORM,NFEV,INFO,(X(J),J=1,N)

c get the covariance matrix from the data
          ldr=nn
          tol=1.d-4
          do i=1,n
            do j=1,n
              r(i,j)=fjac(i,j)
            end do
          end do
          call covar(n,r,ldr,ipvt,tol,wa)
          write(nwrite,'(//,a17)')'covariance matrix'
          do i=1,n
            write(nwrite,1010)('c(',i,',',j,')=',r(i,j),j=1,n)
          end do

c calculate the linear variances
          write(nwrite,'(//,a16)')'linear variances'
          var2exp=fnorm*fnorm/(m-n)
          do i=1,n
            var=dsqrt(abs(r(i,i))*var2exp)
            write(nwrite,'(t3,a4,i1,a3,1pe10.3)')'var(',i,')= ',var
          end do

      STOP
 1000 FORMAT (31H FINAL L2 NORM OF THE RESIDUALS,1pe11.3 /
     *       31H NUMBER OF FUNCTION EVALUATIONS,I10 /
     *       15H EXIT PARAMETER,16X,I10 ///
     *       27H FINAL APPROXIMATE SOLUTION / 3(1pe11.3))
 1010  format(10(a2,i1,a1,i1,a2,1pe10.3,'  '))
      END
c-------------------------------------------------------------
```

```
      SUBROUTINE FCN(M,N,X,FVEC,IFLAG)
c ------------------------------------------------------------
c Simulation of the CD column using ideal solution constant alpha
c VLE for Hexene, Hexane. H2 is not included in the VLE calculation
c and assumed to be uniformally distributed throughout the CD system
c L & V are assumed constant and measurable.
c Reaction is Hexene + H2 --> hexane.
c The system is assumed to be in pseudo equilibrium at each point in
c time, constant P.
c The hold-up in the column and condenser are assumed to be negligible
c The composition at the condenser and reboiler have been measured
c as a function of time
c the solution proceeds from the TOP given the concentration of the
c condenser
c extension of the code to vary the size of the reactive section
c Km and GM Jan 2003
c
==========================================================================
==========
        implicit none
c DDASAC parameters
        integer nstvar,npar,nspar,lrw,liw
      PARAMETER (NSTVAR=4,NPAR=10,NSPAR=0)
      PARAMETER (LRW=5000,LIW=500)
      real*8 Y(NSTVAR)  !dependent variables
        real*8 YP(NSTVAR)  !sensitivity of dependent variables
      integer INFO(18)  !info array
        real*8 RWORK(LRW)  !work array
        integer IWORK(LIW)  !work array
      real*8 RPAR(NPAR)  !model parameters
        integer ipar(npar)
        real*8 rtol,atol
        integer idid,ieform
      EXTERNAL fsub,Esub,Jac,Bsub
```

```
c minpack parameters
      INTEGER M,N,IFLAG
      DOUBLE PRECISION X(N),FVEC(M)
c local variables
          integer i,j,iout,nz,idata
          real*8 z,dz,zdz,zL,pt,xR1,x01,x02,y01,y02,yy,RR,xx
          real*8 zstop1,zstop2,zstop3,R1
c common block
          real*8 alpha,Kya,Kh,L,V,yh,xd(10),xr(10),yh2(10)
          common alpha,Kya,Kh,L,V,yh,xd,xr,yh2

c set the parameters to be estimated
          rpar(1)=x(1)
          rpar(2)=x(2)

c the rest of the programme must be placed in a loop to get the
c error vector
          do idata=1,m  !start idata loop

c system variables
          iout=1  !output unit
          nz=30   !number of steps
          zL=1.   !length
          dz=zL/nz !step size
C Insert the model parameter values
c         Pt=101325.*2.  !system pressure
          alpha=1.1  !relative volatility for 1,2
c         Kh=.0001   !pseudo rxn rate for h2
c         Kya=30.00  !gas-Liq phase overall coeff
          yh=yh2(idata)  !H2 in the gas phase
          L=1.  !this is only the flow of C6
          V=1.
c       RPAR(1)= 30.  !A sensitivity of needed
c       RPAR(2)= 0.1    !B
```

```
C initial values of x and y
c actually need to calculate the values which are consistent with
c initial conditions at the TOP
        x01=xd(idata)  !condenser composition
        y01=x01*(1.-yh)
        y02=1.-y01-yh
        x01=y01/(1.-yh)
        x02=1.-x01
     Y(1)=y01 !hexene y1
     Y(2)=y02  !hexane y2
     Y(3)=x01  !hexene x1
     Y(4)=x02  !hexane x2
C    Insert INFO(j) values
     DO 10 J = 1, 18
      INFO(J)  = 0
10   CONTINUE
c       info(17)=1  !do not let y(1) go negative
c       rwork(42)=1.d-5  !actual value of y
c       rwork(43)=1.d-8  !tolerance
        info(10)=2  !all y(i) must always be positive
C    Suppress t-differencing of f in the initialization:
     Rwork(44)=0.0D0
C    Provide scalar tolerances in accordance with info(2)
     RTOL = 1.D-6
     ATOL = 1.D-8
        z=0.
c       write(iout,1002)'batch CD simulation - km and gm dec 2002'
c       write(iout,1002)
c       write(iout,1001)'z  ','y1  ','y2  ','x1  ','x2  ','y1"  ','x1"  ',
c    &  'Rxn(1/0)'
c       write(iout,1000)z,(y(j),j=1,nstvar)
c start the integration, there will be 3 equal sections
c 1 = distillation, 2 = reaction+distillation, 3 = distillation
c use leform and info(4)=1 to set up the different regions
```

```
c on a 0-1 z interval
        info(4)=1  !integration regions
        zstop1=10.*dz
        zstop2=20.*dz
        zstop3=30.*dz
      rwork(1)=zstop1
        leform=0
        info(1)=0
      DO 40 i=1,nz
       If (z.eq.zstop1) then
            rwork(1)=zstop2
            leform=1
            info(1)=0
          end if
       If (z.eq.zstop2) then
            rwork(1)=zstop3
            leform=0
            info(1)=0
          end if
          zdz=z+dz
       CALL DDASAC(z,zdz,NSTVAR,Y,YP,RTOL,ATOL,INFO,
     1            RWORK,LRW,IWORK,LIW,RPAR,IPAR,IDID,iout,
     2            leform,fsub,Esub,Jac,Bsub)
          z=zdz
          yy=y(1)/(1.-yh)
          if (z.gt.zstop2) then
             R1=rpar(2)*yh*(zstop2-zstop1)
           else
             if (z.gt.zstop1) then
                    R1=rpar(2)*yh*(z-zstop1)
               else
                 R1=0.
             end if
          end if
```

```
c         write(2,'(10(f8.4))')z,R1
c         xx=V/L*(y(1)-y01)/(1.-yh)+x01-R1
c         write(iout,1000)z,(y(j),j=1,nstvar),yy,xx,float(ieform)
40    CONTINUE
c check on reboiler concentration and reaction rate
          xR1=y(1)/(y(1)+alpha*(1.-y(1)-yh))  !mole fraction
c         RR=(L*y(3)-V*y(1)/(1.-yh))  !mole/(sec.area)
c         write(iout,1002)
c         write(iout,1001)'x-reboiler','rxn-rate'
c         write(iout,1003)xR1,RR
c calculate the error vector
      FVEC(idata) = xr(idata)-xr1  !error in reboiler concentration

          end do  !idata loop

50    WRITE(iout,80) (IWORK(J), J=11,15)
60    FORMAT(1X,F6.3,4(1X,1PD12.5))
70    FORMAT(/1X,'Integration failed in step',I6,' with IDID =',I5)
80    FORMAT(//1X,'Number of steps taken so far =',I5/
     1        1X,'Number of function calls    =',I5/
     2        1X,'Number of Jacobian calls    =',I5/
     3        1X,'Number of error test fails  =',I5/
     4        1X,'Number of convergence fails =',I5/)
1000  format(' ',10(1pe11.2))
1001  format('#',10(a11))
1002  format('#',a40)
1003  format('#',10(1pe11.2))

      RETURN
      END
c
=============================================================
==========
      SUBROUTINE fsub(z,NSTVAR,y,f,RPAR,IPAR,Ieform,Ires)
```

```
      IMPLICIT none
      real*8 z,y(*),f(*),RPAR(*)
         integer i,nstvar,ieform,ires,ipar(*)
         real*8 ys(2),R1,NA1,NA2,yy
c common block
         real*8 alpha,Kya,Kh,L,V,yh,xd(10),xr(10),yh2(10)
         common alpha,Kya,Kh,L,V,yh,xd,xr,yh2

c calculate the y* and x* values
c note using 1-y1-yh does not work for ys2 ???????, instability or
c the condition sum(x)=sum(y)=1 is not maintained
         ys(1)=alpha*y(3)*(1.-yh)/(1.+(alpha-1.)*y(3))  !hexene
         ys(2)=y(4)*(1.-yh)/(y(4)+alpha*(1.-y(4))) !hexane
c        NA1=Kya*(y(1)-ys(1))
c        NA2=Kya*(y(2)-ys(2))
         NA1=rpar(1)*(y(1)-ys(1))  !dimensionless flux
         NA2=rpar(1)*(y(2)-ys(2))
         R1=0.
         if (ieform.eq.1) then
c        R1=-Kh*yh  !rxn rate of reactant
           R1=-rpar(2)*yh  !dimensionless formation rxn rate
c          NA1=NA1*0.01  !reduce mass transfer in reaction zone
c          NA2=NA2*0.01
         end if
c function evaluation
      f(1)=NA1*(1.-yh)  !hexene  y(1)=y1
      f(2)=NA2*(1.-yh)  !hexane  y(2)=y2
         f(3)=NA1+R1  !hexene y(3)=x1
      f(4)=NA2-R1  !hexane y(4)=x2
c        write(2,'(10(f8.4))')z,y(1)+y(2),y(1),y(2),y(3)+y(4),y(3),y(4)
c        write(2,'(10(f8.4))')R1
      RETURN
      END
c-----------------------------------------------------------------------
```

```
      SUBROUTINE Esub
      RETURN
      END
C-----------------------------------------------------------------
         SUBROUTINE Jac
      RETURN
      END
C-----------------------------------------------------------------
      SUBROUTINE BSUB
      RETURN
      END
C-----------------------------------------------------------------
```

Appendix F - FORTRAN Code: Concentration Profiles

PROGRAM CDmodelSSc

```
c ------------------------------------------------------------
c Simulation of the CD column using ideal solution constant alpha
c VLE for Hexene, Hexane. H2 is not included in the VLE calculation
c and assumed to be uniformally distributed throughout the CD system
c L & V are assumed constant and measurable.
c Reaction is Hexene + H2 --> hexane.
c The system is assumed to be in pseudo equilibrium at each point in
c time, constant P.
c The hold-up in the column and condenser are assumed to be negligible
c The composition at the condenser and reboiler have been measured
c as a function of time
c the solution proceeds from the TOP given the concentration of the
c condenser
c extension of the code to vary the size of the reactive section
c Km & GM Jan 2003
c
==============================================================
==========
      IMPLICIT none
c DDASAC parameters
          integer nstvar,npar,nspar,lrw,liw
      PARAMETER (NSTVAR=4,NPAR=10,NSPAR=0)
      PARAMETER (LRW=5000,LIW=500)
      real*8 Y(NSTVAR)  !dependent variables
          real*8 YP(NSTVAR)  !sensitivity of dependent variables
      integer INFO(18)  !info array
          real*8 RWORK(LRW)  !work array
          integer IWORK(LIW)  !work array
      real*8 RPAR(NPAR)  !model parameters
          integer ipar(npar)
          real*8 rtol,atol
          integer idid,ieform
      EXTERNAL fsub,Esub,Jac,Bsub
```

```
c local variables
      integer i,j,iout,nz
      real*8 z,dz,zdz,zL,pt,xR1,x01,x02,y01,y02,yy,RR,xx
      real*8 zstop1,zstop2,zstop3,R1
c common block
      real*8 alpha,Kya,Kh,L,V,yh
      common alpha,Kya,Kh,L,V,yh

c system variables
      iout=1  !output unit
      nz=10   !number of steps
      zL=1.   !length
      dz=zL/nz !step size
C Insert the model parameter values
c     Pt=101325.*2.  !system pressure
      alpha=1.1  !relative volatility for 1,2
c     Kh=.0001   !pseudo rxn rate for h2
c     Kya=30.00  !gas-Liq phase overall coeff
      yh=0.8506  !H2 in the gas phase
      L=1.533e-3  !this is only the flow of C6
      V=0.9078
    RPAR(1)= 0.0  !A sensitivity of needed
    RPAR(2)= 3.1672e-3    !B
C initial values of x and y
c actually need to calculate the values which are consistent with
c initial conditions at the TOP
      x01=0.3301
      y01=x01*(1.-yh)
      y02=1.-y01-yh
      x01=y01/(1.-yh)
      x02=1.-x01
    Y(1)=y01 !hexene y1
    Y(2)=y02  !hexane y2
    Y(3)=x01  !hexene x1
```

```
      Y(4)=x02  !hexane x2
C     Insert INFO(j) values
      DO 10 J = 1, 18
       INFO(J)  = 0
10    CONTINUE
c       info(17)=1  !do not let y(1) go negative
c       rwork(42)=1.d-5  !actual value of y
c       rwork(43)=1.d-8  !tolerance
        info(10)=2  !all y(i) must always be positive
C     Suppress t-differencing of f in the initialization:
      Rwork(44)=0.0D0
C     Provide scalar tolerances in accordance with info(2)
      RTOL = 1.D-6
      ATOL = 1.D-8
         z=0.
         write(iout,1002)'batch CD simulation - km dec 2002'
         write(iout,1002)
         write(iout,1001)'z ','y1 ','y2 ','x1 ','x2 ','y1" ','x1" ',
     & 'Rxn(1/0)'
         write(iout,1000)z,(y(j),j=1,nstvar)
c start the integration, there will be 3 equal sections
c 1 = distillation, 2 = reaction+distillation, 3 = distillation
c use leform and info(4)=1 to set up the different regions
c on a 0-1 z interval
         info(4)=1  !integration regions
         zstop1=10.*dz
         zstop2=20.*dz
         zstop3=30.*dz
      rwork(1)=zstop1
         leform=0
         info(1)=0
      DO 40 i=1,nz
       If (z.eq.zstop1) then
            rwork(1)=zstop2
```

```
            ieform=1
            info(1)=0
          end if
        If (z.eq.zstop2) then
            rwork(1)=zstop3
            ieform=0
            info(1)=0
          end if
          zdz=z+dz
       CALL DDASAC(z,zdz,NSTVAR,Y,YP,RTOL,ATOL,INFO,
     1          RWORK,LRW,IWORK,LIW,RPAR,IPAR,IDID,iout,
     2          ieform,fsub,Esub,Jac,Bsub)
          z=zdz
          yy=y(1)/(1.-yh)
          if (z.gt.zstop2) then
            R1=rpar(2)*yh*(zstop2-zstop1)
           else
            if (z.gt.zstop1) then
                  R1=rpar(2)*yh*(z-zstop1)
             else
              R1=0.
            end if
          end if
c         write(2,'(10(f8.4))')z,R1
          xx=V/L*(y(1)-y01)/(1.-yh)+x01-R1
          write(iout,1000)z,(y(j),j=1,nstvar),yy,xx,float(ieform)
40    CONTINUE
c check on reboiler concentration and reaction rate
        xR1=y(1)/(y(1)+alpha*(1.-y(1)-yh))  !mole fraction
        RR=(L*y(3)-V*y(1)/(1.-yh))  !mole/(sec.area)
        write(iout,1002)
        write(iout,1001)'x-reboiler','rxn-rate'
        write(iout,1003)xR1,RR
```

```
50    WRITE(iout,80) (IWORK(J), J=11,15)
60    FORMAT(1X,F6.3,4(1X,1PD12.5))
70    FORMAT(/1X,'Integration failed in step',I6,' with IDID =',I5)
80    FORMAT(//1X,'Number of steps taken so far =',I5/
     1       1X,'Number of function calls    =',I5/
     2       1X,'Number of Jacobian calls    =',I5/
     3       1X,'Number of error test fails  =',I5/
     4       1X,'Number of convergence fails =',I5/)
1000  format(' ',10(1pe11.2))
1001  format('#',10(a11))
1002  format('#',a40)
1003  format('#',10(1pe11.2))
      STOP
      END
c
=============================================================
==========
      SUBROUTINE fsub(z,NSTVAR,y,f,RPAR,IPAR,Ieform,Ires)
      IMPLICIT none
      real*8 z,y(*),f(*),RPAR(*)
         integer i,nstvar,ieform,ires,ipar(*)
         real*8 ys(2),R1,NA1,NA2,yy
c common block
         real*8 alpha,Kya,Kh,L,V,yh
         common alpha,Kya,Kh,L,V,yh

c calculate the y* and x* values
c note using 1-y1-yh does not work for ys2 ???????, instability or
c the condition sum(x)=sum(y)=1 is not maintained
         ys(1)=alpha*y(3)*(1.-yh)/(1.+(alpha-1.)*y(3))  !hexene
         ys(2)=y(4)*(1.-yh)/(y(4)+alpha*(1.-y(4))) !hexane
c        NA1=Kya*(y(1)-ys(1))
c        NA2=Kya*(y(2)-ys(2))
         NA1=rpar(1)*(y(1)-ys(1))  !dimensionless flux
```

```
      NA2=rpar(1)*(y(2)-ys(2))
      R1=0.
      if (leform.eq.1) then
c     R1=-Kh*yh  !rxn rate of reactant
        R1=-rpar(2)*yh  !dimensionless formation rxn rate
c       NA1=NA1*0.01  !reduce mass transfer in reaction zone
c       NA2=NA2*0.01
      end if
c function evaluation
    f(1)=NA1*(1.-yh)  !hexene  y(1)=y1
    f(2)=NA2*(1.-yh)  !hexane  y(2)=y2
      f(3)=NA1+R1  !hexene y(3)=x1
    f(4)=NA2-R1  !hexane y(4)=x2
c     write(2,'(10(f8.4))')z,y(1)+y(2),y(1),y(2),y(3)+y(4),y(3),y(4)
c     write(2,'(10(f8.4))')R1
    RETURN
    END
c-----------------------------------------------------------------
    SUBROUTINE Esub
    RETURN
    END
c-----------------------------------------------------------------
      SUBROUTINE Jac
    RETURN
    END
c-----------------------------------------------------------------
    SUBROUTINE BSUB
    RETURN
    END
c-----------------------------------------------------------------
```